ISBN 978-82-326-2704-2 (printed version)
ISBN 978-82-326-2705-9 (electronic version)
ISSN 1503-8181

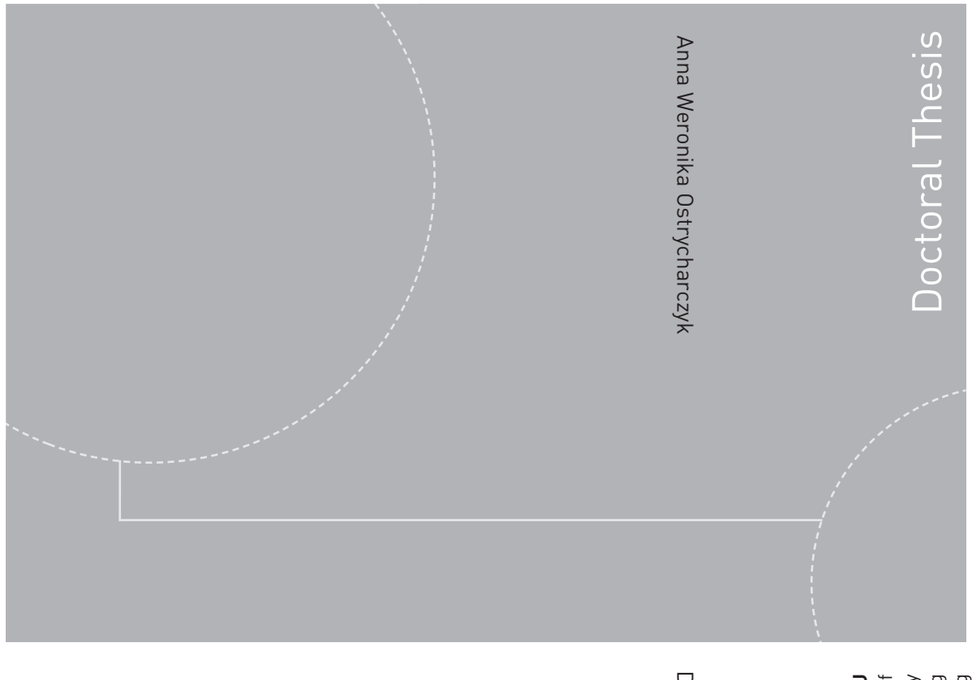

Doctoral theses at NTNU, 2017:318

Anna Weronika Ostrycharczyk

Network arch timber bridges with light timber deck on transverse crossbeams

NTNU
Norwegian University of
Science and Technology
Faculty of Engineering
Department of Structural Engineering

NTNU
Norwegian University of
Science and Technology

Doctoral theses at NTNU, 2017:318

NTNU

NTNU
Norwegian University of
Science and Technology

Anna Weronika Ostrycharczyk

Network arch timber bridges with light timber deck on transverse crossbeams

Thesis for the degree of Philosophiae Doctor

Trondheim, November 2017

Norwegian University of Science and Technology
Faculty of Engineering
Department of Structural Engineering

NTNU
Norwegian University of
Science and Technology

NTNU
Norwegian University of Science and Technology

Thesis for the degree of Philosophiae Doctor

Faculty of Engineering
Department of Structural Engineering

ISBN 978-82-326-2704-2 (printed version)
ISBN 978-82-326-2705-9 (electronic version)
ISSN 1503-8181

Doctoral theses at NTNU, 2017:318

Printed by Skipnes Kommunikasjon as

“Do prawdy nie można dojść w pojedynkę”

(“One cannot reach the truth alone”)

prof. Michał Heller

in *Moralność myślenia* (*Morality of thinking*)

Preface

This doctoral thesis has been submitted to the Norwegian University of Science and Technology (NTNU) for the degree of *Philosophiae Doctor* (PhD). The research was carried out at the Department of Structural Engineering, Faculty of Engineering Science and Technology, at NTNU in Trondheim, Norway.

The supervisor of the PhD project was Professor Kjell Arne Malo from NTNU.

The PhD project was funded by several sources: Norwegian University of Science and Technology, The Research Council of Norway through the project *Rigid Joints for Large Timber Structures* (Grant no. 208052) and WoodWisdom-Net+ through the *DuraTB* (*Durable Timber Bridges*) project (Grant no. 237135 from The Research Council of Norway). Additional financial and technical support was provided by The Association of Norwegian Glulam Producers, Skogtiltaksfondet and Norwegian Public Roads Authorities.

The PhD project started in August 2012 and the thesis was submitted in August 2017. The PhD position included over one year of teaching assistance at the Department of Structural Engineering, NTNU.

The thesis consists of an introduction, four scientific papers in the main part of the thesis and one additional scientific paper on secondary literature study. Three of the scientific papers were submitted to international scientific journals and two were published in international conference proceedings.

The author, Anna Weronika Ostrycharczyk, declares that the thesis and the work presented in it are her own. The thesis contains no material that has previously been submitted for a degree at this university or any other institution.

Anna Weronika Ostrycharczyk

Trondheim, August 2017

Acknowledgements

This PhD work would not have been possible without the technical and moral support I received from many people.

First and foremost, I would like to acknowledge my supervisor prof. Kjell Arne Malo, who gave me the opportunity to get the PhD-experience, as well as for making this thesis completion possible. I highly appreciate his open-door policy, and that I always felt welcome in his office regardless the topic to discuss. The time spent on technical and philosophical disputes was fruitful for my knowledge and perception of the world. I am thankful for those moments and the influence.

I would also like to thank prof. Kolbein Bell for all his help and given advices. Within the time I have spent at the NTNU, he become my inspiration and the role model in the engineering and scientific world.

From practical point of view, this PhD project was possible thanks to funds of many organizations: Norwegian University of Science and Technology, The Research Council of Norway through the project *Rigid Joints for Large Timber Structures* (Grant no. 208052) and WoodWisdom-Net+ through the *DuraTB* (*Durable Timber Bridges*) project (Grant no. 237135 from The Research Council of Norway). Additional financial and technical support was provided by The Association of Norwegian Glulam Producers, Skogtiltaksfondet and Norwegian Public Roads Authorities. I am very grateful for this support.

The working days at the university would not have been as enjoyable as they were if not for my colleagues: Alessia, Elena, Haris, Martin, Mirko and Katarzyna. Coffee breaks, gossips and complaints sessions with them were what I needed to stay sane.

My grateful thanks are extended to all my friends who backed my decision of moving to Trondheim, and to my family which was constantly accepting and supporting all my life decisions. I am here because of them.

Final gratitude goes to Michał. Thank you for being my mentor both in the academic and the everyday life, and for deciding to stay with me through the thick and thin not only for this PhD-adventure. Without you it would not be the same.

Abstract

In modern bridge engineering, timber is more and more often considered as a choice for structural material. The advantages are evident: timber is environmentally friendly, easy to shape, thus it can meet various architectural requirements, and due to current technology, production of long elements of massive glulam is possible. However, due to the narrow history of wood research, in comparison to steel and concrete, this material is less familiar to the engineers. Therefore, the present situation can be amended increasing the research in the field.

The aim of this research project was to create a concept for a long-span timber bridge. Therefore, the idea of network arch, known among steel and concrete structures, was adapted to timber, i.e. in the studied bridge-type both the arch and the deck were made of glulam. For the chosen design concept, the focus of the research was on defining the network pattern suitable for bridges with light timber deck on transverse crossbeams, with equally distributed hangers along the lower chord. In addition, the concept of spoked configuration of hangers was verified. In order to perform such study, the work was divided into two phases: a preliminary study of a laboratory model and a wide-range parametric numerical study.

The scaled laboratory model was used as a benchmark for the validation of a single, detailed numerical model, which in turn was used as a basis to create a software tool for automatic model generation. The tool allows to build a bridge model with arbitrary geometrical, material and structural properties defined by a user.

The developed software was used to performed wide-range parametric studies. First, a comparison of selected existing network patterns with equally distributed hangers along the deck was made for two types of arch shape, i.e. circular and parabolic. Next, the focus of the numerical investigation was on the introduced radial pattern modifications. The influence of the presented pattern modifications on the structural performance of the network bridge, especially moment distribution in the arch, stresses in hangers and number of relaxed hangers, was evaluated for various load conditions. Finally, a possible alternative for wind bracing, i.e. spoked configuration of hangers, was analysed in terms of stability of the bridge.

In conclusion, the introduced pattern modifications have a positive influence on the forces distribution in the bridge structure, in comparison to the existing patterns. In addition, the modifications provide a way of a systematic pattern generation. Therefore, as such, they are promising for further development and application. Moreover, it was shown that spoked hangers configuration might reduce the amount of wind bracing, and

consequently the number of side connections which are the main source of water penetration into timber elements.

List of Papers

The main part of the thesis consists of the following papers.

Major papers

I. **Comparison of network patterns suitable for timber bridges with crossbeams**
A. W. Ostrycharczyk & K.A. Malo
In: *Proceedings of the ICTB 2017, 3rd International Conference on Timber Bridges.* Skellefteå, Sweden, 2017.

II. **Parametric study of radial hanger patterns for network arch timber bridges with a light deck on transverse crossbeams**
A. W. Ostrycharczyk & K.A. Malo
Submitted to Engineering Structures in February 2017.

III. **Parametric study on effects of load position on the stress distribution in network arch timber bridges with light timber deck on transverse crossbeams**
A. W. Ostrycharczyk & K.A. Malo
Submitted to Engineering Structures in July 2017.

IV. **Network arch timber bridges with light timber deck and spoked configuration of hangers – parametric study**
A. W. Ostrycharczyk & K.A. Malo
Submitted to Structural Engineering International in July 2017.

Additional paper

V. **A review of serviceability limit state design criteria for timber footbridges**
A. W. Ostrycharczyk & K.A. Malo
In: *Proceedings of the WCTE 2014, World Conference on Timber Engineering.* Quebec City, Canada; 2014.

Declaration of authorship

The author of the thesis, Anna Weronika Ostrycharczyk, planned, prepared and executed all the numerical experiments, evaluated the results, and wrote the major part of all the papers included in the thesis. The co-author of the papers contributed in planning the experiments, discussing and evaluating the results by assisting in writing the papers. The physical, laboratory model of the bridge was prepared as a part of a master project (students: R. Barli and I. Hakvåg, 2013).

Other publications

In addition to the papers included in the thesis, the author of this thesis has contributed to the following works.

Conference papers

Malo, Kjell A.; Ostrycharczyk Anna W.; Barli Runa; Hakvåg, Idun. "On Development of Network Arch Bridges in Timber". In: *Proceeding of the 2nd International Conference on Timber Bridges, ICTB 2013*. Las Vegas, Nevada USA, 2013.

Ostrycharczyk, Anna W.; Malo, Kjell A. "Experimental evaluation of timber network arch bridge". In: *Experimental Research with Timber: Enhance mechanical properties of timber, engineering wood products and timber structures; (COST Action FP1004).* Prague, Czech Republic, 2014.

Malo, Kjell A.; Ostrycharczyk, Anna W. "Durable Timber Bridges". In: *COST Timber Bridge Conference - CTBC 2014; (COST Action FP1004 and FP1101).* Biel, Switzerland, 2014.

Project report

Pousette, A.; Malo, K.A.; Thelandersson, S.; Fortino, S.; Salokangas, L.; Wacker, J. *Durable Timber Bridges, Final Report and Guidelines*. SP Rapport 2017:25, RISE Research Institutes of Sweden. Skellefteå 2017.

Scientific lectures

Ostrycharczyk Anna W. (2013) "On Development of Network Arch Bridges in Timber". *ICTB 2013, 2nd International Conference on Timber Bridges*. Las Vegas, Nevada USA.

Ostrycharczyk Anna W. (2014) "Experimental evaluation of timber network arch bridge". *COST Action FP1004.* Prague, Czech Republic.

Ostrycharczyk Anna W. (2014) “Durable Timber Bridges”. *COST Action FP1004 and FP1101*. Biel, Switzerland.

Ostrycharczyk Anna W. (2014) “A review of serviceability limit state design criteria for timber footbridges”. *WCTE 2014, World Conference on Timber Engineering.* Quebec City, Canada.

Ostrycharczyk Anna W. (2015) “Development of timber network arch bridges”. Wood Workshop (Tredager), Norwegian University of Science and Technology (NTNU), Trondheim, Norway.

Ostrycharczyk Anna W. (2017) “Comparison of network patterns suitable for timber bridges with crossbeams”. Wood Workshop (Tredager), Norwegian University of Science and Technology (NTNU), Trondheim, Norway.

Ostrycharczyk Anna W. (2017) “Comparison of network patterns suitable for timber bridges with crossbeams”. *ICTB 2017, 3rd International Conference on Timber Bridges.* Skellefteå, Sweden.

Table of contents

PART I

Introduction to the doctoral thesis

1 Introduction

1.1 Background and motivation

Nowadays, wood-based materials and wood engineering are constantly gaining popularity. Not long time ago, the main limitation in design of wooden structure was the size of available wood elements. Currently, the possibility of creating big elements of massive glulam in almost any shape makes timber a competitive material in the nowadays market, especially with the increased complexity of modern structures. Moreover, wood is a natural material and this makes it an environmental friendly choice.

On the other hand, due to the narrow history of wood research, in comparison to steel or concrete, this material is less familiar to the engineers, and thus it might not be their first choice. In addition, legal requirements in Europe for newly designed bridges demand a designed lifetime of 100 years, which raises doubts on the durability of timber constructions. Such legal requirements, in combination with a modest knowledge of the material, make wood a rare alternative especially for long-span bridges for car traffic.

A natural conclusion of the above observation is that more knowledge, and research is needed in the field. Therefore, this thesis, related to the *Durable Timber Bridges* project, deals with the concept of a durable long span timber bridge [1]. The suggested solution is a network arch timber bridge with light timber deck, with hangers in spoked configuration. The durability of the wooden arch elements is highly increased by limiting the number of connections, which are usually the source of moisture penetration. The spoked configuration of hangers allows to limit or remove wind bracing, which usually is mounted to the arch sides. Therefore, all the connections are located under the arch, which is desirable. Furthermore, the durability of the deck is dependent on construction details design, in such a way, that water is immediately removed from the structure. The details design is out of the scope of this thesis; however, the problem is addressed in the *DuraTB* project.

The network arch bridge, due to many unique features was a logical choice for the considered concept of a long timber bridge. Nonetheless, it brings a challenge with the choice of the network pattern, as well as the light weight of the timber deck, which may in consequence enhance the phenomenon of hanger relaxation. In addition, for long footbridges, special care should be given to the vibration analysis of the structure.

Network arch bridges were studied by many researches, and special attention was paid to different network patterns, stability of the bridge structure and vibrations, although mostly in bridges made of steel or concrete. Therefore, the presented thesis aims to extend the research for network bridges made of timber. Norway, as one of the leaders

in wood industry, environmentally friendly country and homeland of Per Tveit, creator of the network arch bridge, is the perfect place for this type of research.

1.2 Objectives

This thesis was connected to the *DuraTB* project, which aimed to "contribute to the development of sustainable timber bridges by making guidelines for moisture design and developing new and improved bridge concepts and details in terms of durability and maintenance aspects" [1]. This PhD project was part of the Work Package 4 (WP4) *Design concepts for durable timber bridges*, under WP4.3 *Medium to long span bridges*. Thus, the focus was on the conceptual study of network arch bridges with both the decks and the arches made of glulam.

In the thesis, the following objectives were defined:

- To verify existing network patterns as possible patterns for bridges with transverse crossbeams, which constitute the base for hangers attachment on the lower chord (deck level).
- To define a new network pattern suitable for network arch bridges with crossbeams and provide a systematic way of pattern creation.
- To prepare a software tool for auto-generation of numerical models of network arch bridges. Validation of numerical models should be based on tests of a scaled laboratory model of a bridge.
- To verify the introduced pattern and its effect on the structural performance of the bridge.
- To verify the introduced concept of double inclination of hangers (spoked configuration of hangers), and the influence on the bridge stability, as possible alternative for a wind-truss.

1.3 Research strategy

To achieve the objectives of this thesis, the following strategy was developed.

The identification process of the laboratory model of the scaled bridge allowed the creation of the numerical model in Abaqus environment.

Next, the numerical model was validated with respect to the laboratory one, using results from modal hammer method analyses.

The further work was focused on the creation of a software tool for the auto-generation of various hanger patterns in 2D, where the geometrical parameters were defined by a user. Next, the tool was extended with the generation of a full 3D model of a bridge. A few predefined load cases were also included.

The further development of the software tool featured automatic creation and execution of vast sets of simulations, data collection of selected results and initial data mining. The completed tool was used for a wide-range parametric study of network patterns.

The analysis of the results led to a proposal of modification of the radial network pattern. The introduced pattern modification was tested and analysed with the same tool.

Finally, the developed software was used to study the spoked configuration of hangers on 3D numerical models of the bridge.

1.4 Research limitations

The main research focus was on long span timber network arch bridges, with light timber deck on transverse crossbeams. To further limit the scope of this thesis, the following limitations were made:

- The 2D numerical analyses were limited to network arches with certain constant geometry parameters like the bridge length, number of crossbeams and the arch shape. These geometrical limitations were chosen to allow for detailed study of the introduced radial pattern modifications (Paper II and Paper III) and for direct comparison with other pattern types (Paper I).

- The static analysis of the 2D numerical models in Paper I and Paper II was limited to eleven load cases, among which nine consist of unsymmetrical load. The chosen load cases do not cover all load situations usually applied during design process of a bridge, however they cover load cases, which expose network arch to adverse force distribution in the structure.

- In general, to minimise the computational time of the wide-range parametric studies, both in 2D and 3D, ranges of parameters were limited. The choice of parameters was based on preliminary studies and realistic dimensions of existing bridges.

- The design of the studied 3D bridges was limited to a structure where hangers in spoked configuration (lack of wind-truss) were attached to the crossbeams (lack of tie). Moreover, both the deck and the arch were pinned to the abutments. Other boundary conditions were not in the scope of the thesis.

- The type of the numerical analysis was limited to static analyses.

- The stiffness properties of an arch in all numerical models are constant along the element, regardless the bridge length. This limitation was applied to study in detail the influence of network patterns on the structural performance of the bridge, even though in reality the arch will not be a one-massive timber element, but few connected elements.

1.5 Outline of the thesis

This PhD thesis consists of three parts.

PART I consists of six Chapters. Chapters 1-3 are an introduction to the research topic. Moreover Chapter 3 contains the description of the modification of the radial pattern introduced in this thesis as well as the spoked configuration of hangers. The literature review is presented in Chapter 4. The laboratory model and experiments are illustrated in Chapter 5. In addition, in the chapter, the developed software is introduced. The final Chapter 6 comprises conclusions and further research.

PART II gathers four scientific papers which constitute the main part of this thesis.

In **Paper I** the comparison of three existing network patterns was made. The patterns were adopted for bridges with crossbeams and equally distributed hangers along the deck. Two arch shapes were tested and compared.

Paper II is about the influence of radial pattern modifications on the structural performance of the bridge. It focuses on moments distribution in the arches and number of relaxed hangers under static, line load conditions.

Paper III is about the influence of radial pattern modifications on the structural performance of the bridge. It focuses on stresses in hangers. Moreover, moments distribution in the arches and number of relaxed hangers are also analysed. The effects were studied under the approximation of moving load.

Paper IV contains a study about the influence of the spoked configuration of hangers on the stability of network arch timber bridges. The spoked configuration is introduced as an alternative to the wind truss.

PART III consists of one, additional paper written as a result of a secondary literature study.

Paper V is about the comparison of serviceability limit state requirements for timber footbridges in Australia, Canada, Europe and United States of America.

2 Structural systems of timber bridges

A timber bridge consists of a timber superstructure and auxiliary elements. The superstructure consists usually of a slab, set of beams, trusses or arches, depending on the chosen structural system, combined with the deck. Sometimes, for long pedestrian bridges, cable stayed or suspension bridges are used. The railings, claddings, protective layers, etc. constitute secondary elements of the bridge.

2.1 Beam bridges

One of the simplest timber bridge designs is a beam-type structure. The superstructure consists of a few longitudinally located beams, often stiffened in the transverse direction with additional timber beams or steel cables located between main beams. Pre-cambered and bowed forms of the beam are common for glulaminated constructions. The top of the beams is covered with the deck, which can be made as a concrete plate or out of wooden planks. The drawback of concrete-timber composite systems is a shear force formed as a result of the difference in creep and temperature behaviour of the two materials [2].

Although beam-type bridges are simple in design, which can lead to effective and economical solutions, their span is quite limited [3]. The common designs spread up to 30 m. The static system can vary from single support beam, through multiple spans or cantilevers [3]. An example of multi-span beam footbridge in Helsinki, Finland is presented in Fig. 2.1.

Fig. 2.1 Beam footbridge in Helsinki, Finland. Photo: A.W. Ostrycharczyk.

2.2 Slab bridges

As opposed to beam bridges, slab bridges consist usually of a single laminated deck only. The most common form is a nail-laminated or a stress-laminated deck. Both types can be made of solid or glulam timber. The span of the slab bridge can be significantly longer than for the beam bridge, however the bridge is much more technologically demanding. For shorter spans, the whole deck can be preassembled in the factory, while

for longer spans it has to be constructed on site. The slab bridge design can be made as a single- or multiple-span bridge [2]. In Fig. 2.2, multi-span slab footbridge is presented.

Fig. 2.2 Dalen slab footbridge in Trondheim, Norway. Photo: A.W. Ostrycharczyk.

2.3 Truss bridges

For medium and long bridge spans, more advanced structures are required. For instance, by using a truss as one of the superstructure elements, combined with stress-laminated deck, high load-carrying capacity can be achieved. The location of a truss can be either beneath or above the deck, see Fig. 2.3 and Fig. 2.4, respectively. It depends on the available free space below the deck, durability considerations or aesthetics [2]. Although long span can be easily achieved with the truss structure, it usually requires a two-stage assembling process. The truss parts of a size which can be transported are preassembled in the factory, while the final construction is connected on site. The typical span of a truss bridge spreads between 10 and 40 m [4]. However, an unique example of a long truss bridge is the Flisa bridge. It is a multi-span construction of a total length of 181.5 m with the middle span being 71 m long [5], see Fig. 2.4.

Fig. 2.3 Kjøllsæter bridge in Åmot, Norway. Photo: M. Čepelka.

Fig. 2.4 Flisa bridge, Norway. Photo: M. Čepelka.

Long-span designs are made possible by very effective connection types, e.g. slotted-in steel plates combined with screws, bolts or dowels.

2.4 Arch bridges

Another alternative for a long-span construction is the use of an arch. Arche bridges can be systemised by different criteria like shape of the arch or structural articulation [6]. The arch usually is either circular or parabolic, while structural articulation can be further divided into location of the deck or boundary conditions.

In general, there are three types of arch bridges which differ in the location of the deck with respect to the arch. Therefore, the deck can be built above the arch, underneath (called through arch bridge [2]), or somewhere between (called half-through arch bridge [2]); see Fig. 2.5. For bridges with deck located above the arch, the load forces are transferred by compressed posts to the arch, while in the two other cases, by hanger-type tensile elements. In all cases, forces from loading on the structure are transferred by the superstructure, i.e. the arch, to the abutments.

Fig. 2.5 Different types of arch bridges varied by location of the deck.

The choice of the boundary conditions is an important aspect for arch bridges. Depending on the chosen static system, a different mechanical behaviour is expected and, in consequence, a different type of bridge is considered. The most common are the two- or three-hinge arches with or without a tie, see Fig. 2.6. The purpose of the tie is

to withstand horizontal thrust forces, as the whole structure works as a simply supported beam.

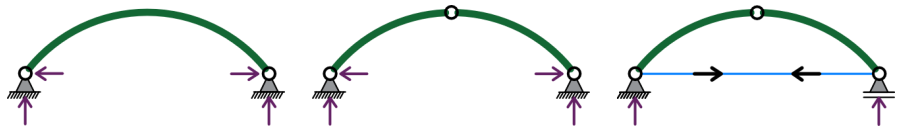

Fig. 2.6 Typical static systems for arch constructions.

Typically, arch timber bridges span between 20-70 m [4]. For such lengths, similarly to truss bridges, transportation and assembly challenges should be taken into account while designing an arch bridge.

An interesting arch bridge example, where the truss and the arch were combined together, is the Tynset bridge presented in Fig. 2.7. It is a three-span, 124 m long bridge, with the longest span of 70 m.

Fig. 2.7 Tynset bridge, Norway. Photo: K. Bell.

In all bridge types, the superstructure should be covered with water-resistant materials, and cladding should be applied on the side of the main structural elements. In addition, proper ventilation should be provided. Paying attention to details allows for designing and constructing durable timber bridges.

3 Network arch bridges

3.1 Tied arch bridges

The arch bridge with hangers is often called *tied arch bridge* or *bowstring arch* [2, 6]. In such a construction, the whole deck or the tie, in form of an edge beam, takes over the horizontal forces, thus the abutments take none or just a small portion of them. The whole structure is often indeterminate internally, but determinate externally, therefore it can be treated just like a simply supported beam.

Among tied arch bridges two important types can be distinguished: the so-called *Langer bridge* and *Lohse bridge*. In the Langer bridge, it is assumed that the arch can carry only compressive forces and the girder carries moments, shear and tensile forces. Therefore, the arch has a strengthening function only [7]. Moreover, the Langer bridge with diagonals, is called *trussed Langer* [7]. An example of the Langer arch bridge is presented in Fig. 3.1.

The arch in the Lhose bridge, on the other hand, can carry all sectional forces and moments, thus it has a function as important as the deck. Therefore, the stiffness ratio between the arch and the deck is decisive for the moment distribution in the structure. Defining such ratio is a designer's choice [7].

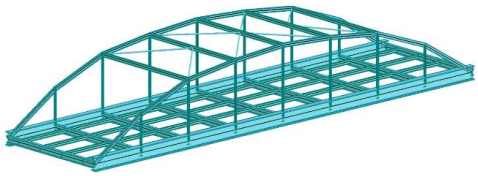

Fig. 3.1 Langer arch bridge.

Fig. 3.2 Fretheim Bridge. Photo: Norwegian Public Roads Administration.

In the aforementioned bridge types, the connection between the upper and the lower chord is usually moment resistant which makes the whole structure quite stiff in the arch plane. A different situation takes place when the arch ends are connected with a tie in form of a steel rod or a cable with very low bending stiffness. Then, the connections between the arch and the tie, as well as at the arch supports, are usually in-plane moment free, thus the biggest bending moment appears in the arch, not at the support. An example of an arch bridge with cable tie is the 38 m long Fretheim Bridge, located in Aurland, Norway [2]; see Fig. 3.2.

3.2 Network arch and Per Tveit

The arch bridge with vertical hangers is a classical arch bridge design. In a bridge with vertical hangers, forces from dead and live load are acting on the deck in the vertical direction, and therefore they are directly transferred to the arch, causing mainly bending moments and minor compressive and shear forces, depending on the angle between the arch tangent and the hanger.

By inclining the hangers, the internal forces in the arch can be distributed more evenly along the entire structure. The horizontal components of the hanger forces in adjacent hangers on the arch act in the opposite directions, see Fig. 3.3.

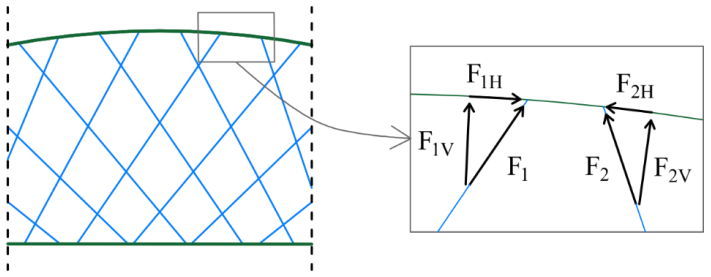

Fig. 3.3 Force components in inclined hangers.

The idea of a positive influence from the inclined elements in a structure was already noticed in the fifteen century by Leonardo Da Vinci, who drew in his manuscript a truss bridge with a curved upper chord [2]. Therefore, truss structures were, in fact, predecessors of arches with hangers. However, truss structures differ from arches with hangers, because truss struts can carry compressive forces, while hangers, regardless of vertical or inclined orientation, carry only tensile forces.

The historical development of truss structures allowed the introduction of the arch bridge with inclined hangers, given by Octavius F. Nielsen in 1925 [2]. Due to limitations around analytical calculations, inclined rods did not cross each other at all.

Around 1955, Per Tveit started to work on arches with inclined hangers which were crossing each other, and called them *network arches*. His publication from 1966 defines network arches as “bowstring arch bridges with inclined hangers which have multiple intersections” [8]. After that, both Per Tveit and other researchers were working on the development of this promising and effective structure.

It is worth to notice that network arch bridges are often mistakenly called *Nielsen-Lohse girder* in Japan, or *X-style arch bridges* in China [2].

3.3 Hanger patterns

The general topology of hanger patterns for arch bridges is shown in Fig. 3.4, where arch with vertical hangers, fan arrangement (two cases, after [9] and [2]), Nielsen-type and network pattern are presented together.

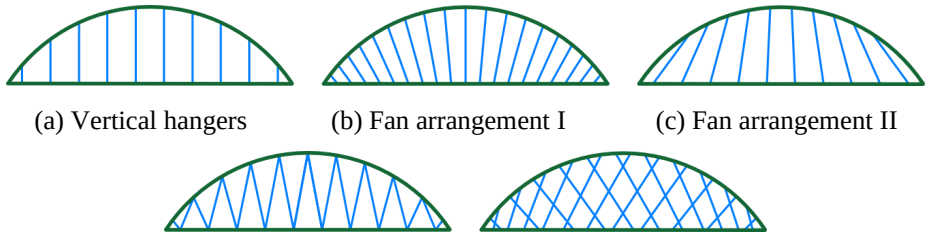

(a) Vertical hangers (b) Fan arrangement I (c) Fan arrangement II

(d) Nielsen pattern (e) Network pattern

Fig. 3.4 Hanger patterns in arch bridges.

3.4 Network hanger patterns

Network arch bridges are considered as light and economical structures which can be very slender. Inclination of hangers influence positively on the moments distribution, especially for uneven loading on the deck; the positive gain, as compared to vertical arrangement of hangers, can be seen in Fig. 3.5. In addition, overall stiffness of network arch bridge is higher than in a corresponding classical bridge with vertical hangers, what yields smaller deformations; confer Fig. 3.6. Moreover, network bridges are considered visually appealing, and as such can fit both in urban and rural areas.

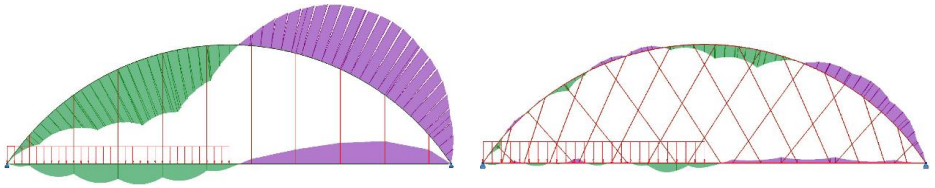

(a) (b)

Fig. 3.5 Example of scaled moments distribution in arch bridge under unsymmetrical loading;
a) bridge with vertical hangers – maximal bending moment in the arch of 983 kNm;
b) network bridge – maximal bending moment in the arch of 212 kNm.

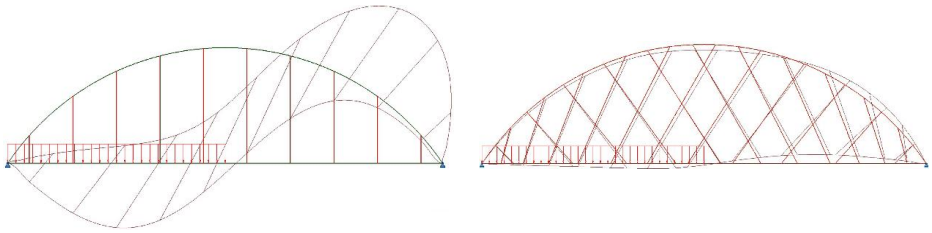

(a) (b)

Fig. 3.6 Example of scaled deflections in arch bridge under unsymmetrical loading;
a) bridge with vertical hangers – maximal deflection of 0.97 m ;
b) network bridge – maximal deflection of 0.11 m .

Among network patterns, Fig. 3.4e, there are known different pattern outlines, generated in a particular, systematic way. In all of them, terms like (*hanger*) *net*, *outline*, *pattern*, *layout* or (*hanger*) *distribution* can be freely replaced with each other. In the literature they are used in the same way, to describe hangers placement in an arch bridge.

In order to describe the network pattern geometry, the following variables shall be considered:

- number of hanger sets in the arch,
- number of hangers in one set,
- distance between hangers in one set,
- hanger inclination, i.e. relation (angle) with the deck, arch or arch radius [10].

A set of hangers is a group of hangers which are inclined towards the same direction, Fig. 3.7a. A second set is usually symmetrical to the first one, with respect to the centreline of the bridge. In practice, the number of hanger sets in a bridge is, most often, equal to two. However, according to [8], three or more hanger sets might be worth considering for temporary bridges with light and flexible decks; see Fig. 3.7b-c. It could also be favourable in bridges that should withstand big concentrated forces on the deck. In this case more than two hangers transfer the load to more than two points on the arch [10]. However, assuming that the arch behaves like a beam on elastic support, the introduction of an additional set of hangers changes the stiffness of such support. The same effect can be gained by increasing the number of hangers or their diameter [10].

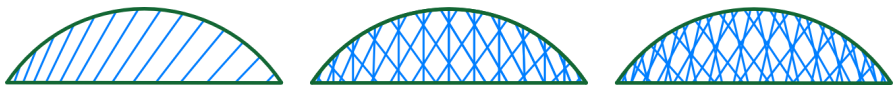

(a) One set of hangers (b) Three sets of hangers (c) Four sets of hangers

Fig. 3.7 Patterns with different number of sets of hangers.

The number of hangers in one set depends primarily on the bridge length and its use, i.e. type of traffic. The longer the bridge and the heavier the traffic, the more hangers are recommended. Moreover, the number of hangers depends on the type of bridge static system and on the boundary conditions, as well as the bridge design. The distances between hangers in one set as well as their inclination vary depending on the pattern type.

A well-designed network pattern is characterised i.a. by small bending moments in the arch and the deck, comparable maximum stresses in the hangers, small stress ranges in the hangers, lack of relaxed hangers and favourable position of the hanger connections with regard to other structural elements [10].

Selected examples of hanger pattern types are described in the following sections.

3.4.1 Rhombic pattern

In the rhombic hanger net, all hangers in one set have the same inclination, i.e. the angle between the hangers and the deck is constant. Such a pattern was proposed by Per Tveit, based on Nielsen pattern [10]. Usually, in rhombic patterns, pairs of hangers inclined in opposite directions are sharing a fastening point on the deck level. The pairs of hangers are often evenly distributed along the deck and therefore the distribution of the hangers along the arch is irregular, see Fig. 3.8a.

3.4.2 Pattern with constant inclination of hangers

As the name suggest, the inclination of the hangers is constant among hanger sets. Therefore, the same rule as for the rhombic pattern is also applied here. The difference between patterns is solely in the distribution of hangers. In the rhombic pattern, they are usually evenly spaced along the deck, while in the pattern with constant inclination of hangers, they are usually evenly distributed along the arch [11], see Fig. 3.8b.

Nowadays both names, the pattern with constant inclination of hangers and the rhombic pattern, are used interchangeably. Moreover, the latter is becoming obsolete.

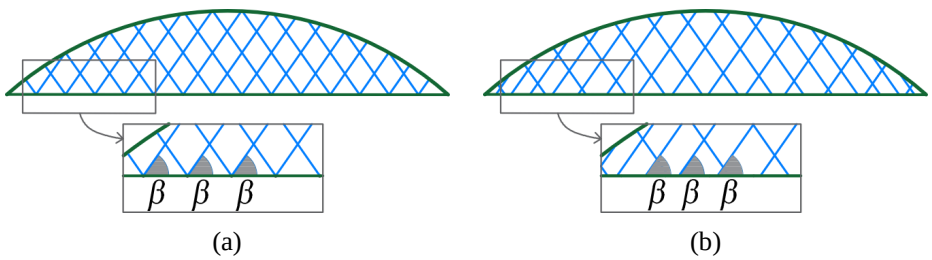

Fig. 3.8 Rhombic pattern / Pattern with constant inclination of hangers; a) equal distribution of hangers on the deck; b) equal distribution of hangers on the arch.

3.4.3 Pattern with constant change of hangers inclination

This pattern is also called *constant-change-of-slope* [9]. In here, hangers in one set are changing their inclination incrementally, with a constant value of change. Therefore, the pattern can be described by two main parameters: the starting angle γ and the constant angle change $\Delta\gamma$. Depending on the desired geometrical effect the angle change can be both positive and negative [11]; see Fig. 3.9a and Fig. 3.9b respectively.

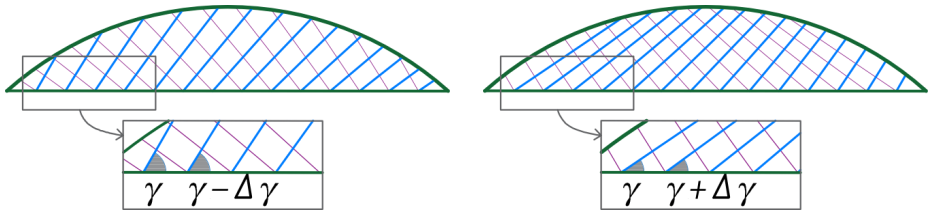

Fig. 3.9 Pattern with constant change of hangers inclination; a) negative angle change; b) positive angle change.

3.4.4 Elliptical pattern

This pattern is characterised by the spacing of the fastening points of the hangers on the lower chord. Those connections are spaced unevenly, although according to a certain scheme. The distance between consecutive points in a single hanger set is calculated using the geometry of an ellipse, see Fig. 3.10.

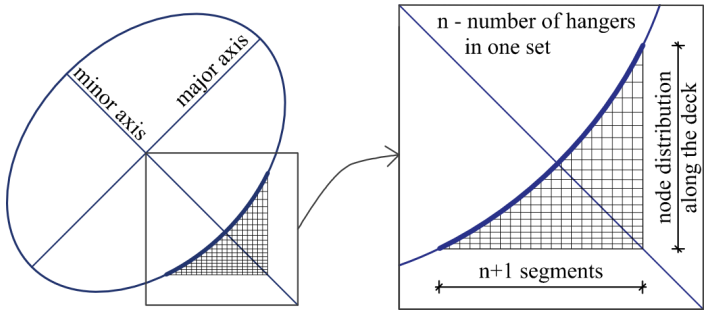

Fig. 3.10 Principle of elliptical pattern.

This method leads to a semi-even distribution of few fastening points located in the middle of the lower chord. Moreover, the remaining fastening points are located quite close to each other at the beginning of the set and are widely spread at the end of the set, see Fig. 3.11, [12].

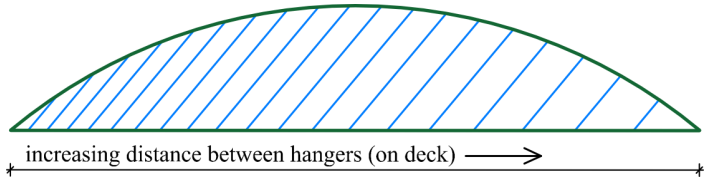

Fig. 3.11 Node distribution along the deck in elliptical pattern; one set of hangers.

Each ellipse can be defined by two parameters, i.e. the minor and the major axes. The choice of axes length influences the geometry of the pattern. For instance, if the length of the minor axis is zero, the ellipse degenerates into a line coinciding with the major axis. In result, all distances between fastening points are equal.

The hanger distribution obtained for a single set is usually combined with another, symmetrical set of hangers, thus there are two sets of hangers in the pattern. In effect, the hangers distribution in the middle of the bridge is semi-even while on the edges it is a combination of close and wide spread of hangers, [12].

The described method for the spacing of the fastening points on the lower chord was originally used with equal distribution of hangers on the arch. However, the method can be easily combined with other hanger outline systems. Moreover, the similar idea of evenly distributed points on the lower chord can be found in [13].

3.4.5 Radial pattern

In the radial pattern type, the angle between arch radius and the hangers is constant. This pattern was developed by Schanack and Brunn [12] after parametric studies performed on a 100 m long bridge designed for train traffic. The outline of the radial pattern, where hangers are equally distributed along the deck, is presented in Fig. 3.12a, while Fig. 3.12b presents a pattern with hangers equally distributed along the arch.

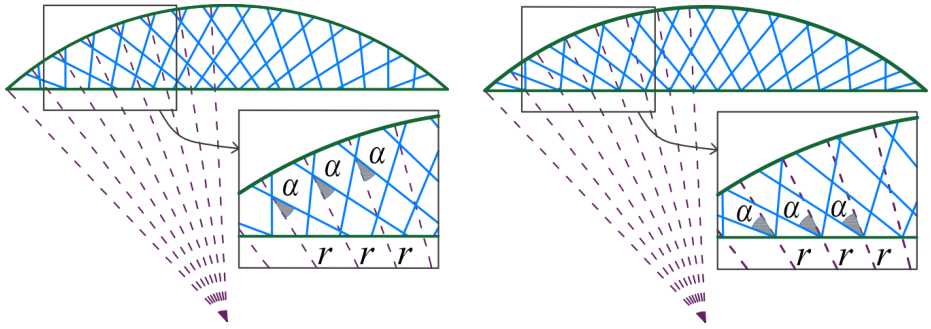

(a) (b)

Fig. 3.12 Radial network pattern; a) equal distribution of hangers on the deck; b) equal distribution of hangers on the arch.

3.5 Modified radial pattern

In this thesis modifications of the radial pattern were introduced. Although the modifications are general in nature, in this thesis they are tailored for bridges with transverse crossbeams evenly distributed along the deck.

In a classical radial pattern the angle between a hanger and the arch radius is kept constant. In the radial pattern with modifications the constant angle spreads between a *radial ray* (instead of the arch radius) and the hanger. The radial ray is created by a straight line from a *focal point* (different from the centre of the arch) through a crossbeam towards the arch. The focal point is the centre for radial rays. The focal point lies in the plane of the arch and can be shifted in the horizontal, the vertical or both directions relative to the centre of the arch. Such modifications are called: X-, Y-, and XY-configuration, respectively.

For shifts in the horizontal direction, two or three focal points need to be created, depending on the number of the crossbeams, see Fig. 3.13. The angle α, denoted in the Fig. 3.14, is called the *spread angle*.

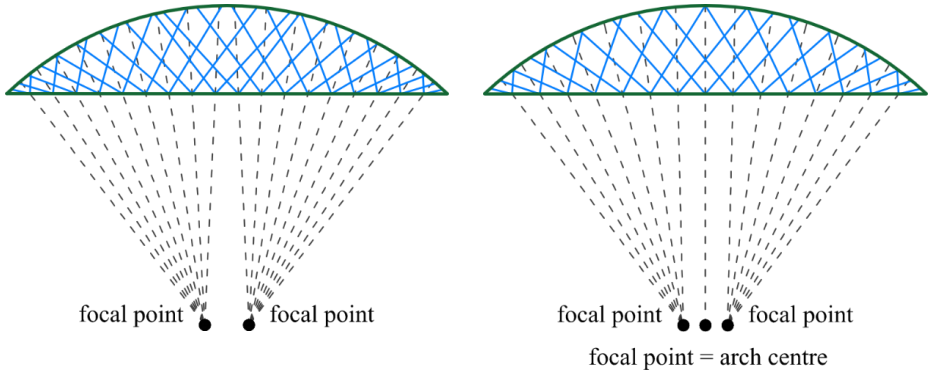

Fig. 3.13 Modified radial pattern; a) even number of crossbeams; b) odd number of crossbeams; X-configuration.

Vertical shifts can go both in the positive or the negative direction. Positive shifts should be performed with caution, avoiding a situation where the focal point is located above the deck.

An example of pattern modification is presented in Fig. 3.14.

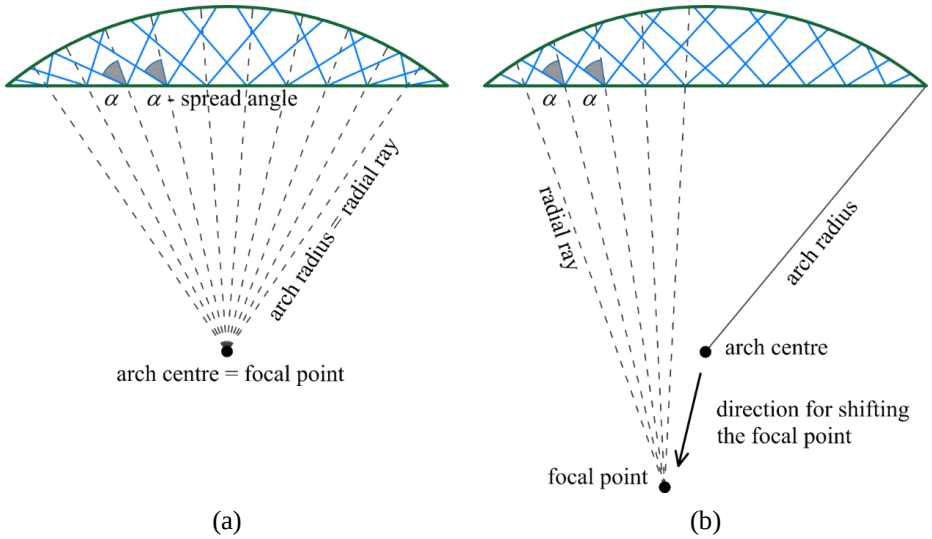

Fig. 3.14 Radial pattern; a) classical; b) modified, with XY-configuration.

Certain combinations of geometric parameters of a bridge, especially those with big spread angles, may result in some hangers located almost horizontally or even not intersecting with the arch, see Fig. 3.15. Thanks to the introduced modifications, such a problem can be limited for patterns with the same big spread angle.

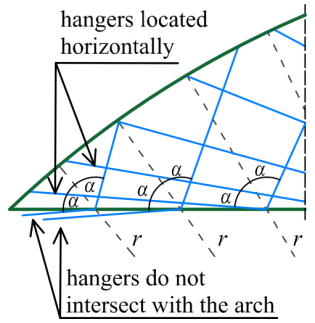

Fig. 3.15 Radial pattern with excluded hangers.

In addition, the introduced modifications allow for precise control over hanger spacing along the arch. The hanger distribution in the upper chord influences bending moments, leading to extremes in degenerated cases, for example two hangers sharing an attachment point on the arch.

3.6 Spoked configuration of hangers

In this thesis, an additional feature of the network pattern, called *spoked* or *spoked wheel configuration* of hangers, was introduced. In the spoked configuration, there are double sets of inclined hangers. The two hangers in the set have coinciding fastening points on the arch, although they are spaced in the transverse direction along the transverse crossbeams. It means that hangers are simultaneously inclined in- and out-of-arch-plane, see Fig. 3.16.

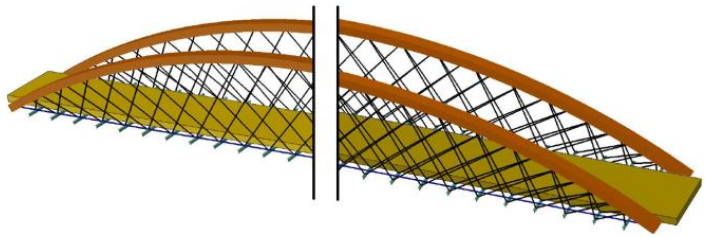

Fig. 3.16 Network arch bridge: classic (on the left) and with spoked configuration of hangers (on the right).

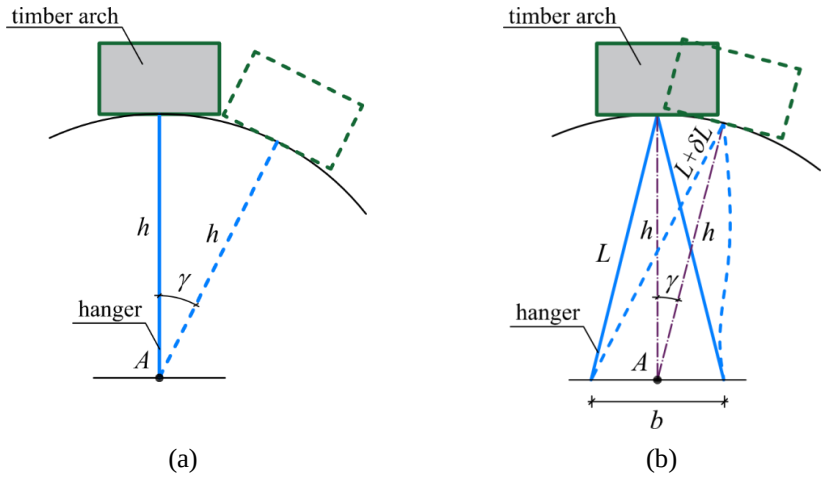

Fig. 3.17 Deflection of network arch; a) hangers in one arch plane; b) hangers in spoked configuration.

A simple model of the possible effects on the stability from the spoked configuration of hangers is presented in Fig. 3.17. The arch deflection for bridges with hangers located only in the arch plane is presented in Fig. 3.17a, where the transversal displacement of the arch is mainly a rotation around the point *A*, located on the lone between arch ends.

In the bridge with spoked configuration of hangers, Fig. 3.17b, the rotation around point *A* results in an elongation of one of the hangers, which in consequence creates a force resisting the lateral displacement. Such transversal component of the hanger force influences positively the stabilization of the arches and can limit the need for wind trusses.

3.7 Example of a network bridge

Network arch bridges are common structures all over the world. They are built with different spans and purposes, for instance as car bridges, train bridges or footbridges. However, in most cases the material used in bridge design is steel or concrete.

In this thesis, one especially interesting example of network bridge with timber truss-arches is presented. Steien bridge was built in Norway in 2016, see Fig. 3.18 and Fig. 3.19. The bridge is located over river Glåma in Alvdal and is the longest network timber arch bridge with a span of 88.2 m. The arch rise is equal to 15 m, while the deck is 19.8 m wide and consists of two traffic lanes and pedestrian and cycle paths on each side of the traffic road. The steel hanger network, made of solid steel bars, is based on the radial pattern with hangers equally distributed along the arch. The arches are made of glulam and the deck is made of light concrete. In addition, the arches are tilted toward each other with an angle of $7°$. The solution with inclined arches is rather popular and can vary from an inclination of a small angle, like in the presented case, to solutions where arches meet in the middle part of the bridge. An extreme example is the Troja Bridge, located in Prague, Czech Republic [14], see Fig. 3.20.

Fig. 3.18 Steien bridge, Norway – view of the network. Photo: Norwegian Public Roads Administration.

Fig. 3.19 Steien bridge, Norway – view of inclined arches. Photo: Norwegian Public Roads Administration.

Fig. 3.20 Troja Bridge, Prague, Czech Republic. Photo: M. Čepelka.

4 Literature review

4.1 Structural performance

The idea of network arch bridges was introduced by Per Tveit. He started to work on the topic in the early stage of his engineering and scientific career. The matured idea was described in one of his papers in mid-sixties entitled *The design of network arches* [8].

In the paper [8], Tveit studied different aspects of network arch bridges. One of them was the structural performance of two bridges taken as examples. Force distribution in hangers, arches and lower chords were analysed based on the influence lines. In addition, two equations for axial force in the arch and in the lower chord were presented. The influence of the cross-section of the arch and the deck dimensions on bending in the chords was also highlighted. Moreover, additional topics covered in the article were arch buckling, effect of hangers breaking, effect of arches with more than two sets of hangers and resistance of hangers against relaxation. The latter was analysed for bridges with different arch rise-to-length ratio, which led to the suggestion of sufficient hangers slope, to avoid their relaxation. The main part of the study was based on patterns with constant change of hangers inclination.

In [15], Tveit studied the design of network arches in more detail. He described four sources of bending moments in the arches: bending due to concentrated load, relaxation of hangers, distance between nodal points and secondary bending. Moreover, he analysed optimal arrangements of network patterns in terms of number of hangers and location of hangers attachment points on the arch or the lower chord. In addition, few remarks on the arch buckling were provided. Another topic covered in the article was the choice of the material. It was suggested to use pre-stressed concrete decks and arches and hangers made of steel, for the network arch bridge design.

The advantages of network bridges were presented in [16]. It was shown that bridge with network arch can be up to 4.5 times lighter than an alternative design with vertical hangers.

The subject of network arch bridges was further studied by Tveit in [17-19]. Moreover, a multitude of materials on the topic can be found on Tveit's webpage [20].

After Tveit, the study was continued by various researchers, i.a. his two master students, Brunn and Schanack. In [12], they described and examined the newly introduced radial network pattern. The study was performed with the premise of the railway bridge.

Next, Schanack and Brunn in [21] gathered fundamental information for designers, highlighting features of well-designed network patterns. In their suggestions, number of hanger sets and hangers in one set, as well as choice of pattern type, were discussed.

In addition, the paper contains notes on manual hangers adjustment and optimal hanger angle. It was showed that for the considered patter outlines (rhombic, radial, constant hanger inclination change) the angle between the hanger and the deck should be around $55°$ in the middle part of the deck.

Another work of Schanack and Brunn presented in [22] was a comparative study of conventional tied arch bridges and network arch bridges with radial patter outlines. The paper highlights that, by use of the network pattern, the bending moments can be heavily reduced in the structure (about ten times) in comparison to the bridge with vertical hangers.

In [23], the work of Brunn et al. was extended with i.a. analyses of different deck types (concrete, steel, composite), arch features (rise, cross-section), hangers connections and radial patter optimization. It was suggested to use angles from the range $45-60°$ for an optimal hanger outline.

The next researcher who studied the subject was Teich. In [24], he compared two bridges: with vertical hangers and with network pattern, showing advantages of the latter solution. In addition, in the paper the number of hangers was studied for different bridge lengths, and some suggestions were given for bridges of 100-200 m. Moreover, design guidelines for the arches, the decks and the network were given. Furthermore, the influence of the hanger inclination and of the live-load to dead-load ratio on the number of relaxed hangers was presented for railway bridges. Finally, the comparison, in terms of weight of used material, of different existing tied arch railway bridges was included in the paper.

The detailed comparison of network patterns can be found in [11]. Here, Teich focuses on patterns with constant inclination of hangers, positive and negative constant change of hangers inclination, radial pattern and elliptical pattern. Four comparative criteria were chosen: stress amplitudes in hangers, hangers relaxation, variation of maximum hanger force and maximum hanger force. The study showed that the radial pattern and the pattern with constant change of inclination seem to be the best. In the paper, some additional information was given, for instance the recommended number of hangers depending on the bridge span, or the recommended slope.

In [25], Teich presented the study on hanger connectors in terms of fatigue. The focus was on the geometry of the hanger connector and topology optimization based on the stress distribution in the steel plate.

The effect of the fatigue on hangers arrangement was also studied in [9]. In here Pellegrino et al. considered stress distribution in hangers in various patterns like fan, radial, pattern with constant change of hangers inclination or with vertical hangers,

under vehicular load. Different comparative criteria were used: maximum or average axial force in hangers, variation of axial force in the hanger, maximum or average axial force variation in the hanger. The paper highlights that an improvement of structural performance of the network can be gained by a slight modification of the hanger arrangement, namely using steeper hangers, near to the ends of the arch.

Additional research conducted by De Zotti and Pellegrino et al. was published in [26]. Here, the authors compared axial forces in arches and hangers as well as bending moments in arches for bridges with various hanger patterns, arch rises and bridge lengths.

The force variation in the hangers was studied by De Backer et al. in [27]. The reference bridge was 200 m long with concrete deck and steel arches. The material model of the hangers was nonlinear and as such did not withstand compressive forces. The main interest of the paper was on hangers relaxation depending on their location in the bridge, the load case and the bridge length. It was concluded that pre-tensioning of hangers caused by the dead load solves the problem of hangers relaxation.

Pipinato in [28] considered steel arches and composite steel concrete decks in the design of a multi-span network bridge. In the paper, studies on materials, stresses in hangers and their connections are performed on different network patterns. The focus was on fatigue analysis pattern optimization.

4.2 Stability

One of the important topics discussed in the literature related to network bridges is the buckling of the arches. Schanack in [29] analysed in-plane buckling of network arches with various number of hangers, under different load cases. He considered the network arch as a curved compression strut on an elastic support. Based on this model, he derived a simple analytical formula for evaluating the critical buckling load and buckling mode for in plane buckling of the network arch, with an error of less than 5%.

Pircher et al. in [30] extended Schanack's work [29] and studied the influence of load patterns on the so-called *local buckling modes* in-plane of the arch. It was noticed that such local modes can occur at significantly lower traffic loading levels than for global loading patterns which are usually used in stability analyses of arch bridges. Therefore, it is highly important to use suitable load cases for stability verification. In addition, it was shown that initial imperfections have a negative influence on the stability under the described load conditions.

The stability of timber network bridges was discussed by Bell and Karlsrud in [31], where a network arch was proposed as an alternative design for Tynset bridge (timber truss-arch bridge with vertical hangers). Buckling analyses were performed i.a. for

various out-of-plane stiffness values of the arch connections to the abutments. It was shown that the sideway stability of the arches demands high stiffness in the out-of-plane.

Wollebæk and Bell in [32] focused on the lateral torsional buckling problem for timber arches. In the paper two case studies were considered. In the first one, an out-of-plane bracing and the arch geometry were studied for a numerical model of a timber arch. The arch was modelled as an orthotropic curved plate or as series of straight 3D beams. The second case study was a numerical model of an arch network timber bridge, where each arch was made of four sub-arches mechanically joined together along their length. The linearized buckling analysis for two load cases was performed for the described bridge model. The results were compared to those obtained for a similar network bridge built with massive arches instead of sub-arches.

The study presented in [33], by the same authors, relates to the previous paper . In here, the focus was on stiffness of connection at which the four sub-arches were joined together. In the study, several values of rotational stiffness were introduced to the numerical model and buckling factors were compared.

4.3 Optimization

In the structural design an optimization procedure is highly important. The process tries to find either the best hanger arrangement or cross-section of bridge elements or material type, etc. As an effect, it leads to a better force distribution in the structure, thus it lowers the cost of the bridge. A popular approach for the optimization of hangers arrangement is a parametric study. This method was used in many papers cited in the previous sections. Moreover, there are also papers that specifically deal with the optimization of network arch bridges.

In [34], Bruno et al. proposed a dedicated, multi-step, design algorithm for network arch bridges. The method contains two optimization criteria: lowest material quantity and best strength performance level in all structural members of the bridge. The authors verified the effectiveness of the algorithm on various bridges of different lengths.

Islam et al. in [35, 36] approached a constrained optimization problem in order to minimize the cost of the superstructure in network arch bridges. Here, the optimized parameters were: hangers outline and their cross-sectional dimensions, geometric shape of the arch, arch cross-section and rise-to-span ratio. The constraints imposed in the optimization process were based on requirements from adequate design standards. This complex problem was solved by the authors with the use of an evolutionary algorithm [37, 38] interfaced with a finite element method analysis software for the evaluation of the structural response. It was concluded that the use of the algorithm can save up to

40% of the total cost of the structure. Moreover, a parabolic arch with optimally designed variables is more economic than a circular one.

4.4 Construction and other highlights

Another topic which raises while studying network bridges is the erection of the structure. The subject was already discussed by Tveit, i.a. in [8, 15, 17, 18]. The author presented several methods of bridge erection like the use of floating cranes to move fully pre-assembled bridges or the bridge steel skeleton from the river bank into the final position. The bridge skeleton can be made with a light temporary lower chord, which can carry the deck while it is being casted. The temporary lower chord is erected by use of traditional timber scaffolding. When the bridge is completed, the scaffolding can be removed.

Another method is to move the steel bridge skeleton, pre-assembled on the river bank, by moving it on the ramps on floating pontoons from one abutment towards the other. As alternative, the bridge can be pre-assembled at the shipyard and floated to the construction site.

In special cases, for instance in cold climates, the ice of the river or lake can be used as an advantage. The ice can be reinforced by steel rebars and additional layer of ice, and used for erecting or moving the temporary structure.

In the erection process sequence of concrete casting is of high importance as correct pre-stress of hangers must be assured. The same applies to pre-stress of edge concrete slabs. The aforementioned methods were also described in more detail in [39] by Räck et al.

A supplementary literature on network arch bridges deals with designed and executed structures. An example of network bridge with concrete arch and concrete deck can be found in [40], while examples of network bridges with steel arches and concrete or composite decks can be found i.a. [41-43]

Moreover, detailed information about the first timber network arch bridge build in Norway can be found in [44, 45] and on the website of Norwegian Public Roads Administration [46]. In the aforementioned publications, the topic of bridge erection is also covered.

An interesting extension of network arch application can be found in [47, 48] where a bowstring arch was used to strengthen the existing bridge construction.

Finally, it is important to note that the literature on the subject is published in few different languages, mainly in German and Spanish, while only few publications are available in English. Therefore, the knowledge is not so widely spread.

5 Background for parametric analyses

This thesis is based on the results obtained from different types of parametric, numerical analyses of a network arch bridge model. To perform the analyses in efficient way, a tool for the automatic generation of the bridge model was prepared.

5.1 Physical and numerical bridge model

The first numerical model was created by hand and validated on the laboratory model of the very same physical bridge. This was the foundation for the further work with the auto-generated numerical models.

5.1.1 Physical model

The laboratory model was a scaled model of a 100 m timber network arch bridge with a tie. The features of the scaled model were:

- length of 10 m;
- arch rise of 1.4 m;
- circular arch shape;
- arch cross-section of 180 mm width and 120 mm height;
- timber pre-stressed laminated deck with height of 98 mm and width of 1000 mm;
- number of crossbeams: 24;
- crossbeams as T-beams with 40 mm height, 40 mm width and 5 mm thickness;
- hanger diameter: 6 mm;
- tie diameter: 16 mm.

The steel elements were made of standard structural steel while the arch and the deck were made of CE L40C glulaminated timber from MOELVEN [49].

In the physical model of the bridge, the radial pattern was chosen as hanger arrangement. The chosen spread angle α was $45°$, while the distance between hangers attachments on the crossbeam, in the transverse direction, was equal 174 mm. For the used 24 crossbeams, there were 48 hangers per arch. Fig. 5.1 presents the laboratory model of the bridge.

Fig. 5.1 Laboratory model of the tested bridge.

The arch was mounted with a pinned connection at the supports, thus it was moment free in the arch plane, see Fig. 5.2a-b. The deck was clamped at the ends thus neither translation nor torsional or transversal rotation was possible, Fig. 5.2a. The tie was attached to the arch mounting point, see Fig. 5.2b. The crossbeams were attached to the bottom of the deck by three pairs of screws, thus giving a stiff connection. The hangers were attached by moment free connections to the crossbeams, confer see Fig. 5.2c, while at the arch they were screwed into the wood giving a pseudo-stiff connection; Fig. 5.2d.

(a) (b)

(c) (d)

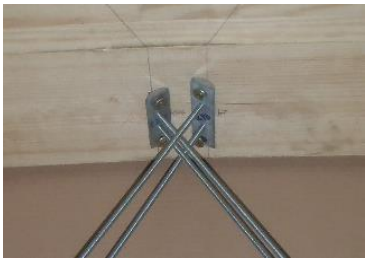

Fig. 5.2 Details of the laboratory model of the bridge; a) arch and deck support; b) connection of the tie; c) hangers attachment to the crossbeams; d) hangers attachment to the arch.

5.1.2 Laboratory tests

A modal analysis with a modal hammer is a technique used to obtain the natural frequencies and the corresponding mode shapes of a tested structure. By impacting the structure with a modal hammer, a wide frequency range is excited, and the motions of the structure are recorded with an accelerometer located on the structure [50]. The force-time history of the impact is also recorded. A basic test result is the frequency response function (FRF), which combines the input force and the movement of the structure caused by the impact. The evaluation of the FRF leads to the recognition of the natural frequencies and the corresponding mode shapes [50].

Two different types of modal hammer were used during the work in the laboratory: Heavy Duty 8208 and 8210 supplied by Brüel & Kjær [51], see Fig. 5.3. The former weighs 1.36 kg, while the latter 5.44 kg. Depending on the tested structure and the expected frequency bandwidth a different tip can be installed on the hammers.

(a) (b)

Fig. 5.3 Modal hammer; a) Heavy Duty Type 8208; b) Heavy Duty Type 8210.

For a bridge response, low frequency excitation at high input force level is usually required. To achieve that, a soft tip of the hammer was used during the tests.

The sensor for the measurements of a bridge response is an accelerometer which can be mounted on any place on the structure. The accelerometer registers the dynamic response of the structure along one direction only and, as such, its position has to be changed when a different element is excited either vertically or horizontally.

In this study, the measurements were performed in the transversal and the vertical direction on the arch and the deck. The accelerometer was positioned close to the support (‘on side’ position) and close to the middle of the bridge (‘centre’ position). The chosen accelerometer position allowed to pick up all the lower mode shapes, see Fig. 5.4.

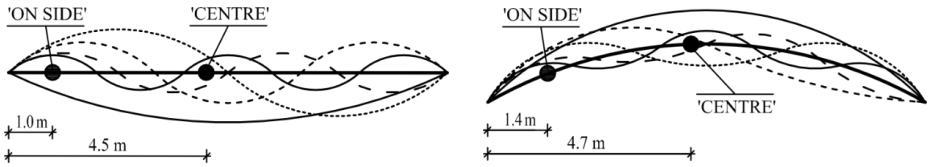

(a) (b)

Fig. 5.4 Mode shapes and position of the accelerometer; a) of the deck; b) on the arch.

The accelerometer and the modal hammer were connected to the computer through the NI Dynamic module, which acquires the data and applies an anti-aliasing filter, installed on a specific frame (NI Chassis) that transmits the data to the PC, and to a unit which supplies power and acts as a signal conditioner. The experimental setup is showed in the following picture; Fig. 5.5, [50].

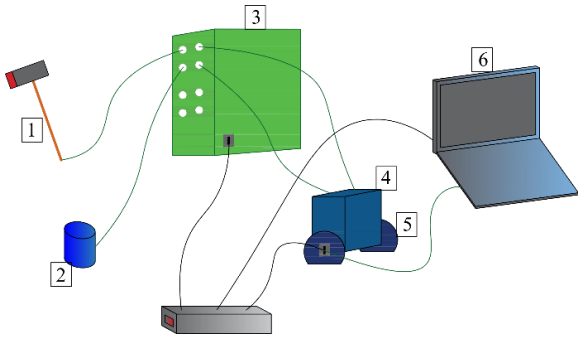

1. Modal hammer
2. Accelerometer
3. Power supply and signal conditioner
4. NI Dynamic module
5. NI Chassis
6. Computer with LabView software

Fig. 5.5 Experimental setup.

The commercial software LabView [52] was used to visualize the mode shapes and to compute the fundamental frequencies and the corresponding damping ratios based on the data recorded from experiments.

In Fig. 5.6, an example of a visualized frequency response function is shown, while Fig. 5.7 depicts an approximation of a mode shape of a deck, obtained from the tests.

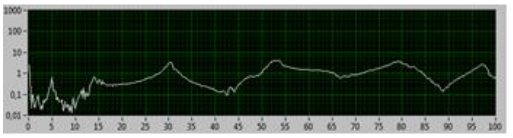

Fig. 5.6 Frequency response function.

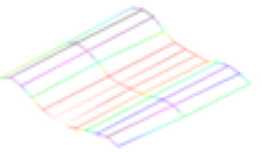

Fig. 5.7 Visualization of the third mode shape of a deck.

The tests on the deck were performed based on a grid with 36 points of excitation, while the tests on the arch assumed linear distribution of 20 points.

Simultaneously to the laboratory tests, a linear modal analysis was performed on a numerical model of the bridge structure under self-weight.

5.1.3 Numerical model of a laboratory bridge

The numerical model of the laboratory bridge was created manually in the Abaqus software.

The deck was modelled as a shell with element type S4R, made of glulam with properties of a transversally isotropic material. The engineering constants describing the glulam properties are presented in Tab. 1.

Tab. 1 Glulam material properties of the deck used in numerical simulations.

E1 [MPa]	E2 [MPa]	E3 [MPa]	v12 [-]	v13 [-]	v23 [-]	G12 [MPa]	G13 [MPa]	G23 [MPa]	Density [kg/m^3]
10308	165	165	0.5	0.6	0.6	660	660	58.2	549

The material properties differ from catalogue values, because they take into account the presence of the pre-stressing steel rods.

The clamping of the deck was modelled as boundary conditions. Just like in the physical model, neither translation nor torsional or transversal rotation was possible at the deck ends.

The 24 transverse crossbeams, modelled as Timoshenko beam elements B31, were attached to the bottom surface of the deck. In this case a node-to-surface connection was used. The bottom of the deck was chosen as a master surface connected to three points on the top of each transverse beam.

Two identical arches were modelled as beam element B31, with the transversally isotropic material properties presented in Tab. 2.

Tab. 2 Glulam material properties of the arch used in numerical simulations.

E1 [MPa]	E2 [MPa]	E3 [MPa]	v12 [-]	v13 [-]	v23 [-]	G12 [MPa]	G13 [MPa]	G23 [MPa]	Density [kg/m^3]
13000	410	410	0.5	0.6	0.6	760	760	76	498

The same boundary conditions were applied to each arch. All degrees of freedom, except rotation about normal to the arch plane, were constrained.

The arch and the crossbeams, which support the deck, were connected by the hangers. In the physical model, the connection between a hanger and the arch and between a hanger and the crossbeams were different, while in the numerical model they are simplified and both are modelled as fully constrained.

The truss element T3D2 was used to represent the hangers. Steel of density 7850 kN/m3, Young Modulus of 210 GPa and Poisson's Ratio of 0.3 was used as material for the hangers. In addition, the hangers can withstand only tensile forces, thus the 'no compression' feature was added in the material properties of hangers. As a result, for negative strains, in pseudo-compressed hangers, the stress value is zero.

The dimensions of all the elements in the numerical model are exactly the same as in the laboratory model.

In order to obtain the values of the natural frequencies and the compatible mode shapes, the modal analysis was performed on the numerical model of a bridge under self-weight.

5.1.4 Validation of numerical model

To validate the numerical model, the natural frequencies obtained for the laboratory model were compared to the corresponding values from the numerical analysis.

The selected results are gathered in Tab. 3. The table gives the natural frequencies for the transversal and the vertical mode shapes (separately) for the deck, and the transversal mode shapes for the arches. The vertical mode shapes of the arches were excluded from the presented results due to the low quality of the recorded frequency response function. Table 3 gathers the results for two positions of the accelerometer and additionally the values of the measured damping ratios.

Tab. 3 Natural frequencies (NF) and damping ratios (DR) of the bridge obtained in the laboratory and NF obtained by numerical tests.

		Tests on the laboratory model				Numerical
		Accelerometer on side		Accelerometer in centre		results
ELEMENT mode shape ↓	Mode number ↓	**NF [Hz]**	**DR [%]**	**NF [Hz]**	**DR [%]**	**NF [Hz]**
DECK transversal	1	16.98	2.13	17.02	2.53	24.90
	2	55.53	1.93	54.74	2.89	58.47
	3	107.43	1.01	107.52	1.34	96.46
DECK vertical	4	38.28	1.12	37.48	1.06	47.63
	5	52.00	0.94	53.14	1.19	61.52
	6	71.40	0.66	68.29	1.63	71.82
ARCH transversal	3	31.23	2.45	31.62	2.14	40.79
	4	53.36	1.97	54.32	2.37	65.01
	5	81.43	0.68	81.36	1.80	84.38

It can be concluded, that the numerical model can be treated as a sufficiently accurate representation of the physical bridge. As a result, further studies regarding timber network arch bridges were performed with numerical models.

5.2 Tool for automatic modelling

Detailed analyses of timber network arch bridges require the construction of many, vastly different, numerical models. Therefore, a tool, which automatically generates models with various geometric and structural features, was created.

The accuracy of the numerical simulations was the foundation for this research, and thus Abaqus software [53] was chosen as a computational and modelling engine. Since Abaqus is easily extendable with Python [54], it was a clear choice for building the framework, as well as it was suitable for integrating with software like MatLab [55] and MSExcel [56], which were used for convenient output data processing.

The tool was prepared for the needs of this research and was used for fundamental studies, detailed parametric studies as well as was a basis for few master theses.

The tool can automatically build a complex numerical model of a bridge based on user-defined parameters. The input parameters can be divided into few following groups:

- structural properties,
- geometric features,
- material properties,
- analysis type,
- model dimensionality (2D, 3D),
- loading,
- pattern type.

The most important structural properties defined by the user include deck and arch shapes, boundary conditions, number of transverse crossbeams, presence of tie and optional pedestrian paths. The deck can be modelled as a flat or as a convex plate, while the arch can have circular or parabolic shape. When a model with pedestrian paths is chosen, they are created outside the arches, see Fig. 5.8.

In addition, the user is able to control the whole geometry of the bridge model, which includes i.a. bridge length and width, arch rise, cross-section and thickness of each element.

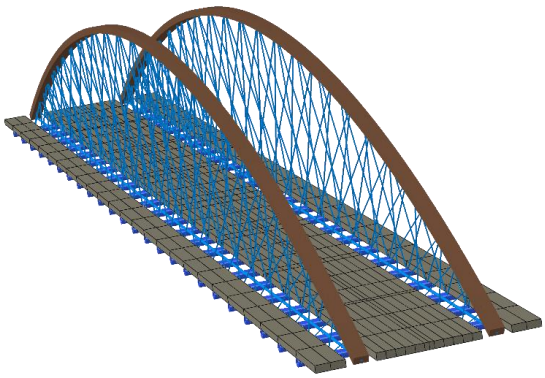

Fig. 5.8 Numerical model of the bridge with separate pavements for pedestrians.

The material properties can be also defined by the user, however in these parametric analyses, they were kept constant. Similar to the numerical model described in Section 5.1.3, a transversally isotropic timber material model was chosen for the arch and the deck, while the crossbeams were made of steel, and the tie and the hangers were made of steel with the 'no compression' feature.

The models can be built both in two and three dimensions. Full 3D models were used for comprehensive study, as well as for buckling and modal analyses, while 2D models were mostly used for in-plane pattern study. Moreover, the tool allows for building a single arch in 3D with a double inclination of the hangers (in- and out-of-plane), with or without series of springs as boundary conditions. This type of model was mainly used for fundamental studies.

Static, buckling and modal analysis types are available. The static analysis can be performed as linear or nonlinear. With the availability of those three analysis types, the basis for an initial and general evaluation of any user-defined network bridge is provided.

The auto-generated models can be subjected to different load scenarios. In the 3D model, different combinations of sub-regions of the deck can be loaded with predefined forces. The embedded loading is based on Load Model 1 (LM1) from Eurocode 1-2 [57] and consists of both an equally distributed load, representing a car traffic, and point loads, representing a single vehicles. The concept of notional lanes is also embedded in the tool. The width of one notional lane can be defined by the user, but by default is equal to 3 m. The lane numbering is defined according to LM1 and therefore the respective load values, which differ for each lane, are used.

In the 2D models, two load scenarios are provided. In the first one, the deck is divided into a selected number of segments. In different combinations, the requested segments are loaded with an equally distributed load. The second scenario consists of a single vehicle passing the bridge in a given time.

The values of the loads can be changed by the user, however in the 3D models, the default values are based on LM1, and the transient combination of loading based on Eurocode 0 and 0/A1 [58, 59] for bridge loaded with traffic and wind. In the 2D models, the default static load is a load corresponding to LM1 for a one lane bridge, while the approximation of the moving load is based on the fatigue load model 3 (FLM3) from Eurocode 1-2 [57] .

An additional feature is the pre-stress which can be applied to ties and hangers. This feature was only used for the fundamental studies.

The most important part of the tool is a pattern generator. The following in-plane pattern types are implemented:

- vertical hangers equally distributed along the arch or the deck,
- rhombic pattern or constant inclination of hangers,
- constant change of hanger inclination - hangers equally distributed along the arch or the deck,
- radial pattern with equally distributed hangers along the arch or the deck,
- radial pattern with modifications - hangers equally distributed along the deck.

The presented pattern types are described in Sections 3.4 and 3.5.

To build a numerical model of a bridge, the pattern has to be chosen by the user, as well as auxiliary data like values of inclination angles, number of crossbeams or the coordinates of the focal point in case of modified radial pattern. Moreover, when a chosen input gives a degenerated pattern (hangers are located out of the deck-arch contour), unnecessary hangers are automatically removed.

To create a spoked configuration of hangers, the out-of-plane displacement should also be provided by the user.

As it was mentioned above, many parameters shall be defined by the user. The way of providing input data is twofold, either by graphic user interface (GUI) in Abaqus (suitable for singular tests) or by an external configuration file. The syntax of a configuration file allows for defining ranges of values for each parameter, so it can be used for automatic wide-range parametric studies. An example of an input table for Abaqus GUI and part of a configuration file are presented in Fig. 5.9 and Fig. 5.10, respectively.

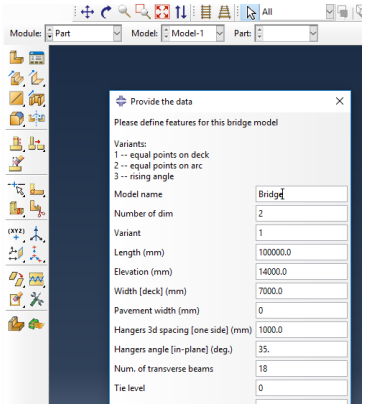

Fig. 5.9 Example of input table in Abaqus.

```
*       :: name: Bridge
*       :: numOfDim: 2
*       :: variant: 1
*       :: slsUls: 2
*       :: compute: 1
*       :: length: 100000.0
*       :: deckElevation: 0000.0
*       :: width: 7000.0
*       :: computed_width: 0
*       :: pavementWidth: 0.0
*       :: hangersZspacing: 0
*       :: numOfHangers: 10
*       :: tieLevel: 0.0
*       :: createTie: True
*       :: tieBeamConnectors: True
*       :: numOfBolts: 10
*       :: numOfBoltsP: 0
*       :: numEigen: 10
*       :: virtual: True
*       :: truss: True
*       :: virtualTruss: True
```

Fig. 5.10 Example of configuration text file.

In case of wide-range studies, from a single configuration file, many instances of the numerical model are created for all combinations of parameters. Next, the numerical analysis is executed and output data, from each simulation, are gathered to the common database. The data of interest can be exported to MSExcel or MatLab for further analysis. The architecture of the framework is shown in Fig. 5.11.

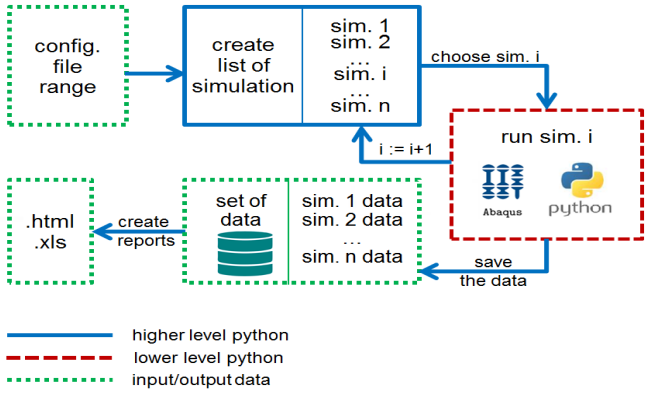

Fig. 5.11 Architecture of the framework.

During the study, stresses and forces in the bridge structure were of interest. Therefore, the auto-generated MSExcel spreadsheet contained i.a. maximal values of axial force or moment in the arch, as well as the maximal stress value in each hanger or the average value of the stress in a hanger set, the number of relaxed hangers for particular load case etc. Fig. 5.12 and Fig. 5.13 present example plots obtained automatically with MatLab. The overall output data were used in fundamental studies of a bridge behaviour.

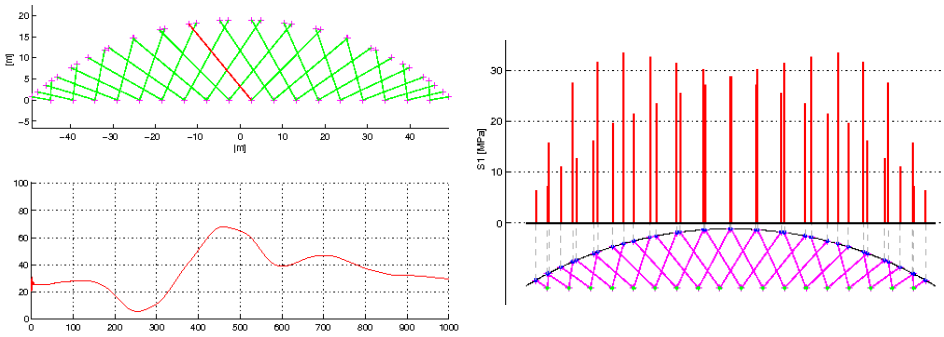

(a) (b)

Fig. 5.12 Exemplar plots of performance of the hangers; a) influence line of highlighted hanger; b) stress distribution in hangers.

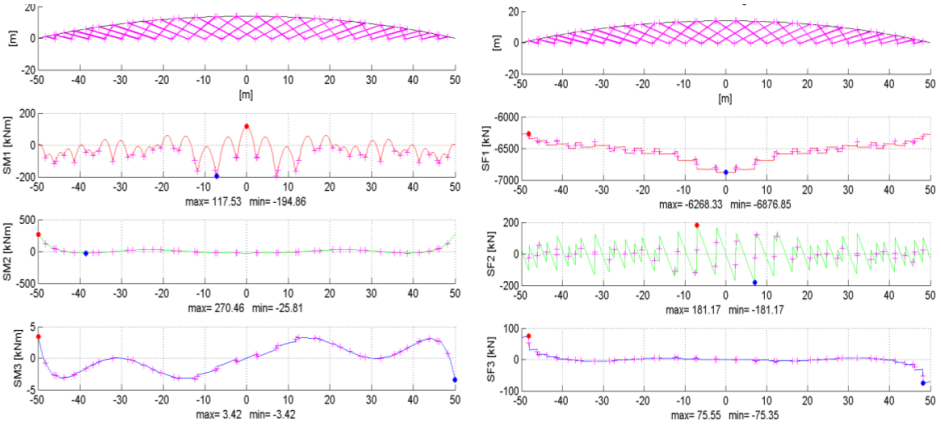

(a) (b)

Fig. 5.13 Exemplar plots of structural performance of the arch; a) bending moments in the arch; b) axial and shear forces in the arch.

6 Summary

6.1 Conclusions

Paper I

In the literature related to network patterns, most studies are focused on patterns with equal distribution of hangers along the arch. This results from technological solutions used in steel and concrete bridges. For timber bridges, an equal distribution of hangers along the deck is desired. Therefore, in Paper I, three types of network patterns with hangers spread uniformly along the deck were compared, i.e. radial pattern, pattern with constant inclination of hangers and pattern with constant change of hangers inclination. Circular and parabolic arch shapes, as well as six different arch rises, were taken into account.

The presented study, based on numerical analyses of more than 2000 pattern outlines, shows that, depending on the arch rise, different pattern types are most efficient. For shallow arches the radial pattern appears to be slightly better than the others, while for medium and high-rise arches, pattern with constant change of hangers inclination is preferable. Moreover, for these patterns a circular arch shape is recommended. On the other hand, for pattern with a constant inclination of hangers, a parabolic arch shape yields better results.

The recommended angle range for the radial pattern and circular arch shape spreads from $\alpha = 45°$ to $\alpha = 55°$ for shallow arches, and from $\alpha = 40°$ to $\alpha = 50°$ for medium and high-rise arches. The recommended angle range for the parabolic arch shape is from $\alpha = 45°$ to $\alpha = 60°$ for all arch rises.

For hangers with constant inclination, and for both arch shapes, the best performance is obtained for the range between $\beta = 35°$ and $\beta = 45°$ for shallow arches, between $\beta = 40°$ and $\beta = 50°$ for medium arches and between $\beta = 45°$ and $\beta = 55°$ for high-rise arches.

For the pattern with constant change of hangers inclination and circular arch shape, the suggested starting angle spreads from $\gamma = 50°$ to $\gamma = 65°$ for shallow arches, from $\gamma = 60°$ to $\gamma = 80°$ for medium arches and from $\gamma = 65°$ to $\gamma = 85°$ for high-rise arches. The suggested angle change spreads from $\Delta\gamma = -1.5°$ to $\Delta\gamma = -3.0°$ for all arch rises. For parabolic arch shape, the suggested starting angle spreads from $\gamma = 50°$ to $\gamma = 60°$ for shallow arches, and from $\gamma = 60°$ to $\gamma = 70°$ for medium and high-rise arches. The recommended angle change varies from $\Delta\gamma = -1.5°$ to $\Delta\gamma = -3.0°$, from

$\Delta\gamma = -1.0°$ to $\Delta\gamma = -3.0°$, and from $\Delta\gamma = -0.5°$ to $\Delta\gamma = -2.5°$ for shallow, medium and high arch rises respectively.

The percentage of relaxed hangers corresponding to the best outlines is acceptably low, however some relaxation of hangers always takes place. Patterns without hanger relaxation have higher values of bending moments, and often in those patterns, hangers become located almost horizontally. Such location of hangers results in a high value of stress range in the pattern and therefore it should be avoided.

Paper II

The paper presents results from a very large number of hanger patterns for a 100 m long network timber arch bridge with a light deck on crossbeams. The analyses, performed for different arch rises, include the influence of the number of crossbeams and of the hanger spread angle on the structural performance of the bridge.

The main conclusion from the first part of the analysis is that the optimal number of crossbeams for a 100 m long bridge is between 15 and 21. Whether the number of crossbeams is odd or even seems to be insignificant.

While using a coinciding centre of the arch and the focal point, a general recommendation is to use a hanger spread angle in the range from $43°$ to $51°$ in the design process. Depending on the arch rise, more specific ranges are between $48° - 65°$, $40° - 55°$ and $38° - 54°$, for shallow, medium and high-rise arches, respectively. These ranges lead to the smallest bending moments in the arch. It should be noted that spread angles bigger than $45°$ lead to hangers that are oriented almost horizontally at the ends of the bridge. However, they do not relax (as might be expected). Nevertheless, such location of hangers would not be accepted in the engineering practice. For an actual hanger pattern, it is recommended to avoid that hangers meet at the arch, since this will increase the bending moment in the arch.

A horizontal offset of the focal point can reduce bending moments by almost 50%. Furthermore, the number of relaxed hangers can be reduced almost by half. Horizontal offsets should be less than 10 m. In most cases, offsets up to about 5.5 m are beneficial. However, horizontal offsets up to 10 m can be beneficial for patterns with medium or high-rise arches and spread angle lower than $40°$.

In case of vertical offset of the focal point, the bending moment for the best modified pattern is only about 25% of the bending moment for the reference (classical) pattern. The number of relaxed hangers can be reduced by 80% (from 10 to 2 relaxed hangers). The recommended values of the vertical offset are in the range between -110 m to 30 m. For medium and high-rise arches and spread angle below $45°$, the largest benefit is

obtained for negative offsets which are almost equal to four times the radius of curvature of the circular arch.

Comparing effects from the X- and Y-configuration, the latter is clearly more beneficial for the structural performance of the bridge. However, the combined (XY) modification is in general the most advantageous.

The loading is an important premise for the performed analyses. The key bending moment values, i.e. the maximum bending moment for each pattern, may occur for any one of the load steps (i.e. load cases). Therefore, it is suggested to use several load cases while testing or comparing different network patterns.

The study presented in Paper II shows that the introduced pattern modifications yield significant improvements in the structural performance of network timber arch bridges with light decks on transverse crossbeams.

Paper III

In Paper III, various radial network patterns for a 100 m long network arch bridge with light deck on 18 transverse crossbeams were tested and analysed under varying load positions (approximation of moving loading). The patterns were generated based on different arch rises, spread angles and locations of the focal point with equidistant distribution of hangers along the deck.

From the analyses performed on classical radial patterns (without modifications), it is recommended to use spread angle from the range $48-55°$ for shallow arches and $38-54°$ for medium and high-rise arches. Based on these analyses it became clear that the comparative criteria, i.e. stress range in the hangers and bending moment in the arch, give divergent results for constant angle rise.

From the study on pattern modifications, it can be concluded that horizontal offsets do not significantly change the stress distribution in the hangers. However, small modifications, i.e. offset under 15 m for a bridge of 100 m length, can be beneficial in terms of bending moment, especially for small angles, below $35°$. Here, the moment can be reduced more than 50% compared to the patterns without modifications.

The effect of a vertical offset gives larger improvements. The introduction of a vertical offset enhances the results up to 32% in terms of stress range in the hangers, and up to 78% for moments in the arch. However, in order to create the best pattern in terms of stress range in the hangers, a positive offset is required, while considering bending moments, a negative one is beneficial. Based upon the available data, it is recommended primarily to apply the negative offset in the search for the best pattern. Thus, the recommended vertical offset ranges from -150 m to -30 m for a 100 m long bridge. However, for cases with the spread angle bigger than $55°$, no offset should be applied.

The combined modification has the largest potential for optimization. However, the difference between the Y-configuration and the XY-configuration is quite small. In general, it is recommended to use a dual offset, or start with only a vertical offset in the pattern optimizing process. The ranges for the spread angle for classical patterns are also valid for modified patterns.

In general, it is recommended to put emphasis on the bending moment criterion in comparison to the stress ranges criterion.

Paper IV

The Paper IV presents a study on network timber arch bridges with spoked configuration of hangers.

The main conclusion from the study is that a double inclination of hangers can be considered as an alternative to a wind bracing. Moreover, based on the performed analyses, a few designing guidelines can be proposed.

It is suggested to keep the out-of-arch-plane spacing of the fastening points of the hangers within the vertical projection of the arch. For properly chosen proportions of the arch cross-section, such distance should be sufficient to resist buckling. Moreover, it does not increase the length of the crossbeams.

The width of the arch cross-section should be bigger than the height of the arch cross-section. The ratio width-to-height should not be smaller than 1.5.

It is equally important to carefully choose both the outline of the in-plane hanger pattern and the out-of-plane spacing of the hangers. The first one is critical for skew loading, while the latter influences mainly the out-of-plane buckling.

Final conclusions

The final conclusions drawn from the conducted research are hereby reported according to the objectives they answer to.

Objective 1. Verify existing network patterns as possible patterns for bridges with transverse crossbeams, which constitute the base for hangers attachment on the lower chord (deck level).

The radial network pattern, the pattern with constant inclination of hangers and the pattern with constant change of hangers inclination can be adapted for bridges with transverse crossbeams, which constitute the base for hangers attachment on the lower chord (deck level).

Objective 2 and Objective 4. Define new network pattern suitable for network arch bridges with crossbeams and provide a systematic way of pattern creation. Verify the introduced pattern and its effect on the structural performance of the bridge.

A new network pattern was defined based on a modification of an existing radial pattern. It was shown that the introduced modifications improve the structural performance of the bridge and new patterns can be easily created in a systematic way.

Objective 3. Prepare a software tool for the auto-generation of numerical models of network arch bridges. The validation of the numerical models should be based on tests of a scaled laboratory model of a bridge.

Although it was not the main goal of the research, the auxiliary work was performed to constitute a foundation for further research. For this, the software was implemented. The software tool was validated using the laboratory model.

Objective 5. Verify the introduced concept of double inclination of hangers (spoked configuration of hangers), and its influence on the bridge stability, as a possible alternative for wind truss.

During the study, it was shown that double inclination of hangers can be considered as a valid alternative to the wind bracing.

6.2 Further work

The following recommendations for further research are given:

Analysis of patterns with different boundary conditions

In the presented thesis, it was assumed in all numerical models, that both the arch and the deck are pinned to the ground. It is recommended to verify the results on the model of classical bowstring arch, i.e. a construction with the tie and unsymmetrical boundary conditions – like a simply supported beam.

Influence of the stiffness of the connection at the arch end

The 3D studies described herein share the common assumption of a constant stiffness of connection between the arch ends and the abutments, in the transversal direction. Therefore, the logical extension of the presented work would be to study the influence of the connection stiffness on the stability of the bridge.

Arch partition

To simplify the numerical analysis the arch was modelled as a single element. Nevertheless, the physical solution would require partitioning into several sub-elements, mainly due to transport limitation. As the introduction of new connections into the arch can modify the behaviour of the bridge, the structural performance and the bridge stability should be studied under the new conditions as well. This particular issue was addressed as a part of the *DuraTB* project, confer [1, 60, 61].

Different type of cables

The scope of this thesis was limited to hanger networks made of solid steel rods only. The recommended future work should concentrate on the application of steel cables as an alternative, and on the comparison of both solutions in terms of structural performance of the bridge. Special attention should be paid to the phenomena of hangers relaxation and deflection.

Bridge dynamics

Since the detailed studies of the bridge dynamic response were out of the scope of this thesis, the issue should be further investigated, especially for network arch timber footbridges.

Bridge erection method

Although the matter of network bridge erection is far from the scope of the thesis and was already studied for steel and concrete structures, the issue should be again addressed for bridges with a light timber deck discussed in this thesis. The light construction of the deck may not guarantee sufficient hangers pre-stressing, and the

building technology is different than for concrete decks, thus specific erection solutions should be defined.

References

1. Pousette, A., et al., *Durable Timber Bridges, Final Report and Guidelines*. 2017, RISE Research Institutes of Sweden: Skellefteå
2. Pipinato, A., *Innovative Bridge Design Handbook : Construction, Rehabilitation and Maintenance*. 2016: Butterworth-Heinemann.
3. Mettem, C.J., *Timber Bridges*. 2011, New York TRADA Technology Ltd.
4. Pousette, A., *Träbroar - konstruktion och dimensionering (in Swedish)*. 2008, Stockholm: SP Sveriges Tekniska Forskninginstitut, SP Trätek.
5. International Database for Civil and Structural Engineering. *Available at:* https://structurae.net.
6. Ryall, M.J., G.A.R. Parke, and J.E. Harding, *The manual of bridge engineering*. 2000, London: Thomas Telford.
7. Chen, W.F. and E.M. Lui, *Handbook of Structural Engineering, Second Edition*. 2005, New York: CRC Press.
8. Tveit, P., *The design of network arches.* The Structural Engineer, 1966. **44**(7): p. 249-259.
9. Pellegrino, C., G. Cupani, and C. Modena, *The effect of fatigue on the arrangement of hangers in tied arch bridges.* Engineering Structures, 2010. **32**(4): p. 1140-1147.
10. Schanack, F., *Puentes en Arco Tipo Network, (Network Arch Bridges). Doctoral Thesis*. 2008, Department of Structural Engineering and Mechanics, Technical College of Road, Channel and Port Engineering, University of Cantabria, Spain.
11. Teich, S., *Development of general design principles for the hanger arrangements of network arch bridges (in German).* Stahlbau, 2011. **80**(2): p. 100-111.
12. Brunn, B. and F. Schanack, *Calculation of a double track railway network arch bridge applying the European standards. Graduation Thesis.* 2003, Dresden University of Technology.
13. Tveit, P. *Network Arches*, in *11th Congress of International Association for Bridge and Structural Engineering (IABSE)*. 1980. Vienna, Austria.
14. Gregora, D., et al., *New Troja Bridge in Prague – Concept and Structural Analysis of Steel Parts.* Procedia Engineering, 2012. **40**: p. 131-136.
15. Tveit, P., *Considerations for Design of Network Arches.* Journal of Structural Engineering (United States), 1987. **113**(10): p. 2189-2207.
16. Tveit, P., *Comparison of Steel Weights in Narrow Arch Bridges with Medium Spans* Stahlbau, 1999. **68**(9): p. 753-757.
17. Tveit, P., *An introduction to the optimal network arch.* Structural Engineering International, 2007. **17**(2): p. 184-187.

18. Tveit, P., *Network Arches: The World's Lightest Arch Bridges*, in *9th Asia Pacific Transportation Development Conference*. 2012: Chongqing, China. p. 473-480.
19. Graße, W., et al. *Network Arches for Road Bridges*, in *International Conference on Arch Bridges, ARCH'04*. 2004. Barcelona, Spain.
20. Tveit, P. *The Network Arch. Findings on network arches during 54 years. Available at:* http://home.uia.no/pert/.
21. Schanack, F. and B. Brunn, *Generation of network arch hanger arrangements (in German).* Stahlbau, 2009. **78**(7): p. 477-483.
22. Schanack, F. and B. Brunn, *Analysis of the structural performance of network arch bridges.* Indian Concrete Journal, 2009. **83**(1): p. 7-13.
23. Brunn, B., F. Schanack, and U. Steimann. *Network Arches for Railway Bridges*, in *International Conference on Arch Bridges, ARCH'04*. 2004. Barcelona, Spain.
24. Teich, S., *The network arch bridge, an extremely efficient structure - Structural behaviour and construction (in German).* Stahlbau, 2005. **74**(8): p. 596-605.
25. Teich, S. *Fatigue Optimization in Network Arches*, in *International Conference on Arch Bridges, ARCH'04*. 2004. Barcelona, Spain.
26. De Zotti, A., C. Pellegrino, and C. Modena. *A parametric study of the hanger arrangement in arch bridges*, in *5th International Conference on Arch Bridges, ARCH '07*. 2007. Madeira, Portugal.
27. Backer, H., et al. *Force Variation and Slackness in Tied Arch Bridges with Crossing Hangers*, in *International Conference on Arch Bridges, ARCH'04*. 2004. Barcelona, Spain: CIMNE.
28. Pipinato, A., *Structural analysis and design of a multispan network arch bridge.* Proceedings of the Institution of Civil Engineers: Bridge Engineering, 2016. **169**(1): p. 54-66.
29. Schanack, F., *Calculation of the critical in-plane buckling load of network arches (in German).* Bautechnik, 2009. **86**(5): p. 249-255.
30. Pircher, M., M. Stacha, and J. Wagner, *Stability of network arch bridges under traffic loading.* Proceedings of the Institution of Civil Engineers: Bridge Engineering, 2013. **166**(3): p. 186-192.
31. Bell, K. and E. Karlsrud. *Large Glulam Arch Bridges - A Feasibility Study*, in *Innovative Wooden Structures and Bridges, IABSE Conference*. 2001. Lahti, Finland: IABSE report
32. Wollebæk, L. and K. Bell. *Stability of glulam arches*, in *8th World Conference on Timber Engineering, WCTE*. 2004. Lahti, Finland.
33. Bell, K. and L. Wollebæk. *Large, mechanically joined glulam arches*, in *8th World Conference on Timber Engineering, WCTE*. 2004. Lahti, Finland.
34. Bruno, D., P. Lonetti, and A. Pascuzzo, *An optimization model for the design of network arch bridges.* Computers and Structures, 2016. **170**: p. 13-25.

35. Islam, N. and R. Ahsan. *Optimization of hanger arrangement of network arch bridges*, in *IABSE-JSCE Joint Conference on Advances in Bridge Engineering-II*. 2010. Dhaka, Bangladesh.

36. Islam, N., et al., *An Optimized Design of Network Arch Bridge using Global Optimization Algorithm.* Advances in Structural Engineering, 2014. **17**(2): p.197-210.

37. Ghani, S.N., *A versatile algorithm for optimization of a nonlinear non-differentiable constrained objective function*. UKAEA Harwell Report Number R-13714. 1989, London: HMSO Publications Centre.

38. Ghani, S.N. *Performance of global optimization algorithm EVOP for non-linear non-differentiable constrained objective functions*, in *IEEE International Conference on Evolutionary Computation, IEEE ICEC'95*. 1995. Perth, Australia.

39. Räck, M., F. Schanack, and P. Tveit. *Erection of Network Arches*, in *International Conference on Arch Bridges, ARCH'04*. 2004. Barcelona, Spain.

40. Stetter, H., S. Hentschinski, and T. Fritsche, *Innovation concentrated - Regenbrücke Stefling: A tied arch bridge in concrete (in German).* Beton- und Stahlbetonbau, 2015. **110**(10): p. 710-719.

41. Millanes, F., M. Ortega, and S. Nebreda, *Design and Construction of Composite Tubular Arches with Network Suspension System: Recent Undertakings and Trends.* Journal of Civil Engineering and Architecture, 2011. **5**(3).

42. Millanes, F., M. Ortega, and A. Carnerero, *Palma del Río Arch Bridge, Córdoba, Spain.* Structural Engineering International, 2010. **20**(3): p. 338-342.

43. Millanes, F., et al. *The Use and Development of The Network Suspension System for Steel Bowstring Arches*, in *VII Congresso de Construção Metálica e Mista*. 2009. Lisbona.

44. Veie, J. and R.B. Abrahamsen. *Steien Network Arch Bridge*, in *2rd International Conference on Timber Bridges, ICTB*. 2013. Las Vegas, Nevada, USA.

45. Veie, J. *Network arch bridge with glulam arches. Lessons learned and further development*, in *3rd International Conference on Timber Bridges, ICTB*. 2017. Skellefteå, Sweden.

46. Norwegian Public Roads Administration. *Avaiable at:* https://www.vegvesen.no.

47. Valenzuela, M.A. and J.R. Casas. *Bridge strengthening by network arch: Structural performance and design criteria*, in *6th International Conference on Bridge Maintenance, Safety and Management*. 2012. Stresa, Lake Maggiore, Italy.

48. Valenzuela, M.A. and J.R. Casas, *Bridge strengthening by conversion to network arch: Design criteria and economic validation.* Structure and Infrastructure Engineering, 2016. **12**(10): p. 1310-1322.

49. MOELVEN. *Available at:* http://www.moelven.com/.

50. Labonnote, N., *Modal hammer for dummies*. 2012, Norwegian University of Science and Technology, NTNU: Trondheim, Norway.
51. Kjær, B., *Product Data: Heavy-duty Impact Hammers Types 8207, 8208 and 8210*. Available at: https://www.bksv.com/media/doc/bp2079.pdf.
52. National Instruments, *LabView 2010*. Austin, Texas, United States.
53. Hibbit, K., Sorensen, *ABAQUS/Standard Analysis User's Manual* 2007.
54. Python, *Python Software Foundation*. Available at: https://www.python.org/: Wilmington, Delaware, United States.
55. The MathWorks Inc., *MatLab, Release 2012b*. Natick, Massachusetts, United States.
56. Microsoft Corporation, *Excel 2016*. Redmond, Washington, United States.
57. CEN, *EN 1991-2: Eurocode 1: Actions on structures -Part 2: Traffic loads on bridges*, in 2003: Brussels, Belgium.
58. CEN, *EN 1990: Eurocode 0: Basis of structural design* 2002: Brussels, Belgium.
59. CEN, *EN 1990: Eurocode 0/A1: Basis of structural design* 2005: Brussels, Belgium.
60. Cepelka, M. and K.A. Malo. *Effect of on-site splice joints for timber network arch bridges*, in *3rd International Conference on Timber Bridges*. 2017. Skellefteå, Sweden.
61. Cepelka, M. and K.A. Malo, *Moment resisting splice of timber beams using long threaded rods and grout-filled couplers – Experimental results and predictive models.* Construction and Building Materials (submitted), 2017.

PART II

Appended major papers

Paper I

Comparison of network patterns suitable for timber bridges with crossbeams

(In: *Proceedings of the ICTB 2017, 3rd International Conference on Timber Bridges*)

Comparison of network patterns suitable for timber bridges with crossbeams

Anna Weronika OSTRYCHARCZYK
MSc, PhD Candidate
Norwegian University of Science and Technology (NTNU)
Trondheim, Norway
anna.w.ostrycharczyk@ntnu.no

Anna Weronika Ostrycharczyk is working in the field of timber structures. Current research topic is related to structural performance of network arch timber bridges.

Kjell Arne MALO
Professor, Dr. ing
Norwegian University of Science and Technology (NTNU)
Trondheim, Norway
kjell.malo@ntnu.no

Kjell Arne Malo is professor of timber structures at NTNU. His research topics are methods for increased strength and stiffness of connections for timber structures and vibrations in timber structures.

Summary

This article presents a comparison of different types of network patterns with evenly spaced hanger pairs on the deck level, which is suitable for timber bridges with transversal crossbeams. Bending moments in the arch and the number of relaxed hangers, obtained for skew loading, have been the comparative criteria. The numerical parametric studies focus of three pattern types, two arch shapes and six different arch rises. In conclusion, values of geometric parameters are suggested in order to achieve optimal structural performance of bridges with network hanger patterns.

Keywords: timber, network arch, network pattern, circular arch, parabolic arch

1. Introduction

Network arch bridge concepts are well known among bridge engineers. The concept was defined by the Norwegian engineer Per Tveit. The basic assumption for the network arch is that the hangers are crossing each other multiple times [1]. When this assumption is combined with fine-tuned hanger arrangement, it is possible to achieve approximately uniform distribution of forces in the structure, especially for bending moments in the arch and axial forces in the hangers. It can result in better material utilization and thus material savings. This is considered to be the main advantage of network arches.

In the literature, many hanger arrangements are defined [2-4]. Not all of those patterns belong entirely to the network group. The most common patterns are: vertical hangers [5], fan arrangement [5], radial network pattern [6], network pattern with constant inclination of hangers [3] or with constant change of hangers inclination [3].

In [7] Teich compared four network patterns to a pattern with vertical hangers, in terms of i.a. arch utilization related to axial forces, bending moments or both. Moreover, necessary amount of steel weight of the arch was also presented. It was shown that arch with vertical hangers required almost double amount of steel in comparison to arches with network patterns.

In the other article [3], Teich presented parametric studies of five different network patterns, with varying parameters like number of hangers, bridge span, arch rise or hangers inclination. The main comparative criteria were related to stress values in hangers.

Schanack [6] compared bending moment distributions in upper and lower chords of network bowstring arches with different hanger arrangements with radial patterns as well as patterns with vertical hangers.

De Zotti et al. [8] compared structural performance of arches with vertical hangers, network and fan patterns for different arch to span ratios. The same set of patterns as in [8] was considered by Pellegrino et al. [5]. The main comparative criteria were related to stress values in hangers. In the paper, individually arranged outline of hangers located close to supports were tested and compared.

The vast majority of the patterns from the described studies share a common feature, namely hanger attachment points are evenly distributed along the arch; the distribution along the deck is hence likely to be uneven. Such distributions are suitable for network bridges made of steel or concrete, i.e. hanger attachment on the deck level can be located anywhere on edge beams of the deck.

In this paper however, the network concept is adapted to the timber bridges with light timber deck supported by transversal crossbeams. It is assumed that hangers are attached to the crossbeams. Consequently, the hangers should be evenly distributed along the deck. Although all the previously published papers studied different patterns in detail, the results are most useful for outlines with even distribution of hangers on the arch. This publication attempts to extend the results for outlines suitable for timber bridges with crossbeams.

The present study focuses on comparison of three network patterns adapted for even distribution of hangers along the deck. The comparison is performed for two types of arch shapes and six different arch rises.

2. Methodology

2.1 Analysed patterns

In the paper three types of network patterns are discussed: radial, pattern with constant inclination of hangers (CIH) and pattern with constant change of hanger inclination (CCI).

The radial pattern [6] is characterised by a constant angle between arch radius and hanger. The pattern was developed by Brunn and Schanack [9] as a result of parametric studies performed on the 100 m long steel bridge with concrete deck. Fig.1a shows the outline of the radial pattern. In this specific instance hangers are equally distributed along the arch. Fig. 1b presents corresponding pattern with uniform distribution of hangers on the deck level.

The tested range of angles α for the radial pattern spreads from $0°$ to $70°$ with steps of $1°$. It should be highlighted that patterns with angle α above a certain value depending on the arch rise, bridge span and number of hangers, can be classifies as a network pattern. Moreover, the pattern where $\alpha = 0°$ is denoted a fan arrangement [5].

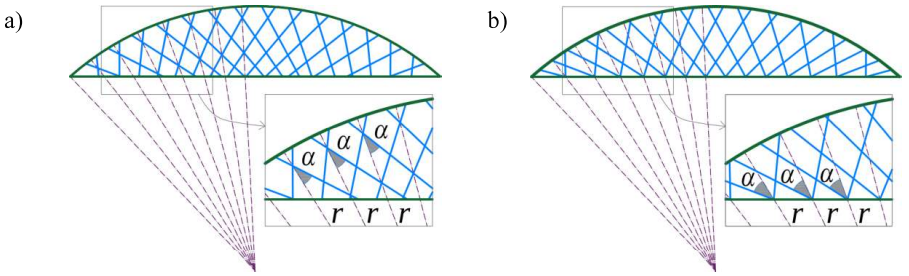

Fig. 1 Radial pattern with hangers equally distributed along the arch (a); along the deck (b)

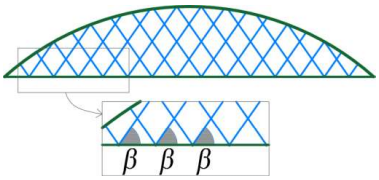

Fig. 2 Pattern with constant inclination of hangers (CIH)

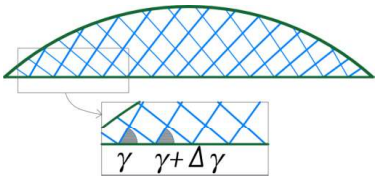

Fig. 3 Pattern with constant change of hangers inclination (CCI)

In the pattern with constant inclination of hangers (CIH), as the name suggests, the angle between the deck and each hanger is constant for the whole pattern, see Fig. 2. This pattern, with the hangers evenly distributed along the deck, is known also as a rhombic pattern [10].

In the numerical study presented herein, the angle β is in range from $30°$ to $90°$ with steps of $2.5°$. When $\beta = 90°$, it becomes a special case with vertical hangers.

The third analysed pattern is a variation of the previous pattern. This pattern is often denoted pattern with constant change of hanger inclination (CCI). Here, the angle between the deck and the hanger changes its value incrementally for each consecutive hanger. The increment is constant. Two parameters are needed to unambiguously describe the pattern: a starting angle γ and an angle change $\Delta\gamma$. Depending on the desired geometrical effect, the angle change can be both positive and negative. An example of CIH pattern is depicted in Fig. 3.

The tested range of starting angle γ spreads from $45°$ to $90°$ with steps of $5°$ while the angle change $\Delta\gamma$ is from $0°$ to $4.5°$ with steps $0.5°$. For some combinations of γ and $\Delta\gamma$ certain patterns cannot be constructed, so they were excluded from the analysis.

2.2 Numerical model

A parametric numerical model was created to study the patterns and to compare them. The model is two-dimensional and consists of beam elements in arch and deck, and truss elements in hangers. In the model, the hangers are of steel and can only carry tensile forces, as in the material properties the elastic modulus is zero, for negative strains. Both the arch and the deck are made of glulam GL30c and GL24c, respectively [11]. The arch cross-section is 1000 x 600 mm, while the deck is 3000 x 500 mm. The deck width corresponds to the width of one notional car-lane, according to EN1-2 [12]. The density of timber associated to the deck takes into account the presence of 18 steel crossbeams and an asphalt layer of 120 mm. Moreover, pinned boundary conditions are applied both to the arch and the deck.

In this paper all comparisons are made with bridge length $l = 100$ m and number of crossbeams $n = 18$. Other parameters, like an arch rise f and angles are varied. In the study, six arch rises are considered, i.e. $f = (11,14,17,20,23,26)$ expressed in meters. For a 100 m bridge span, $f = 11$ m $(14$ m$)$ constitutes 11% (14%) of the deck length and represents a shallow arch. Accordingly, $f = (17,20)$ refers to medium arch rises and $f = (23,26)$ refers to high-rise arches. The values of the considered angles α, β and γ are given in Section 2.1. For an instance given by f and l, it is possible to construct only one particular circle or one particular parabola that will constitute the arch. Both shapes are considered and compared.

All analyses have been performed with Abaqus software [13] with implicit procedure allowing nonlinear analysis. Abaqus software was extended with Python [14] scripting, in order to create pattern outlines automatically.

2.3 Comparison criteria

One of the advantages of network arches is a possibility to achieve uniformly distributed bending moments along the arch. Bending moment is sensitive to skew loading, and therefore different skew load cases are considered in the numerical studies. The loading was applied on the deck structure in 11 steps, leading to 11 load cases. Starting from left, the loaded part of the deck was increased by 10% of the deck length in each step. The first step includes only the self-weight, while the last step represents uniformly loaded deck.

For different network patterns with the same arch rise, the values of axial forces are similar (they only differ by approximately 5%). Therefore, the main comparative criterion takes into account solely bending moments. For a given pattern, the absolute maximum bending moment along the arch M is obtained for the most unfavourable load case. The value M for each hanger outline is then used to compare the structural performance of the network arch layouts.

The arch utilization is usually the governing design criterion. However, in the considered patterns, analysis of the bending moments and the utilization function leads to similar conclusions. In Fig. 4 an example of maximum bending moment M and utilization U for a range of patterns is presented. The utilization U is calculated as combination of the bending moment and an axial force, according to EN5-1-1 [15]. Both functions reach minimum for similar geometric feature of the pattern, i.e. angle. Moreover, the same behaviour can be observed for all types of tested patterns.

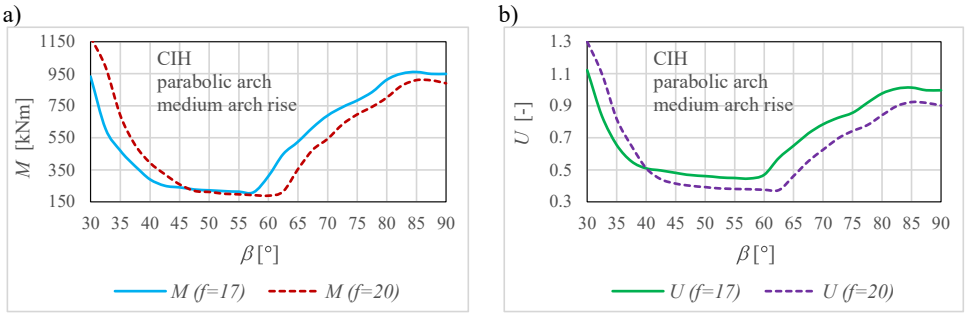

Fig. 4 Maximum bending moment M (a) and arch utilization U (b) as a function of angle β, for patterns with constant inclination of hangers(CIH), n=18 and arch rise f=17m and f=20m

A secondary comparative criterion is the maximum percentage of relaxed hangers, H, chosen from all load cases. It might be an important design characteristic since, as opposed to a heavy concrete deck, the self-weight of a light timber deck is insufficient for adequate hanger prestressing.

3. Results

For each studied pattern type two comparative criteria are presented in a single figure. In each figure, the left-hand-side vertical axis corresponds to the bending moment value, while the right-hand side vertical axis refers to the percentage of relaxed hangers. The horizontal axis, depending on tested pattern type, refers to angle α, β or γ and $\Delta\gamma$.

In most figures, the results for two arch rises are presented simultaneously. The bending moment is marked as solid or dotted line, while open dots and plus symbols mark the percentage of relaxed hangers.

3.1 Radial pattern

The results for the radial pattern are presented in Fig. 5 and Fig. 6. Only the medium arch rises are chosen for visualisation, since the results for all tested arch rises have common characteristic. The critical values for all arch rises and pattern types are gathered in Tab.1 in Section 3.4.

The function of bending moment to angle α, presented in Fig. 5, is decreasing for increasing α, until function starts to rise with fluctuations. The function of percentage of relaxed hangers is constantly decreasing with increasing angle. The highest M and lowest H is achieved for $\alpha = 0°$, i.e. the fan arrangement of hangers.

For the radial pattern, the most promising angle is corresponding to the lowest value of M. In Fig. 5a this angle is $\alpha \approx 45°$. For such angle, the number of relaxed hangers is around 10% what is an acceptable value. It can be noticed that for angles $\alpha \geq 55°$, values of H reach zero, which is of course desired. However for such inclination some hangers are located almost horizontally, which should be avoided.

Comparing the results for circular and parabolic shape of the arch, the latter reaches slightly higher values of M and H. The results have the same characteristic, but are shifted up and right.

The results presented in Fig. 5 refer to the model of 100 m long bridge with 18 transversal crossbeams, while the results presented in Fig. 6 refer to a similar bridge with 24 transversal crossbeams. By comparing both figures, it can be concluded that number of crossbeams does not change the characteristics of the results. Only the negligible changes of M and H values, are direct consequences of a change of the number of hangers.

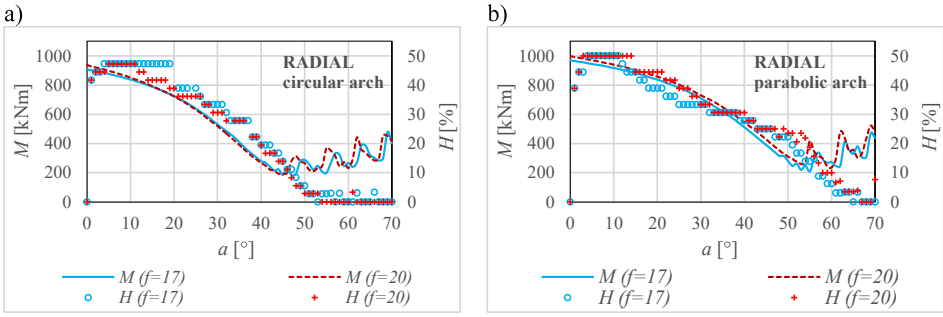

Fig. 5 Bending moment and percentage of relaxed hangers for medium arch raises and arch shape as circle (a); parabola (b). Number of crossbeams n=18. Radial pattern.

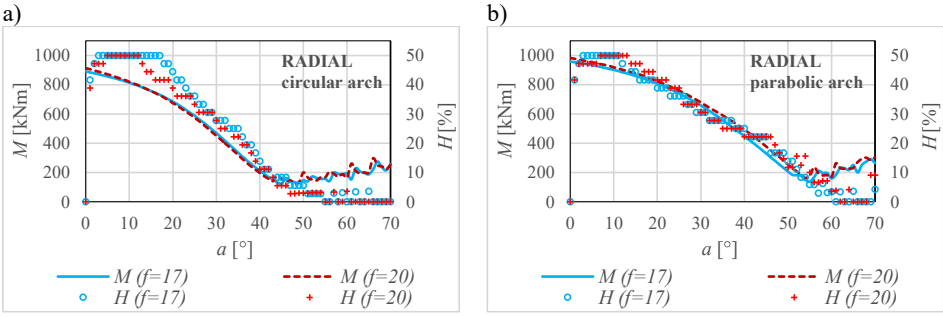

Fig. 6 Bending moment and percentage of relaxed hangers for medium arch raises and arch shape as circle (a); parabola (b). Number of crossbeams n=24. Radial pattern.

3.2 Pattern with constant inclination of hangers

The results related to the pattern with constant inclination of hangers for medium arch rises are depicted in Fig. 7. The function of the bending moments has similar characteristics for both arch shapes. Clearly it has an optimal range of β around $40° - 50°$.

The functions of hanger relaxation H for both arch shapes also have similarities. The graph shows, approximately, independence of β for small values, but for $\beta > 45°$ a steady increase of H takes place for increasing β.

The outline with angle $\beta \approx 50°$ seems to be most promising, regardless the arch shape. It is worth to notice that for parabolic shape the pseudo optimal range of angles is wider than for circular shape and spreads from $\beta \approx 40°$ to $\beta \approx 60°$.

Note that the highest values of M and the lowest value of H are for $\beta = 90°$, thus for a pattern with vertical hangers. Such pattern often constitutes the basic pattern for comparison of network patterns to show a scale of improvement from inclined hangers.

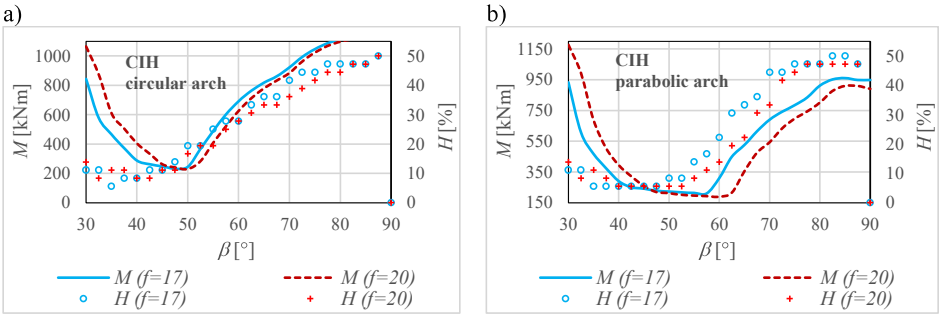

Fig. 7 Bending moment and percentage of relaxed hangers for medium arch raises and arch shape as circle (a); parabola (b). Number of crossbeams n=18. Pattern with constant inclination of hangers (CIH).

3.3 Pattern with constant change of hangers inclination

In this section the pattern with constant change of hangers inclination is taken under consideration. In Fig. 8 the bending moment and the percentage of relaxed hangers are shown as a function of the starting angle γ and angle change $\Delta\gamma$. The arch rise is 17 m and arch shape is circular. In Fig. 9 similar results are presented for parabolic arch shape. Further results have been obtained for other arch rises, thus Fig. 8 and Fig. 9 are only shown as examples.

The lowest values of M can be obtained for various combinations of γ and $\Delta\gamma$. In general, the higher the starting angle, the bigger angle change shall be used. It applies to both arch shapes.

The percentage of relaxed hangers is low for starting angle $\gamma = 45°$ for any angle change $\Delta\gamma$. For the circular arch shape, H increases with increasing γ, and is larger for small changes $\Delta\gamma$. For the parabolic shape, H remains low for $\gamma \leq 60°$ and increases drastically with an increase of γ, regardless of $\Delta\gamma$.

On the plots in Fig. 8 and Fig. 9, zero values of M or H correspond to pattern outlines which cannot be geometrically constructed.

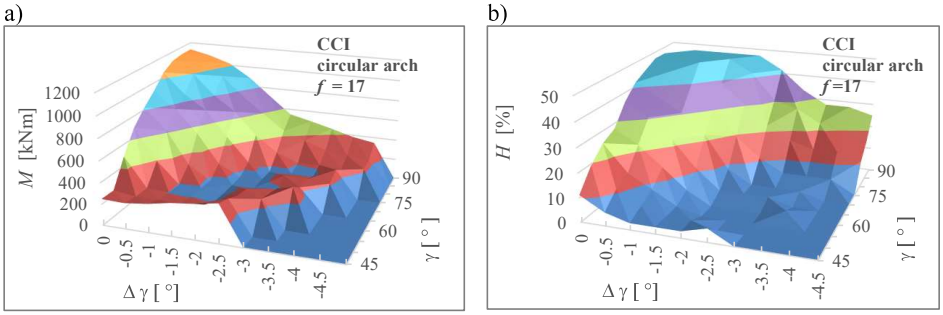

Fig. 8 Bending moment (a) and percentage of relaxed hangers (b) in circular arch with $f = 17$ and $n = 18$. *Pattern with constant change of hanger inclination.*

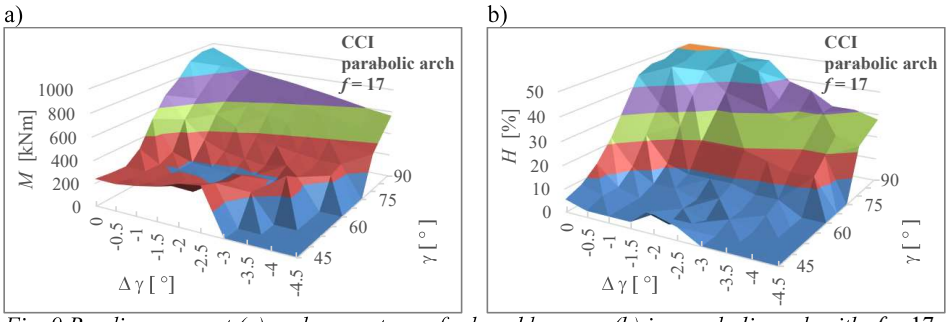

Fig. 9 Bending moment (a) and percentage of relaxed hangers (b) in parabolic arch with $f = 17$ and $n = 18$. *Pattern with constant change of hanger inclination.*

3.4 Collected results

The most promising outlines are those with the lowest value of M and possibly the lowest value of H. The lowest values of the bending moment for all tested arch rises f, two arch shapes, and three pattern types are collected in Tab. 1. Percentages of relaxed hangers, corresponding to M values from Tab.1, are given in Tab. 2.

Table 1 Lowest given bending moment in the arch for different arch rises, shape of the arch, and type of the pattern

Arch rise	Lowest bending moment on the arch M [kNm]					
	radial		constant inclination of hangers (CIH)		constant change of inclination (CCI)	
f	circular	parabolic	circular	parabolic	circular	parabolic
11	185	209	328	327	195	224
14	176	209	261	250	183	199
17	183	208	231	210	163	172
20	193	237	230	189	153	173
23	209	256	239	175	146	158
26	223	316	281	165	156	152

* the lowest values for particular arch rise is highlighted in grey

Table 2 Percentage of relaxed hangers corresponding to lowest M in the arch, for different arch rises, shape of the arch, and type of the pattern

Arch rise	H [%] corresponding to M from Tab. 1					
	radial		constant inclination of hangers (CIH)		constant change of inclination (CCI)	
f	circular	parabolic	circular	parabolic	circular	parabolic
11	6	11	19	17	8	3
14	8	11	14	17	3	3
17	11	14	14	17	3	8
20	14	10	17	14	3	3
23	3	18	14	14	6	3
26	0	23	17	11	8	3

In Tab. 1, for each arch rise the lowest value of M is highlighted in grey. It can be noticed that for shallow arches radial pattern strikes as best, while for medium and high arch rises it is the pattern with constant change of hangers inclination. In addition, for radial and CCI patterns, the circular arch shape is more beneficial. The parabolic arch shape is better for CIH.

The percentage of relaxed hangers corresponding to *M*-results from Tab. 1, is smallest for CCI patterns, while it is the highest for CIH pattern and varies for circular and parabolic arch shape.

4. Conclusions

In the literature related to network patterns, most studies are focused on patterns with equal distribution of hangers along the arch. It results from technological solutions used in steel and concrete bridges. For timber bridges, equal distribution of hangers along the deck is desired. Therefore in this paper, three types of network patterns with hangers spread uniformly along the deck are compared. Circular and parabolic arch shape as well as six different arch rises are taken into account.

The present study, based on numerical analyses of more than 2000 pattern outlines, shows that, depending on arch rise, different pattern types are most efficient. For shallow arches the radial pattern appears to be slightly better than the others, while for medium and high-rise arches, pattern with constant change of hangers inclination is preferable. Moreover, for these patterns circular arch shape is recommended. On the other hand, for pattern with constant inclination of hangers, parabolic arch shape yields better results.

The recommended angle range for radial pattern and circular arch shape spreads from $\alpha = 45°$ to $\alpha = 55°$ for shallow arches, and from $\alpha = 40°$ to $\alpha = 50°$ for medium and high-rise arches. Recommended angle range for parabolic arch shape is from $\alpha = 45°$ to $\alpha = 60°$ for all arch rises.

For hangers with constant inclination (CIH), and for both arch shapes, best performance is obtained for the range between $\beta = 35°$ and $\beta = 45°$ for shallow arches, between $\beta = 40°$ and $\beta = 50°$ for medium arches and between $\beta = 45°$ and $\beta = 55°$ for high-rise arches.

For the last pattern, CCI, and circular arch shape, the suggested starting angle spreads from $\gamma = 50°$ to $\gamma = 65°$ for shallow arches, from $\gamma = 60°$ to $\gamma = 80°$ for medium arches and from $\gamma = 65°$ to $\gamma = 85°$ for high-rise arches. Suggested angle change spreads from $\Delta\gamma = -1.5°$ to $\Delta\gamma = -3.0°$ for all arch rises. For parabolic arch shape, the suggested starting angle spreads from $\gamma = 50°$ to $\gamma = 60°$ for shallow arches, and from $\gamma = 60°$ to $\gamma = 70°$ for medium and high-rise arches. The recommended angle change is from $\Delta\gamma = -1.5°$ to $\Delta\gamma = -3.0°$, and from $\Delta\gamma = -1.0°$ to $\Delta\gamma = -3.0°$, and from $\Delta\gamma = -0.5°$ to $\Delta\gamma = -2.5°$ for shallow, medium and high arch rises respectively.

The percentage of relaxed hangers corresponding to the best outlines is acceptably low, however some relaxation of hangers always takes place. Patterns without hanger relaxation, according to criterion *H*, have higher values of bending moments, and often hangers become located almost horizontally. Such location of hangers results in high value of stress range in the pattern and therefore should be avoided.

5. Acknowledgements

This work has been made possible by a project grant received from The Research Council of Norway (208052) and financial and technical support from The Association of Norwegian Glulam Producers, Skogtiltaksfondet and Norwegian Public Road Authorities. These contributions are gratefully acknowledged. This work was also supported by the WoodWisdom-Net+ project DuraTB ("Durable Timber Bridges") and the support from the partners is appreciated.

6. References

1. Tveit P., *The design of network arches.* The Structural Engineer, 1966. **44**(7): p. 249-259.
2. Pipinato A., *Innovative Bridge Design Handbook: Construction, Rehabilitation and Maintenance*. 2016: Elsevier Science.

3. Teich S., *Entwicklung allgemeiner Entwurfsgrundsätze für Hängernetze von Netzwerkbogenbrücken, (Development of general design principles for the hanger arrangements of network arch bridges).* Stahlbau, 2011. **80**(2): p. 100-111.
4. Schanack F., *Puentes en Arco Tipo Network, (Network Arch Bridges). Doctoral Thesis*. 2008, Department of Structural Engineering and Mechanics, Technical College of Road, Channel and Port Engineering, University of Cantabria, Spain.
5. Pellegrino C., G. Cupani, and C. Modena, *The effect of fatigue on the arrangement of hangers in tied arch bridges.* Engineering Structures, 2010. **32**(4): p. 1140-1147.
6. Schanack F. and B. Brunn, *Analysis of the structural performance of network arch bridges.* Indian Concrete Journal, 2009. **83**(1): p. 7-13.
7. Teich S., *Die Netzwerkbogenbrücke, ein überaus effizientes Brückentragwerk - Tragwirkung und Konstruktion, (The network arch bridge, an extremely efficient structure - Structural behaviour and construction).* Stahlbau, 2005. **74**(8): p. 596-605.
8. De Zotti A., C. Pellegrino, and C. Modena. *A parametric study of the hanger arrangement in arch bridges*. in *5th international conference on arch bridges ARCH '07*. 2007.
9. Brunn B. and F. Schanack, *Calculation of a double track railway network arch bridge applying the european standards. Graduation thesis*. 2003, Dresden University of Technology.
10. Schanack F. and B. Brunn, *Netzgenerierung von Netzwerkbogenbrücken, (Generation of network arch hanger arrangements).* Stahlbau, 2009. **78**(7): p. 477-483.
11. CEN, *EN 14080: Timber structures - Glued laminated timber and glued solid timber - Requirements*. 2013: Brussels, Belgium.
12. CEN, *EN 1991-2: Eurocode 1: Actions on structures -Part 2: Traffic loads on bridges*, in 2003: Brussels, Belgium.
13. Hibbit K., Sorensen, *ABAQUS/Standard Analysis User's Manual* 2007.
14. *Python Software Foundation*. https://www.python.org/.
15. CEN, *EN 1995-1-1: Eurocode 5: Design of timber structures -Part 1-1: General - Common rules and rules for buildings*, in 2004: Brussels, Belgium.

Paper II

Parametric study of radial hanger patterns for network arch timber bridges with a light deck on transverse crossbeams

(*Accepted by Engineering Structures on 10 October 2017*)

Parametric study of radial hanger patterns for network arch timber bridges with a light deck on transverse crossbeams

Anna Weronika Ostrycharczyk & Kjell Arne Malo

ABSTRACT: This paper studies network arch timber bridges. The network patterns considered in the paper are suitable for bridges with a light deck on evenly spaced transverse crossbeams. Therefore, the equidistant distribution of hangers fastening points along the deck is assumed. In bridges made of steel and concrete, hangers are usually equally distributed along the arch. In presented cases, hangers distribution along the arch results from values of parameters like: a number of hangers, an arch rise, a bridge span and hangers inclination. This paper introduces a new network pattern as a modification of a radial pattern. The presented analyzes were performed as a parametric study of variable geometric parameters, on a vast set of 2D FEM models of the network arch with modified radial pattern. The focus was on bending moment distribution on the arch, as it is highly sensitive to even small changes in hanger arrangement. In addition, as a light deck may increase hanger relaxation, the number of relaxed hangers was also analyzed. Values of bending moments were obtained from static analyzes of different load cases, with symmetrical and unsymmetrical load applied on the deck. The results indicate, that introduced radial network pattern modification can improve the performance of the network arch.

KEYWORDS: Network arch, arch bridge, timber, transverse crossbeams, radial pattern, parametric studies, circular arch; timber deck

NOTATION:

l	– deck length [m]
f	– arch rise [m; %]
r	– arch radius [m]
n	– number of transversal crossbeams [-]
α	– spread angle in radial pattern [°]
C_a, $C_a(0,0)$	– arch centre origin
C_h, $C_{h,L}$, $C_{h,R}$	– centre for hanger ray (focal point); $C_{h,L}$ - left centre; $C_{h,R}$ - right centre
x, y	– coordinate system
X, Y	– particular coordinate
$\mathbf{X}$, $\mathbf{Y}$	– set of coordinates; $\mathbf{X} = \{X_1, X_2, ..., X_n\}$; $\mathbf{Y} = \{Y_1, Y_2, ..., Y_n\}$
$p_{f^*\alpha^*}$	– reference pattern; a particular pattern in which values of l, n, f, α are fixed, and $X = 0$ and $Y = 0$
$\mathbf{P}_{f^*\alpha^*\mathbf{XY}}$	– set of modified patterns; a group of patterns where values of l, n, f, α are fixed and equal to such values for reference pattern $p_{f^*\alpha^*}$, while $X \in \mathbf{X}$ and $Y = 0$ for X-configuration; $X = 0$ and $Y \in \mathbf{Y}$ for Y-configuration; one or both $X \in \mathbf{X}$ and $Y \in \mathbf{Y}$ for XY-configuration
$M_{\max}$	– maximum (absolute) value of the in-plane bending moment in the arch obtained for the most unfavourable position of the loading; [kNm]
$\mathbf{M}_{f^*\alpha^*\mathbf{XY}}$	– set of bending moments $M_{\max}$ obtained for all patterns in one set of modified patterns $\mathbf{P}_{f^*\alpha^*\mathbf{XY}}$; [kNm]
$M_{\min,\, f^*\alpha^*\mathbf{XY}}$	– lowest bending moment out of set of bending moments $\mathbf{M}_{f^*\alpha^*\mathbf{XY}}$ obtained for one set of modified patterns $\mathbf{P}_{f^*\alpha^*\mathbf{XY}}$; [kNm]
$R_{f^*\alpha^*\mathbf{XY}}$	– ratio of lowest bending moment $M_{\min,\, f^*\alpha^*\mathbf{XY}}$ to bending moment $M_{\min,\, f^*\alpha^*}$ for adequate reference pattern: [-]
H, $H_{f^*\alpha^*}$, $H_{f^*\alpha^*\mathbf{XY}}$	– maximum number of relaxed hangers in individual pattern, as a percentage of all hangers in the pattern [%]; H – in any pattern; $H_{f^*\alpha^*}$ – in reference pattern; $H_{f^*\alpha^*\mathbf{XY}}$ – in a single modified patterns with $M_{\min,\, f^*\alpha^*\mathbf{XY}}$; [%]
$\Delta H_{f^*\alpha^*\mathbf{XY}}$	– difference between percentage of relaxed hangers $H_{f^*\alpha^*}$ for reference pattern and $H_{f^*\alpha^*\mathbf{XY}}$ for modified pattern; [%]

1 Introduction

Hanger patterns used in steel or concrete network arch bridges are usually based on an equidistant distribution of hangers along the arch. This paper deals with parametric studies of a particular type of hanger pattern, namely a radial pattern, in which, additionally, the hangers are distributed equidistantly along the deck. Such patterns are suitable for timber arch bridges with transverse crossbeams.

The network arch bridge concept was introduced in Norway by Per Tveit [1] in the early 1960 as bowstring arches with multiple crossing hangers. In the classic arch bridge, the hangers are vertical. The great advantage of the network arch compared with an arch with vertical hangers, is the more efficient use of materials due to a fairly uniform force distribution in the structure. A steel bridge with vertical hangers may require up to 4.5 times more material than a corresponding network bridge [2]. Force distribution depends on many parameters; the number of hangers and pattern type are perhaps the most important. A good design gives small values of bending moments in arch and deck, as well as nearly constant axial forces in arch and hangers. The most popular patterns such as: radial, fan, constant or changeable inclination of hangers, have been studied by several researchers; see Figure 1. Tveit [1] and [2] analyzed structural performance and weight of different network bridges with constant inclination of the hangers. Teich [3] compared structural performance of bridges with vertical, constant inclination and changeable inclination of hangers, while in [4] he performed a wide range studies of five different patterns, focusing on force distribution in the hangers. Parametric studies on radial patterns were performed by Brunn and Schanack in [5] and in [6]. More studies on structural performance in bridges with vertical, fan and network patterns were performed by De Zotti et al. [7] while Pellegrino et al. [8] used hanger forces as a basic comparative criterion.

In the above-mentioned studies, the reference concrete or steel bridges were usually made with heavy concrete decks, suitable for car or train traffic. Different comparative criteria have been used, focusing on forces in the hangers, important for the fatigue phenomena, or moment distribution in the arch, enhancing the structural performance and reducing material costs. A common feature for most of these studies is the premise of equidistant distribution of hangers along the arch leading to uneven spacing between hangers at the deck.

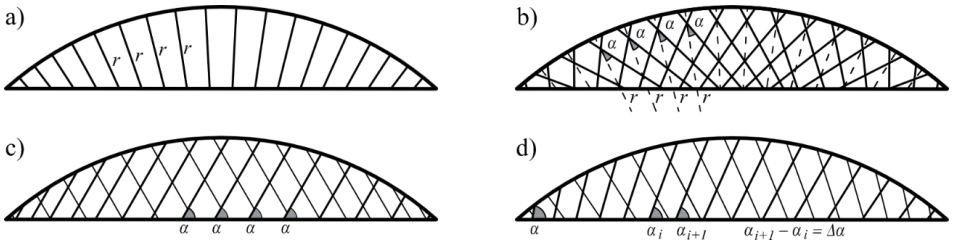

Figure 1 Different hanger patterns; a) fan; b) radial; c) constant hanger inclination; d) constant change of hanger inclination.

In this study, the reference bridge has both arches and deck made of timber. The deck is therefore light and relatively soft, and it rests on transverse crossbeams. The crossbeams are hence the natural fastening points for the hangers as well as supports for the deck structure. Equidistant location of the hangers at the deck level is a basic premise for this class of network bridges. Examples of use of this premise can be found in [9] in which both the design and execution process of such a network bridge are described. In [10] equidistant location of hangers at the deck level is mentioned among different pattern options for a 1.1 km long multi-span bridge. The present paper put the emphasis on network arch bridges having equidistant location of hangers at the deck.

2 Methodology – general information

The reference bridge has two identical circular arches, and for each arch the centre of curvature, denoted C_a, is the origin at which $X = Y = 0$, see Figure 2. The reference hanger pattern has radial arrangement, with respect to C_a and equidistant crossbeams; see Figure 2 and Figure 3. The radial hanger pattern is obtained in the following way: a radial ray, from the origin $C_a(0,0)$ to the location of the crossbeam at the deck level, defines the average direction of a pair of hangers. At the crossbeam, one hanger of the pair is rotated to the left of the ray by the spread angle α, while the other hanger is rotated to the right by the same spread angle (α). A consequence of this approach is that the distance between the fastening points on the arch will vary. Furthermore, each hanger's fastening location on the arch depends on configuration parameters such as: deck length l, arch rise f, number of crossbeams n and spread angle α. The radius r is the radius of curvature of a circular arch through three points, one at each end and one at the crown. While the location of C_a and magnitude of r are defined by the circular arch through the three specified points, the actual arch shape may also be a parabola through the three specified points.

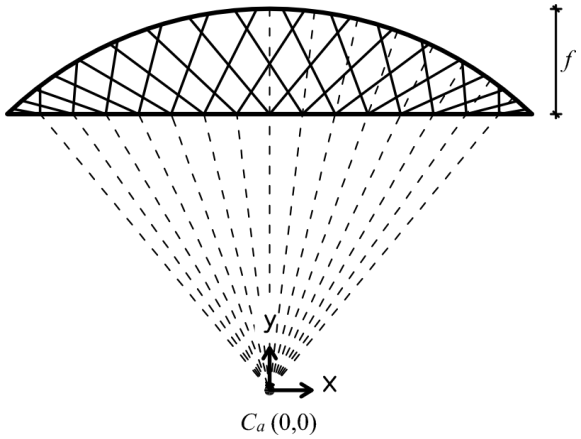

Figure 2 Radial pattern for bridge with crossbeams.

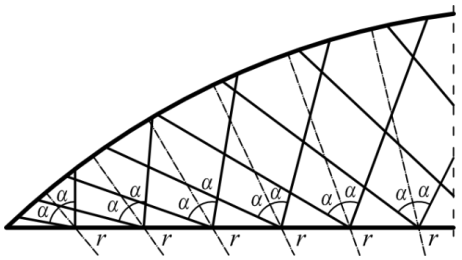

Figure 3 Pair of hangers in radial pattern for bridge with equidistant crossbeams.

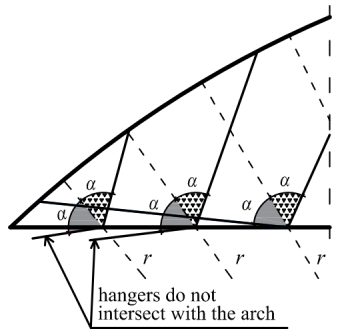

Figure 4 Radial pattern with excluded hangers.

In this study, only one type of arch shape is considered, namely the circular shape, and the three mentioned points define uniquely one circular arch. For a network pattern based on the location of the crossbeams, it is possible that, for high values of α, high f or low number of n, some hangers may not intersect the arch. Figure 4 illustrates a pattern with the following parameters: $n=15$, $f=20$ and $\alpha=55°$. For this configuration, two hangers h_1 and h_2, associated with the two outermost crossbeams do not intersect the arch. Consequently, they are removed from the pattern.

The parametric study reported here, deals with a number of radial hanger patterns. In the basic, reference hanger configuration the centre of the arch $C_a=(0,0)$ and the centre of the radial hanger rays, $C_h(X,Y)$, coincide, such that the coordinates X and Y of the centre of the hanger rays are both equal to zero. Three modifications of the radial pattern were investigated.

In the first modified configuration, the centre C_h is given an offset in the horizontal x-direction. In order to retain pattern symmetry, two centres, $C_{h,L}$ and $C_{h,R}$, located on negative and positive part of the x-axis, respectively, are introduced in the case of an even number of crossbeams; see Figure 5a. For an odd number of crossbeams, three centres $C_{h,L}$, $C_h = C_a$ and $C_{h,R}$ are introduced; confer Figure 5b. For patterns with an odd number of crossbeams, the hangers from the central crossbeam are based on the centre $C_h = C_a\ (0,0)$ while those located on the negative side of the x-axis originate from centre $C_{h,L}$ and those located on the positive side of x-axis originate from centre $C_{h,R}$. The patterns modified by the x-direction offsets are denoted X-configuration.

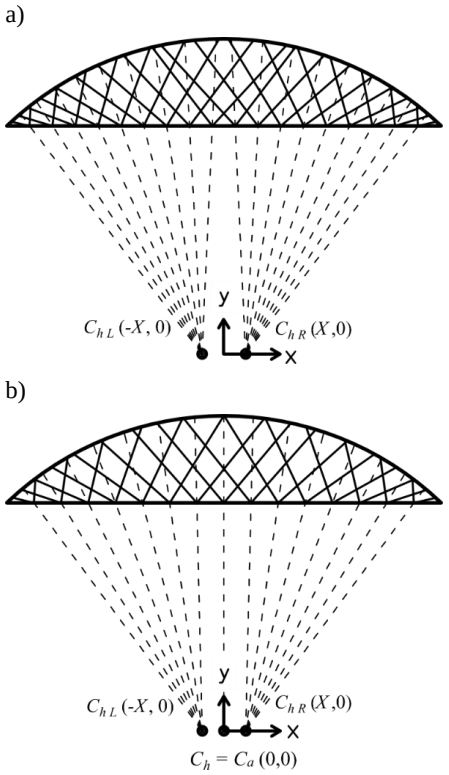

Figure 5 Modified radial pattern with horizontal offset (X-configuration) for a bridge with a variable number of crossbeams; a) even number; b) odd number.

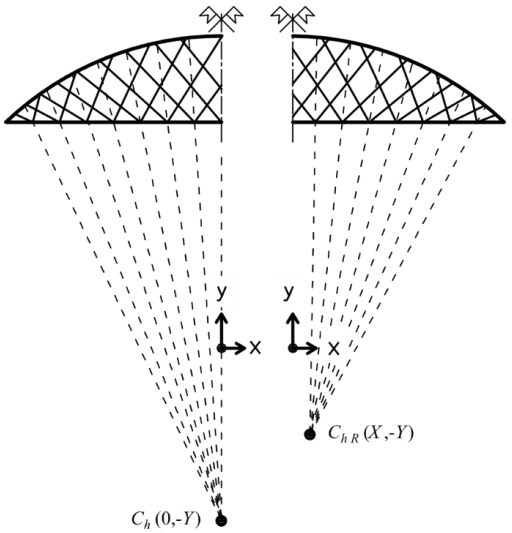

Figure 6 Modified radial pattern; Vertical offset (Y-configuration) on the left-hand side; Horizontal and vertical offset (XY-configuration) on the right-hand side

The second modification applied to the reference radial pattern is an offset of the C_h centre in the vertical y-direction only; see left-hand side of Figure 6. For this modification, no splitting of the C_h centre is necessary. The C_h centre can be moved up or down the y-axis. This pattern modification is denoted Y-configuration.

The third modification applied to the basic radial pattern, denoted XY-configuration, is obtained by simultaneous offsets of the C_h centre in both the horizontal and the vertical direction; see right-hand side of Figure 6. This results in a splitting of the centre C_h as in the X-configuration. Note that there are now two centres $C_{h,L}$ and $C_{h,R}$ in the x-direction, but the Y offset must be the same for both of them.

The analyses presented herein are based on 2D models of the different hanger configurations. To define geometrical and material properties of the 2D model, a reference 3D FEM model of the complete bridge was used. The reference bridge is a two-lane car bridge having a 7 m wide and 100 m long deck, the arch rise is 14 m and the loading is in accordance with Load Model 1 defined in [11]. The glulam arches have a constant cross-section of 1000×600 mm and the wooden deck has a thickness of 500 mm. Material properties for arches and deck are according to the relevant European codes for glulam GL30c and GL24c, respectively. The hangers are made of steel and have diameter of 60 mm. The 3D numerical model of the reference bridge was created in Abaqus software [12], and designed according to the requirements in the European codes. For the present study of the in-plane behaviour, the 3D model was simplified into a 2D model. All dimensions of the arch and the hangers in 2D model remained as in the 3D model, while the deck in 2D model become a 3500×500 mm beam, which constitute half of the deck in 3D. Both the arch and the deck (in 2D), are modelled as beam elements pinned on both ends, thus the horizontal forces are transferred from the deck to the abutments.

The parameters to be varied are: arch shape, arch rise, number of crossbeams, spread angle and location of the centre of the hanger rays. The analysis of each configuration is performed in 11 steps, one for each of 11 different load cases (LC). The self-weight of the structure is applied in the first step as a gravity load. The effects of the gravity are included in all further steps. For the next load cases, a vertical live load is applied on the deck with a stepwise increase of the loaded length, from 10% of the deck length up to 100%. The step size is 10% of the full deck length, and the load is applied sequentially from left to right of the model. By this approach, the applied load in the last load step becomes uniformly distributed along the entire deck. This load variation methodology provides a systematic and comparable load application, independent of the hanger arrangement. Furthermore, it allows for determining the largest arch bending moment related to the most unfavorable skew loading. The value of the live load in 2D models is

set to 38 kN/m, and is obtained by a linear interpolation of Load Model 1 values, defined for the 3D FEM model for the ultimate limit state, after persistent and transient combination of action according to [13]. For simplification, there are no point loads form wheel axels, present in Load Model 1 [11], in any of the 2D models considered.

The objective of the present study is to explore and develop optimized radial patterns for the inclined hangers of timber arch bridges with crossbeams. The parametric studies were organized in 5 steps. In the first step a suitable range of the number of crossbeams was determined. Second, the influence of the spread angle α was investigated. The first and the second steps were performed on basic radial hanger patterns only. The last three steps of the study focused on the three different radial pattern configurations; X-, Y- and XY-configuration. Several python scripts [14] were developed and coupled to the Abaqus software [12], thus providing efficient tools for systematic studies. The scripting procedure is based on a general configuration file defined by the user, in which all parameters are defined as a series of values. The general configuration file constitutes the base for creating specific sets of particular files representing the specific sets of parameters in the range. Each file is fed into Abaqus, in which the particular hanger arrangement is established and executed. The results from all individual analyses are collected into a common database, created for comparison of the results. Since the hangers can only take tension forces, all analyses performed are nonlinear, using the Abaqus implicit solver method.

In the present study two criteria were chosen for the comparison of the hanged configurations. The main criterion is the magnitude of the maximum (absolute) value of the in-plane bending moment, $M_{\max}$ [kNm], in the arch, as obtained for the most unfavorable position of the loading. The second criterion is the number of relaxed (stressless) hangers. Since the reference timber bridge is a relatively light structure, self-weight of the deck alone does not prestress the hangers sufficiently to maintain tensile forces for all load cases. Hence, some hangers may become relaxed, which means that they do not transfer any load. The criterion of maximum number of relaxed hangers, denoted H, is expressed as the percentage of simultaneously relaxed hangers for the most unfavorable load case.

3 Parametric study of radial reference hanger patterns

The results of the study are presented in two parts: the reference patterns and the modified patterns as described in Section 2. In this section the basic reference patterns are dealt with, while the modified patterns are presented in the next section. The length of the bridge is in all cases 100 m. Six different arch rises (f) were included in the studies. The value of f is given in meters, but it can also be expressed as percentage of the bridge

span. The shallow arches have $f = 10$ and $f = 13$, the medium rise arches $f = 16$ and $f = 19$, and high rise arches have $f = 22$ and $f = 25$.

3.1 Number of crossbeams

The number of crossbeams determines the number of fastening points for the hangers, and thus the number of hangers. This is one of the crucial parameters, not only for the present studies, but also for the design of network arch bridges in general. Intuitively, the more hangers present in the pattern, the lower will the arch bending moment and the hanger forces be. Theoretically, a very large number of hangers will almost eliminate the bending moment in the arches, but it will also rise the cost of crossbeams, hangers and human labour related to production and installation. If the hangers are attached to a steel edge beam, or to the deck itself in case of a concrete deck, the cost of the hangers is proportional to their number. For timber bridges with crossbeams, each hanger pair is attached to a crossbeam, and therefore it is important to find a balance, between the number of hangers and number of crossbeams.

In the first part of the study, the parameters varied are:

- number of crossbeams n from 8 to 35 in steps of 1,
- arch rise f from 10 to 25 in steps of 3, and
- spread angle α from $25°$ to $70°$ in steps of $5°$.

The deck length is constant and equal to 100 m. The specified parameter ranges result in a total of 1680 different patterns. All patterns are subjected to the gravity load as well as to the ten load cases (LC) from 10% to 100% in steps of 10%.

Figure 7a and Figure 7b show the relation between the maximum bending moment in circular arches and the number of crossbeams for hanger spread angles $\alpha = 30°$ and $50°$, respectively. Increasing the number of crossbeams noticeably changes the moment curves. After reaching a certain number of crossbeams the curves flatten out. For shallow arches this happen at about 12 crossbeams, for medium rise arches at about 15 and for high rise arches at about 23 crossbeams. For more than 26 crossbeams, the moment decrease is insignificant (gives no benefit), but causes extra costs. Free spans of stress-laminated timber decks can be up to 15.8 m (52 feet) according to [15] and in some cases up to 18m [16]. However, the deck crossbeam spacing is typically much shorter. For instance, the timber deck of the Tynset car bridge in Norway is supported by crossbeams at about every 5.4 m.

a)

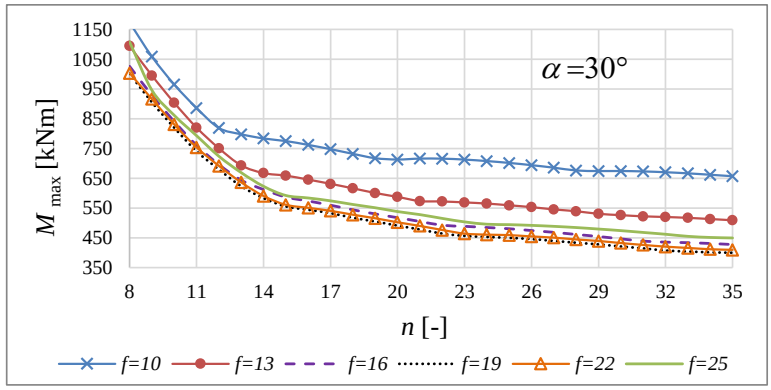

b)

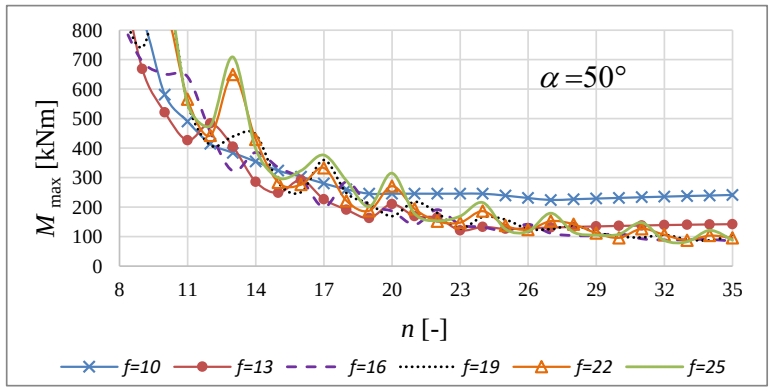

Figure 7 Maximum bending moment $M_{\max}$ as a function of the number of crossbeams n, for different arch rise f and spread angle α; a) $\alpha = 30°$; b) $\alpha = 50°$.

For low spread angle values, in the range from $25°$ to $40°$, the moments as functions of the number of crossbeams relation are steadily decreasing curves; see Figure 7a. For spread angles above $40°$ the corresponding curves show fluctuations. This property is more noticeable for larger angles and higher arches. The cause of this effect is an unfavourable position of two hangers attached very closely to the arch. Such coinciding locations produce high values of bending moments. The closer the hanger attachments are, the higher local moment is to be expected, especially in the central part of the arch. Figure 8 shows hanger patterns for 12, 13, 14 and 15 crossbeams, respectively, for a constant spread angle $\alpha = 50°$ and an arch rise $f = 25$. In the figures, the locations of the maximum moments are marked with circles, while the moment value and the load case that caused it, are given in the figure text; see also Figure 7b.

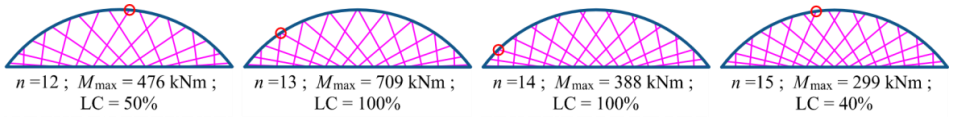

Figure 8 Location of M_{max} for patterns with different number of crossbeams, arch rise $f = 25$, and spread angle $\alpha = 50°$; LC – load case, represents percentage of loaded deck length that causes M_{max}.

Based on all results from the first part of the parameter studies, the best range for the number of crossbeams seems to be between 15 and 21 for a 100 m long bridge. There is no visible influence coming from odd or even number of crossbeams. However, the effect of hangers coinciding at the arch, appears to be more noticeable in bridges with an odd number of crossbeams.

In order to simplify the comparison of the analyses, all further hanger patterns are established on models having $n = 18$ crossbeams, which is a mean value of the suggested range, and which gives a spacing of 5.55 m between the crossbeams.

3.2 Effect of the hanger spread angle α

In the second part of the parametric study, the influence of the spread angle α on the structural performance of the reference bridge was investigated. The deck length (100 m) and the number of crossbeams (18), were kept constant in these studies. The parameter variation is:

- arch rise f from 10 to 25 in steps of 3, and
- spread angle α from 0° (fan outline) to 70° with the step size 0.5°.

The selected ranges results in a total of 846 patterns. Figure 9a-c show the influence of the spread angle α with respect to shallow, medium and high rise arches, respectively. Continuous and dashed lines represent maximum moment values for a particular arch rise, while circles and plus signs represent maximum number of relaxed hangers. The trend in all moment curves is similar. Initially, for increasing spread angles the moment decreases and reaches a local minimum. Thereafter the moment increases slightly, with some fluctuations. An enlarged view of these fluctuations, for an arch rise $f = 19$ and load on 80% of the deck length, is plotted in Figure 10. The cause of the fluctuations is similar to the previous discussion with respect to Figure 7b, i.e. coinciding locations of fastening points of the hangers at the arch.

a)

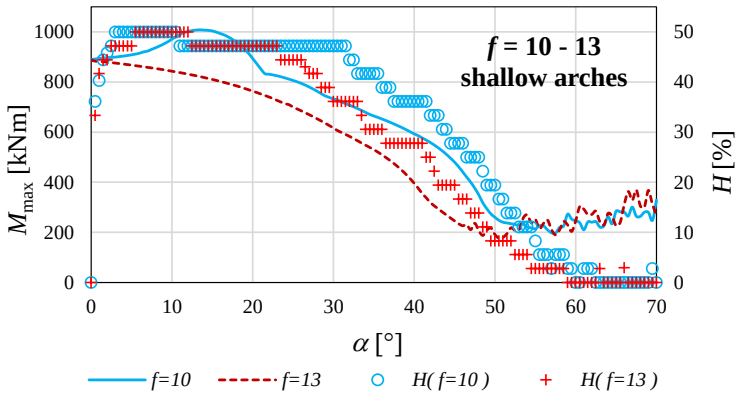

b)

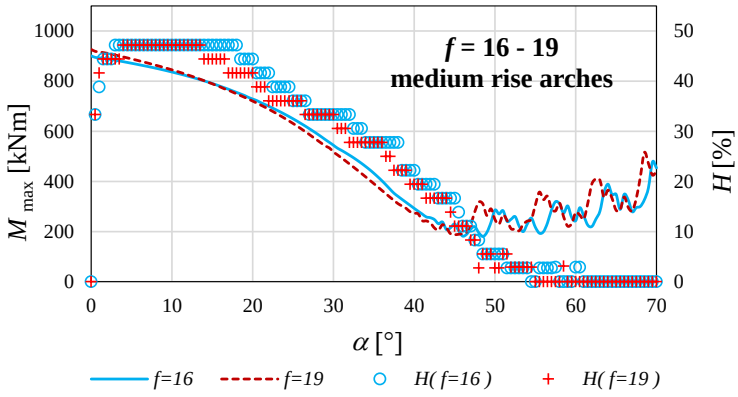

c)

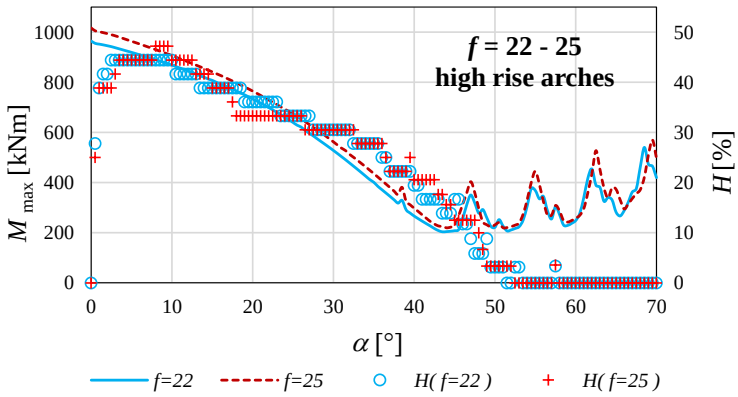

Figure 9 Maximum bending moment M_{max} and number of relaxed hangers H as function of angle α; a) shallow arches; b) medium rise arches; c) high rise arches.

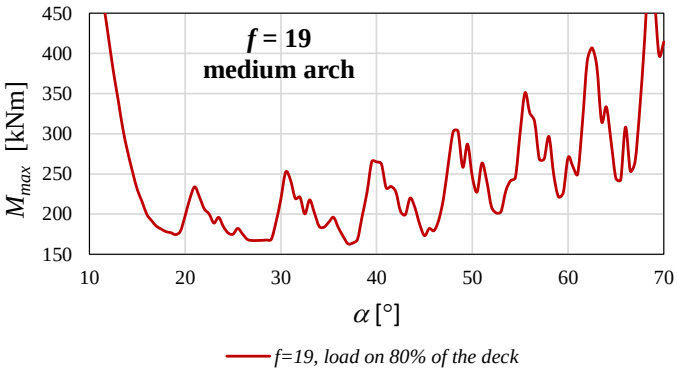

Figure 10 Maximum bending moment $M_{\max}$ as function of angle α for arch rise $f = 19$ and load on 80% of the deck.

The maximum values of the moment usually occur for fan arrangement of hangers. Only for a very shallow arch (with $f = 10$), the moments increase within the first $15°$ and thereafter follow the general decreasing trend. Furthermore, for shallow arches, there is a clear difference between the two curves representing the bending moments for the two arch rises, a difference that is not present for medium and high-rise arches. There are no relaxed hangers ($H = 0\%$) among patterns with fan hangers outline, but for spread angles α in the range of $0.5°$ to $20°$, H reaches a peak value at almost 50%. For spread angles above about $20°$ the number of relaxed hangers decreases almost linearly from 50% to 0% for spread angles α at about $50-60°$, depending on the arch rise. For spread angles α above this level there are no relaxed hangers. It is worth noting that hangers in patterns with spread angle α above $45°$ may be oriented almost horizontally. Note also that some hangers in such patterns are excluded from the outline; see Figure 4 and Figure 8.

Table 1 Summary of lowest $M_{\max}$ and corresponding α and H for variable arch rises

f [m; %]	lowest $M_{\max}$ [kNm]	α [°]	H [%]
10	197	57.5	5.6
13	176	50.5	8.3
16	180	48.5	5.6
19	187	45.0	11.1
22	203	43.5	13.9
25	219	44.0	15.6

The lowest magnitudes of the bending moments $M_{\max}$, for all arch rises considered, are presented in Table 1 along with corresponding spread angle α and percent of relaxed hangers. It can be observed that it is, in theory, possible to reduce the maximum moment to only 1/5 of the maximum moment in a corresponding bridge with fan arrangement of hangers. This, however, requires quite a large spread angle α. Furthermore, it appears that the number of relaxed hangers H, increase with increasing arch rise.

4 Modified patterns

The study of modified patterns is related to a set of reference patterns chosen on the basis of the results presented in Section 3.

4.1 Organization of modified pattern analyses

In the subsequent study of modified patterns, each pattern is a function of four parameters: f-arch rise, α-spread angle, and coordinates X and Y of the ray centre, C_h. The number of crossbeams and the deck length, are kept constant at values $n=18$ and $l=100$.

The pattern identification is:

$$P(f,\alpha,X,Y) \qquad (1)$$

where :

- arch rise f, spanning from 10 to 25 in steps of 3,
- spread angle α, spanning from $25°$ to $70°$ using steps of $5°$,
- offset coordinates $X \in \mathbf{X}$ and $Y \in \mathbf{Y}$ of the ray centre (C_h), where the centre of curvature, C_a, of the circular arch through the 3 defining points, is defined as the origin,
- $\mathbf{X}$ is a set of *X*-values which defines offset of C_h in the horizontal direction, and
- $\mathbf{Y}$ is a set of *Y*-values which defines offset of C_h in the vertical direction.

The reference pattern is defined as:

$$p_{f^*\alpha^*} = p_{f^*\alpha^*,0,0} = P(f^*\alpha^*,0,0), \text{ so } X=0 \text{ and } Y=0; \qquad (2)$$

where the asterisk (*) symbolizes a fixed value that applies to a reference pattern and the set of modified patterns.

A set of patterns with modifications is defined as

$$\boldsymbol{P}_{f^*\alpha^*\boldsymbol{XY}} = P(f^*, \alpha^*,\ X \in \boldsymbol{X},\ Y \in \boldsymbol{Y}), \tag{3}$$

where f and α are kept constant, while X and Y are varied.

The moment function for a certain pattern (configuration) is given by:

$$M(P(f, \alpha, X, Y)). \tag{4}$$

The maximum (absolute) value of the bending moment for a certain pattern (configuration) is:

$$M_{\max} = M_{\max, f, \alpha, X, Y} = M_{\max}(P(f, \alpha, X, Y)). \tag{5}$$

A set of maximum moments for modified patterns is defined by:

$$\boldsymbol{M}_{f^*\alpha^*\boldsymbol{XY}} = M_{\max}(P(f^*, \alpha^*,\ X \in \boldsymbol{X},\ Y \in \boldsymbol{Y})). \tag{6}$$

The minimum value of the maximum bending moments occurring in a set of maximum moments is denoted by:

$$M_{\min,\ f^*\alpha^*\boldsymbol{XY}} = \min\left(\boldsymbol{M}_{f^*,\alpha^*,\boldsymbol{X},\boldsymbol{Y}}\right), \tag{7}$$

identified by the pattern

$$P_{\min,\ f^*\alpha^*\boldsymbol{XY}}. \tag{8}$$

It should be noted that there are 60 sets of modified patterns, corresponding to ten angles and six arch rises considered in the analysis. Consequently, there are also 60 sets of maximum moments for modified patterns and 60 values of $M_{\min,\ f^*\alpha^*\boldsymbol{XY}}$. In the above notation, bold-face style, e.g. $\boldsymbol{M}$, always refers to a set of values, or set of patterns, while regular typeface style, e.g. M, refers to a particular value or pattern.

4.2 Effect of separate centres for arch and radial rays. Horizontal offset. X-configuration.

In the third step of the study, horizontal offsets were applied at the location of the C_h centre. The X-coordinates of centres $C_{h,L}$ and $C_{h,R}$ were shifted with offsets from $X = 0.5\,\text{m}$ to $X = 50\,\text{m}$ using a step size of $0.5\,\text{m}$, in both negative and positive x-direction. Thus different sets $\boldsymbol{P}_{f^*\alpha^*\boldsymbol{X}}$, Equation (3), of patterns with modifications are based on $\boldsymbol{X} = \{0.5, 1, 1.5, ..., 50\}$ [m] and $Y = 0\,\text{m}$. In total 6060 patterns were analyzed. An

X -coordinate equal to 0 m represents a basic, reference radial pattern, see Figure 2 and Equation (2). Examples of pattern outlines, where $X = 5,\ 25$ and $50\,\text{m}$, for $f = 16\,\text{m}$ and $\alpha = 35°$, are presented in Figure 11.

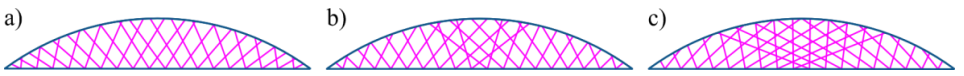

Figure 11 Pattern outlines for different X-configurations; a) P ($f = 16, \alpha = 35°, X = 5,\ Y = 0$); b) P($f = 16, \alpha = 35°,\ X = 25,\ Y = 0$); c) P($f = 16, \alpha = 35°,\ X = 50,\ Y = 0$).

Figure 12 shows selected results for the X-configuration. In the graphs, the moment $M_{\max}$, Equation (5), is presented with reference to the X -coordinate value, limited to the range between 0 m and 14 m. The plots show results for arch rises $f = 10$, 16 and 22 m, which represent shallow, medium and high-rise arches. The general tendency is that for low values of horizontal offset, moment value decreases and reaches a local minimum. Thereafter an increase takes place. For shallow arches, the curves are quite smooth, while for higher values of f rise increasing fluctuations appear. For horizontal offsets larger than 14 m, the maximum moments are higher than for the reference patterns; hence, they give no benefits.

The X -coordinates of $C_{h,R}$, which refer to patterns $P_{\min,\, f^* \alpha^* \boldsymbol{x}}$, defined by Equation (8) have been determined and presented in Table 2. For $\alpha < 35°$, the increase of the horizontal offset, is likely to be beneficial for increasing arch rise. However, for large spread angles α, the benefit of horizontal offset seems to be limited.

Table 2 X -coordinates [m] for patterns $P_{\min,\, f^* \alpha^* \boldsymbol{x}}$; X-configuration.

α [°]	**25**	**30**	**35**	**40**	**45**	**50**	**55**	**60**	**65**	**70**
$f = 10$	0	0.5	3	3.5	5	1	0	2	2.5	2
$f = 13$	3	3.5	3.5	7	4	0	1.5	0	0	0.5
$f = 16$	3,5	4	7.5	4.5	4	2.5	0	1	0.5	1
$f = 19$	4	7.5	5.5	3.5	0	0	2.5	1	0.5	1
$f = 22$	8.5	9.0	4.5	0.5	0	0.5	1.5	0	0	1.5
$f = 25$	10.5	9.0	7.5	2.5	0	1	2	0	1.5	1

a)

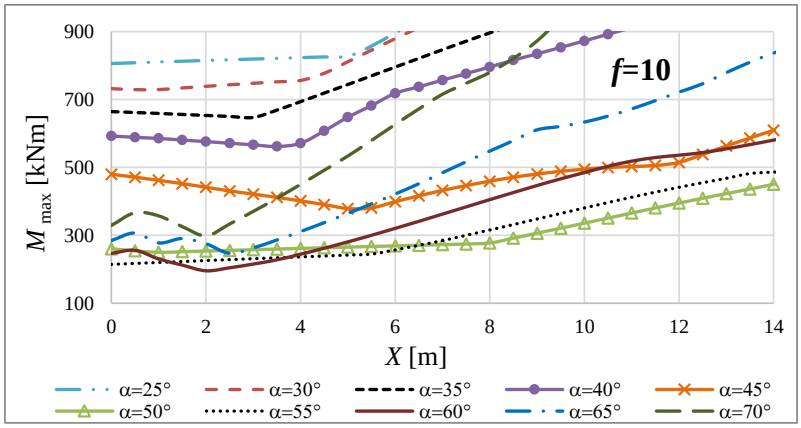

b)

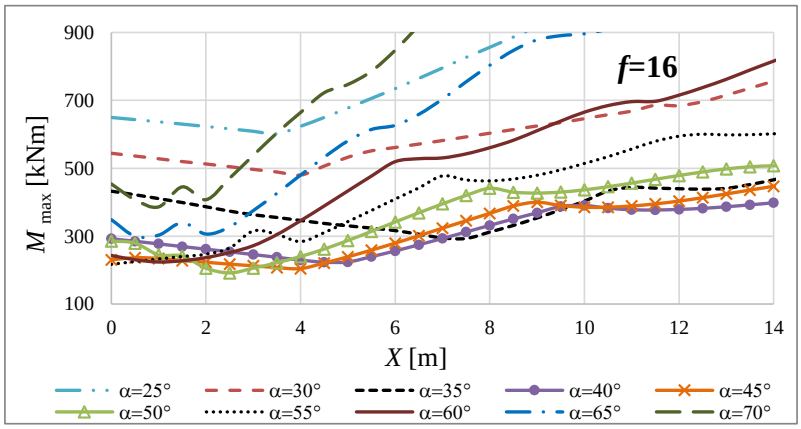

c)

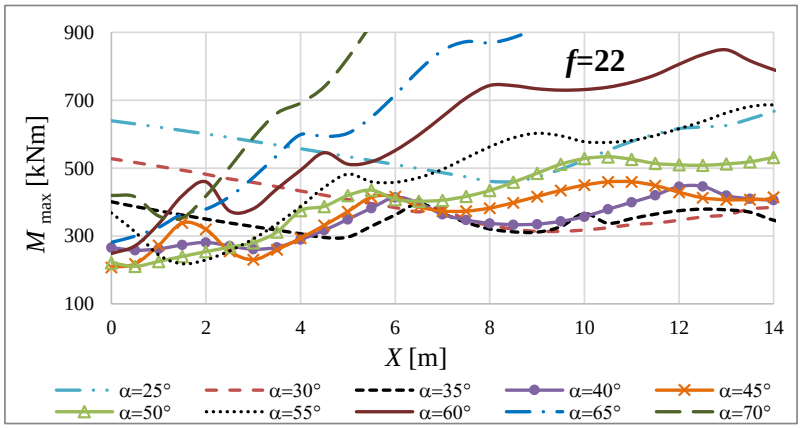

Figure 12 Maximum bending moment M_{max} as a function of the horizontal offset X, for various α and different arch rise; a) $f = 10$ m; b) $f = 16$ m; c) $f = 22$ m; X-configuration.

A ratio, denoted $R_{f^*\alpha^*\blacksquare}$, is defined (in percentage) as:

$$R_{f^*\alpha^*\blacksquare} = \frac{M_{\min,\, f^*\alpha^*\blacksquare}}{M_{\max,\, f^*\alpha^*}} \cdot 100 \ [\%] \qquad (9)$$

where $M_{\min,\, f^*\alpha^*\blacksquare}$, Equation (7), is the lowest value of the maximum bending moment obtained for the set of modified patterns $\mathbf{P}_{f^*\alpha^*\blacksquare}$, Equation (3), and $M_{\max,\, f^*\alpha^*}$, Equation (5), is the maximum bending moment for the reference pattern $p_{f^*\alpha^*}$, Equation (2). The result is presented in Figure 13. The maximum bending moment of any reference pattern $p_{f^*\alpha^*}$ is equal to 100%. Applying the most favorable horizontal offset can reduce the maximum bending moment by almost 50%. For the best case, that is for $f = 25$ and $\alpha = 30°$, the moment drops from 562 kNm to 322 kNm. Nevertheless, for some combinations of arch rise and angle α, the reference pattern is better, in terms of structural performance of the arch, than any pattern with horizontal offset; these combinations have an X-value of zero in Table 2.

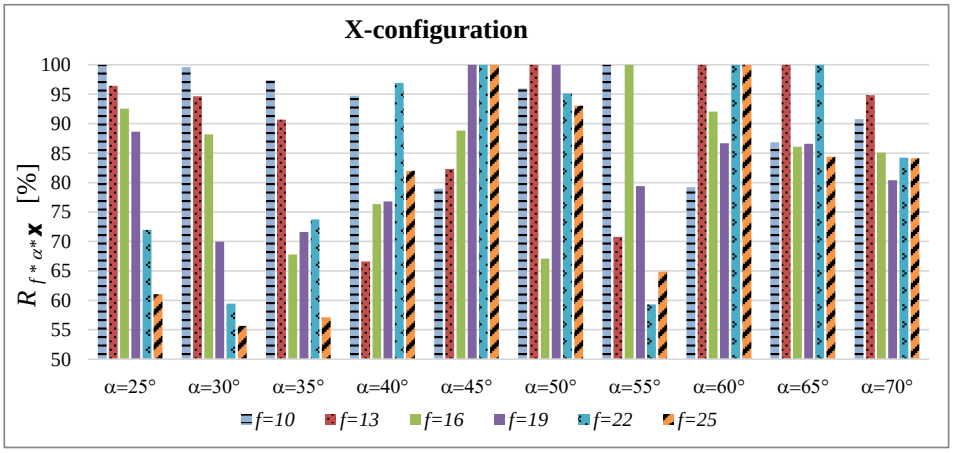

Figure 13 The ratio $R_{f^*\alpha^*\blacksquare}$ for different combinations of f and α; X-configuration.

The columns in Figure 14 show the percentage of relaxed hangers $H_{f^*\alpha^*\blacksquare}$ for $P_{\min,\, f^*\alpha^*\blacksquare}$. In this graph, additional percentage numbers located above some columns, express the difference $\Delta H_{f^*\alpha^*\blacksquare}$ between the percentage of relaxed hangers for the reference pattern $p_{f^*\alpha^*}$ and for the modified pattern $P_{\min,\, f^*\alpha^*\blacksquare}$, i.e.

$$\Delta H_{f^*\alpha^*\blacksquare} = H_{f^*\alpha^*} - H_{f^*\alpha^*\blacksquare}(P_{\min,\, f^*\alpha^*\blacksquare}). \qquad (10)$$

For angle $\alpha \le 45°$ the horizontal offset is advantageous in terms of H. However, for angle $\alpha \ge 55°$, the value of H is not relevant since the number of relaxed hangers, both for the modified and the reference patterns, is very low or equal to zero. The largest influence of a horizontal offset on H, is observed in the pattern with $f = 25$ and $\alpha = 35°$. In this case $H_{25,35,\mathbf{X}} = 16.7\%$, which means 6 relaxed hangers for the modified pattern, while $H_{25,35} = (16.7\% + 11.1\%) = 27.8\%$ for the reference pattern; in other words, 10 relaxed hangers.

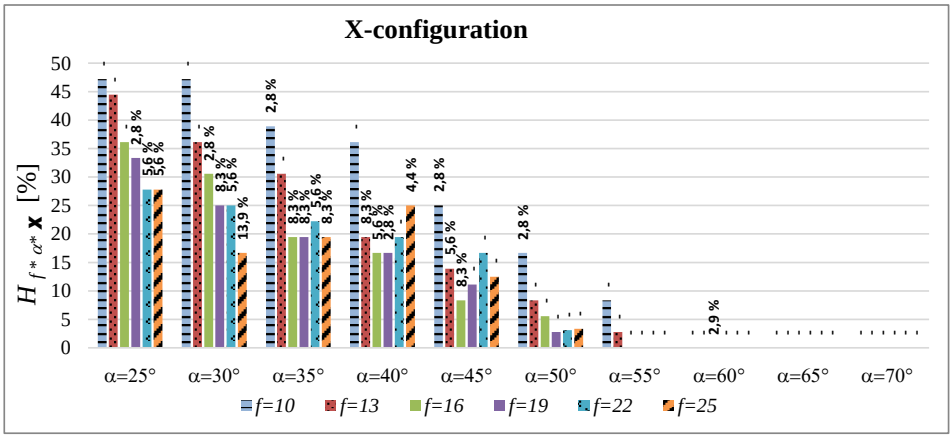

Figure 14 Percentage of relaxed hanger $H_{f^*\alpha^*\mathbf{X}}$ for modified patterns (columns), and differences $\Delta H_{f^*\alpha^*\mathbf{X}}$ between number of relaxed hangers for reference pattern and modified patter (percentage in numbers above columns); X-configuration.

4.3 Effect of separate centres for arch and radial rays. Vertical offset. Y-configuration

In this part a second modification of radial patters was applied. The location of centre C_h is moved along the y-axis, in the range from $Y = -200$ m to $Y = 30$ m, in steps of 10 m. Thus different sets of patterns with modifications, $\mathbf{P}_{f^*\alpha^*\mathbf{Y}}$, Equation (3), are based on $\mathbf{Y} = \{-200, -190, -180, ..., 30\}$ [m] and $X = 0$ [m]. As for the previous section, six different arch rises (f) and ten different angles (α) are considered; hence, a total of 1440 patterns were analysed.

Figure 15 presents selected results for the Y-configuration. In the graphs, the moment $M_{\max}$ is presented with reference to the Y-coordinate value, limited to the range between -150 m and 30 m for all arch rises. The general tendency, especially visible for medium and high-rise arches, is as follows: for a certain offset range, bending moment reaches

local minimum. The moment value grows rapidly for positive values of Y-coordinate. For large negative values of Y-coordinate, the moment increases slightly or the curves flatten out. Some fluctuations of bending moment can be noticed in vicinity of zero value of the Y-coordinate.

The Y-coordinates of C_h, which refer to patterns $P_{\min,\, f^*\alpha^*\blacktriangledown}$, are collected in Table 3. In general, negative vertical offset is beneficial: the majority of Y-coordinates presented in Table 3 is negative. For $\alpha \le 45°$ and medium and high-rise arches, large negative values of vertical offset is the most advantageous. For $\alpha \ge 55°$, positive influence on the moment comes from both small positive or negative value of vertical offset.

Table 3 Y-coordinates [m] for patterns $P_{\min,\, f^*\alpha^*\blacktriangledown}$; Y-configuration.

α [°]	**25**	**30**	**35**	**40**	**45**	**50**	**55**	**60**	**65**	**70**
$f = 10$	10	0	-30	-70	-90	-10	10	-20	10	10
$f = 13$	-30	-70	-60	-60	-40	-30	-40	-50	0	0
$f = 16$	-60	-60	-80	-80	-20	-40	-60	30	20	10
$f = 19$	-60	-70	-110	-50	-60	-70	-30	-30	20	10
$f = 22$	-60	-70	-100	-90	-100	-50	10	-20	0	10
$f = 25$	-60	-90	-110	-100	-60	-30	-10	0	-20	-20

a)

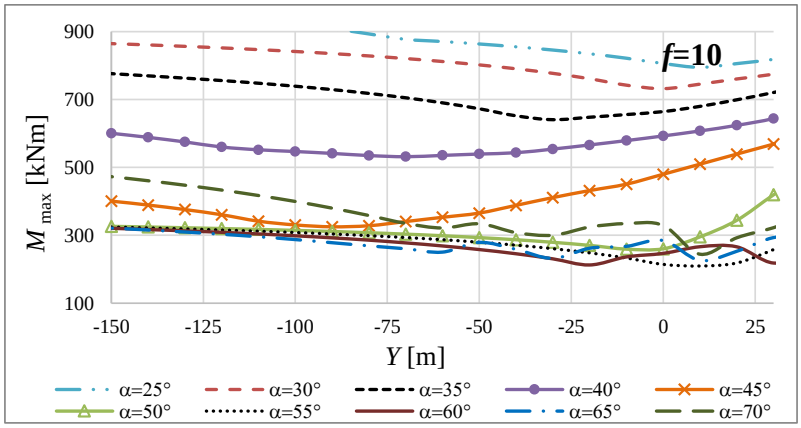

b)

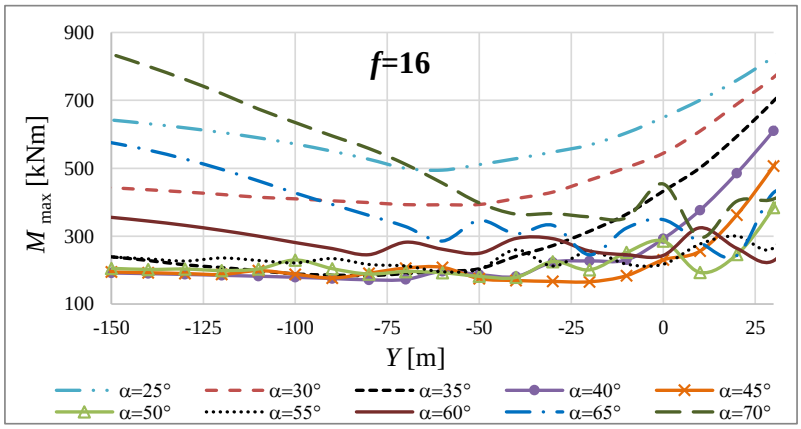

c)

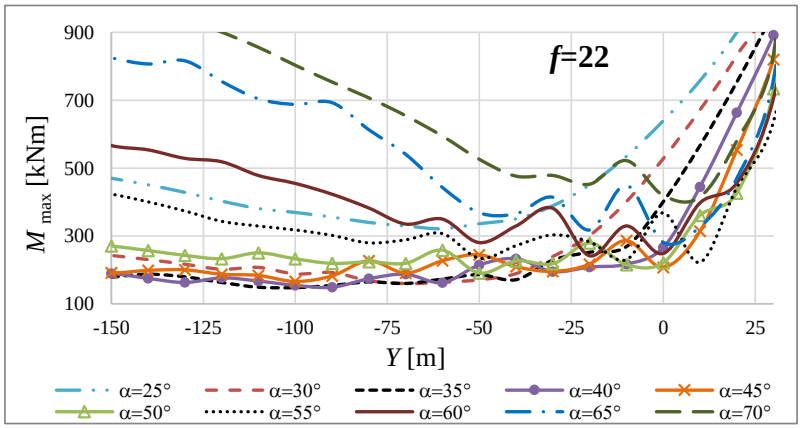

Figure 15 Maximum bending moment as a function of the vertical offset Y, for various α and different arch rise; a) $f = 10$ m; b) $f = 16$ m; c) $f = 22$ m; Y-configuration.

The ratio

$$R_{f^*\alpha^*\blacktriangledown} = \frac{M_{\min,\, f^*\alpha^*\blacktriangledown}}{M_{\max,\, f^*\alpha^*}} \cdot 100\ [\%] \qquad (11)$$

is presented in Figure 16. Applying the vertical offset can reduce the maximum bending moment by almost 1/4 of the maximum moment value for the reference pattern. It is visible in Figure 16, for $f = 25$ and $\alpha = 30°$, where the moment in the reference pattern is equal 526 kNm, and in modified pattern only 148 kNm. For some combinations of arch rise and angle α, a vertical offset gives no benefit; these combinations have an *Y*-value of zero in Table 3.

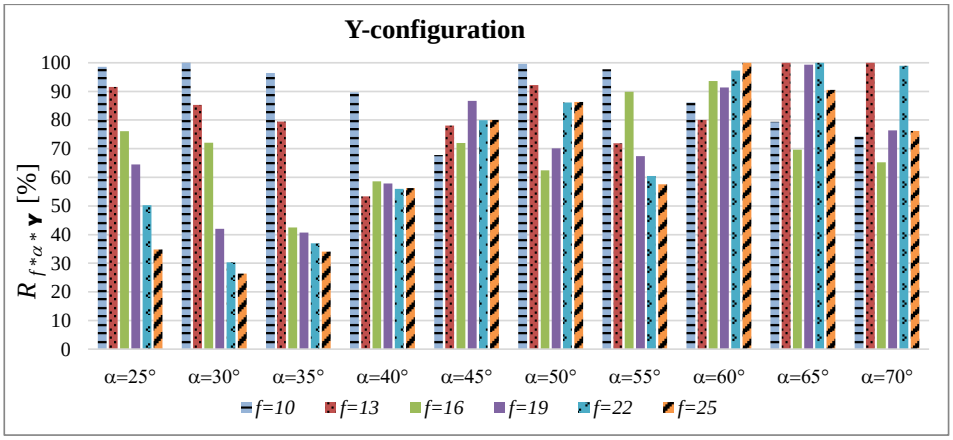

Figure 16 The ratio $R_{f^*\alpha^*\blacktriangledown}$ for different combinations of f and α; Y-configuration.

The columns in Figure 17 show the percentage of relaxed hangers $H_{f^*\alpha^*\blacktriangledown}$ for $P_{\min,\, f^*\alpha^*\blacktriangledown}$. In this graph, percentage numbers located above some columns, express the difference $\Delta H_{f^*\alpha^*\blacktriangledown}$ between the percentage of relaxed hangers for the reference pattern $p_{f^*\alpha^*}$ and for the modified pattern $P_{\min,\, f^*\alpha^*\blacktriangledown}$, i.e.

$$\Delta H_{f^*\alpha^*\blacktriangledown} = H_{f^*\alpha^*} - H_{f^*\alpha^*\blacktriangledown}(P_{\min,\, f^*\alpha^*\blacktriangledown}). \qquad (12)$$

For angle $\alpha \le 50°$ the vertical offset is, in general, beneficial in terms of H; among all the patterns in this group, for only one ($\alpha = 25$, $f = 16$) the slight increase of hanger relaxation was observed, while in most other cases, big decrease can be noticed (up to 22.2 %). Similar to the modifications analyzed in Section 4.2, for angle $\alpha \ge 55°$, value of H is not relevant since the number of relaxed hangers, both for the modified and the reference patterns, is very low or equal to zero. The biggest influence of a vertical offset

on H, is observed for two patterns with $f = 22$ and $f = 25$, and $\alpha = 35°$. In both cases, $H_{22,35,\mathbf{Y}} = H_{25,35,\mathbf{Y}} = 5.6\%$ which means only 2 relaxed hangers for the modified pattern, and $H_{22,35} = H_{25,35} = 27.8\%$ for the reference pattern; in other words, 10 relaxed hangers. In a few cases, values of percentage numbers are negative. Thus, by introducing a vertical offset, number of relaxed hangers slightly increases, namely by 2 hangers in the most unfavourable case, that is for $f = 16$ and $\alpha = 60°$.

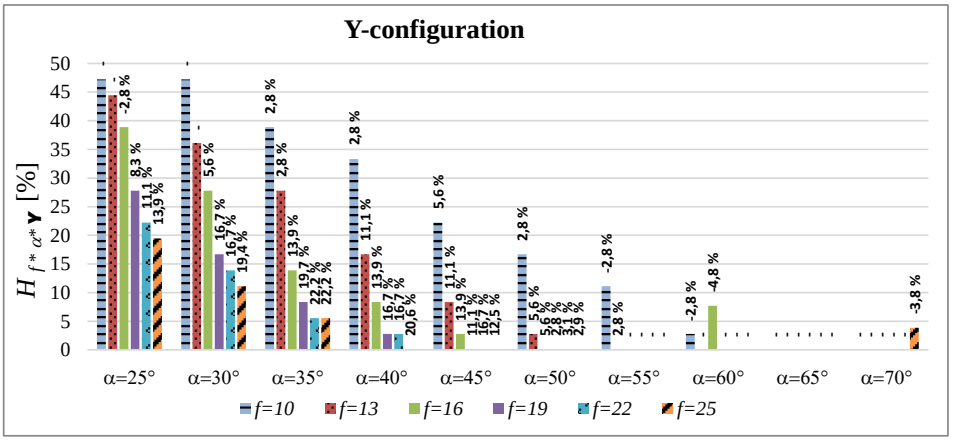

Figure 17 Number of relaxed hanger $H_{f^*\alpha^*\mathbf{Y}}$ for modified patterns (columns), and differences $\Delta H_{f^*\alpha^*\mathbf{Y}}$ between number of relaxed hangers for reference pattern and modified patter (percentage in numbers above columns); Y-configuration.

4.4 Effect of separate centres for arch and radial rays. Simultaneous horizontal and vertical offset. XY-configuration

In the fifth part of the study, offsets in both x- and y- directions were introduced simultaneously. Different sets $\mathbf{P}_{f^*\alpha^*\mathbf{XY}}$ with modifications $\mathbf{X} = \{1, 2, ..., 15\}$ [m] and $\mathbf{Y} = \{-100, -90, -80, ..., 20\}$ [m] were created, and in this part of the study, 12480 patterns were analysed.

Figure 18 presents selected results for the XY-configuration analysis, for arch rises f equal to 10, 16 and 22 m respectively. For each set of modified patterns $\mathbf{P}_{f^*\alpha^*\mathbf{XY}}$, a semi-transparent light grey area was plotted. This area includes all positions of $C_{h,R}(X, Y)$, for which the maximum moment $M_{\max, f^*\alpha^* XY}$ is lower or equal to the moment $M_{\max, f^*\alpha^*}$ of the reference pattern. Thus, white space indicates modifications that give no benefits. All semi-transparent layers are plotted on top of each other. The darker the area is, the more

layers overlap. Thus, the darkest regions indicate greatest likelihood for improvement. It is seen that for shallow arches, the darkest region is the most compact and spreads between 0 m and 4 m on the x-axis, and from $-40\,\text{m}$ to 20 m on the y-axis. An increase in the arch rise leads to decrease of the white region, and the darkest region shifts toward negative values of the Y-coordinate.

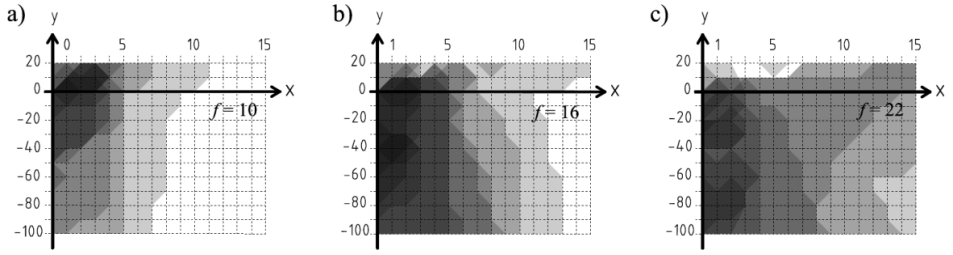

Figure 18 Location of most favorable position of $C_{h,R}$ for arch rise;
a) $f = 10\,\text{m}$; b) $f = 16\,\text{m}$; c) $f = 22\,\text{m}$.

Values of $M_{\max,f^*\alpha^*}$ calculated for each reference pattern, and $M_{\min,f^*\alpha^*\mathbf{XY}}$ calculated for each set of modified patterns $\boldsymbol{P}_{f^*\alpha^*\mathbf{XY}}$, are given in Table 4. The smallest of the presented values is emphasized (grey background). Values of X- and Y-coordinates of $C_{h,R}$, for patterns $P_{\min,f^*\alpha^*\mathbf{XY}}$, are presented in Table 5. For high rise arches with $\alpha \geq 60°$, the values of the X-coordinates are small, one meter or less. The largest offsets for the Y-coordinate are obtained for high arches and $\alpha \leq 50°$.

Table 4 Overview of bending moments $M_{\max,f^*\alpha^*}$ and $M_{\min,f^*\alpha^*\mathbf{XY}}$; XY-configuration.

	$\alpha[°]$	**25**	**30**	**35**	**40**	**45**	**50**	**55**	**60**	**65**	**70**
$f=10$	$M_{\max,f^*\alpha^*}$	806	732	664	593	480	260	214	247	285	329
	$M_{\min,f^*\alpha^*\mathbf{XY}}$	789	727	637	520	320	247	206	195	226	244
$f=13$	$M_{\max,f^*\alpha^*}$	700	616	530	396	246	191	252	247	227	268
	$M_{\min,f^*\alpha^*\mathbf{XY}}$	634	519	412	206	179	176	181	195	225	268
$f=16$	$M_{\max,f^*\alpha^*}$	650	544	432	292	230	286	217	243	349	454
	$M_{\min,f^*\alpha^*\mathbf{XY}}$	488	383	184	165	165	175	180	224	243	296
$f=19$	$M_{\max,f^*\alpha^*}$	631	517	391	273	187	248	306	276	285	440
	$M_{\min,f^*\alpha^*\mathbf{XY}}$	399	218	153	158	162	173	198	223	266	336
$f=22$	$M_{\max,f^*\alpha^*}$	673	562	435	297	229	231	445	257	373	496
	$M_{\min,f^*\alpha^*\mathbf{XY}}$	313	160	148	149	161	191	217	242	281	359
$f=25$	$M_{\max,f^*\alpha^*}$	673	562	435	297	229	231	445	257	373	496
	$M_{\min,f^*\alpha^*\mathbf{XY}}$	234	148	147	167	183	199	214	245	337	378

Table 5 X - and Y -coordinates [m] for bending moment $M_{\min,\, f^*\alpha^*\mathbf{XY}}$; XY-configuration.

	$\alpha[°]$	**25**	**30**	**35**	**40**	**45**	**50**	**55**	**60**	**65**	**70**
$f=10$	X	4	3	2	3	2	4	2	2	0	0
	Y	20	10	-20	-50	-50	10	10	0	10	10
$f=13$	X	1	1	2	3	2	0	0	1	1	0
	Y	-30	-60	-40	-40	-20	-30	-40	-50	20	0
$f=16$	X	1	2	0	2	1	2	1	1	0	0
	Y	-60	-40	-80	-30	-30	-50	-50	0	20	10
$f=19$	X	1	0	2	0	0	1	1	1	1	0
	Y	-50	-70	-60	-50	-60	-70	-10	-30	0	10
$f=22$	X	1	0	0	0	1	0	2	0	0	1
	Y	-50	-70	-100	-90	-90	-50	-40	-20	0	0
$f=25$	X	0	0	1	0	0	0	1	1	0	0
	Y	-60	-90	-100	-100	-60	-30	-30	-10	-20	-20

The ratio

$$R_{f^*\alpha^*\mathbf{XY}} = \frac{M_{\min,\, f^*\alpha^*\mathbf{XY}}}{M_{\max,\, f^*\alpha^*}} \cdot 100\ [\%] \qquad (13)$$

is presented in Figure 19. It is found that among the analyzed modified patterns, the lowest value of $R_{f^*\alpha^*\mathbf{XY}}$ is 26.4%. It is associated with the pattern for which $f=25$, $\alpha=30°$, $Y=-90$ m and $X=0$ m. It is in fact the same configuration that yields most improvement also in Section 4.3 (for the Y-configuration analysis). Thus, for certain cases, additional X modifications give no further improvement. For some arch rises (f) and angles (α), offsets in the vertical and/or the horizontal direction give very small or no benefit at all.

For angle $\alpha \le 50°$, vertical and/or horizontal offsets in XY-configuration are beneficial in terms of H. For angle $\alpha \ge 50°$, the value of H is not relevant since the number of relaxed hangers, both for the modified and the reference patterns, is very low or equal to zero. The largest influence of a double offset on H is observed in the same patterns as in the analysis for Y-configuration, i.e. for $f=22$, 25 and $\alpha=35°$, see Figure 20. In these cases $H_{25,35,\mathbf{Y}} = H_{22,35,\mathbf{Y}} = 5.6\%$, which means 2 relaxed hangers for the modified patterns, while $H_{25,35} = H_{22,35} = 27.8\%$ for the reference patterns, which means 10 relaxed hangers. The negative value of percentage number, appears for some combinations of arch rises (f) and spread angles (α), similarly to the analysis from

previous section. However, the number of additionally relaxed hangers is equal to 1, so is insignificant.

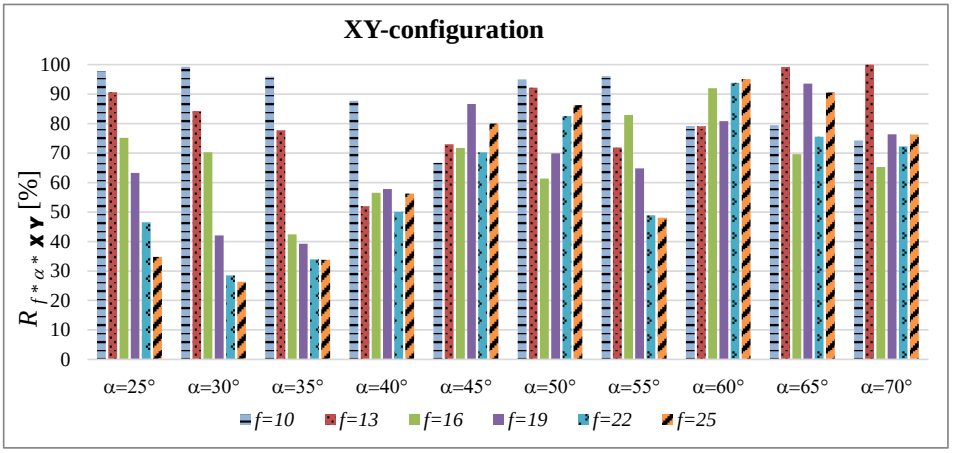

Figure 19 The ratio $R_{f^*\alpha^*\mathbf{XY}}$ for different combinations of f and α; XY-configuration.

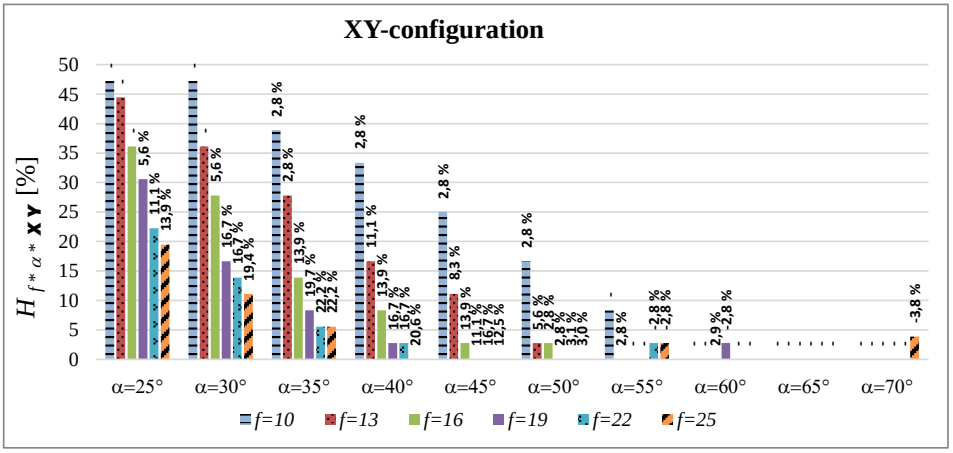

Figure 20 Number of relaxed hanger $H_{f^*\alpha^*\mathbf{XY}}$ for modified patterns (columns), and differences $\Delta H_{f^*\alpha^*\mathbf{XY}}$ between number of relaxed hangers for reference pattern and modified patter (percentage in number above columns); XY-configuration.

5 Summary

The paper presents results from a very large number of hanger patterns for a 100 m long network timber arch bridge with a light deck on crossbeams. The analyses, performed for different arch rises (f) include the influence of the number of crossbeams and of the hanger spread angle (α) on the structural performance of the bridge.

The main conclusion from the first part of the analysis is that the optimal number of crossbeams (n) for a 100 m long bridge is between 15 and 21. Whether n is odd or even seems to be insignificant.

Based upon analyses performed in Section 3.2, using coinciding centres of the arch (C_a) and the hanger patterns (C_h), a general recommendation is to use a hanger spread angle α in the range from $43°$ to $51°$ in the design process. Depending on the arch rise, more specific ranges are between $48°-65°$, $40°-55°$ and $38°-54°$, for shallow, medium and high-rise arches, respectively. These ranges lead to the smallest bending moments in the arch. It should be noted that spread angles $\alpha \geq 45°$ lead to hangers that are oriented almost horizontally at the ends of the bridge. However, they do not relax (as might be expected). Nevertheless, such location of hangers would not be accepted in the engineering practice. For an actual hanger pattern, it is recommended to avoid that hangers meet at the arch, since this will increase the bending moment in the arch.

In Section 4.2 the influence of horizontal offset of the centre for hanger creation C_h is analysed. This modification can reduce bending moments by almost 50%. Furthermore, the number of relaxed hangers can be reduced almost by half. Horizontal offsets should be less than 10 m. In most cases, offsets up to about 5.5 m are beneficial. However, horizontal offset up to 10 m can be beneficial for patterns with medium or high-rise arches and spread angle $\alpha \leq 40°$.

The analysis in Section 4.3 focuses on the influence of vertical offset on C_h. In this case, the bending moment for the best modified pattern is only about 25% of the bending moment for the reference pattern. The number of relaxed hangers can be reduced by 80% (from 10 to 2 relaxed hangers). The recommended values of the y-offset are in the range between -110 m to 30 m. For medium and high-rise arches and $\alpha \leq 45°$, the largest benefit is obtained for negative offsets which are almost equal to the four times radius of curvature of the circular arch.

Comparing effects from the X- and Y-configurations, the latter is clearly the most advantageous for the structural performance of the bridge.

Table 6 Ratios $R_{f^*\alpha^*\mathbf{X}}$, $R_{f^*\alpha^*\mathbf{Y}}$, $R_{f^*\alpha^*\mathbf{XY}}$ in [%] for X-, Y- and XY-configuration.

	$\alpha[^\circ]$	**25**	**30**	**35**	**40**	**45**	**50**	**55**	**60**	**65**	**70**
	$R_{f^*\alpha^*\mathbf{X}}$	100,0	99,6	97,4	94,8	78,9	96,0	100,0	79,2	86,8	90,8
$f=10$	$R_{f^*\alpha^*\mathbf{Y}}$	98,6	100,0	96,4	89,7	67,7	99,6	97,8	86,2	79,4	74,3
	$R_{f^*\alpha^*\mathbf{XY}}$	97,8	99,3	95,9	87,7	66,7	94,9	96,1	79,2	79,4	74,3
	$R_{f^*\alpha^*\mathbf{X}}$	96,4	94,6	90,7	66,6	82,3	100,0	70,8	100,0	100,0	94,8
$f=13$	$R_{f^*\alpha^*\mathbf{Y}}$	91,6	85,3	79,5	53,4	78,0	92,2	71,9	80,0	100,0	100,0
	$R_{f^*\alpha^*\mathbf{XY}}$	90,6	84,3	77,8	52,0	73,0	92,2	71,9	79,0	99,2	100,0
	$R_{f^*\alpha^*\mathbf{X}}$	92,6	88,2	67,8	76,4	88,8	67,1	100,0	92,0	86,1	85,1
$f=16$	$R_{f^*\alpha^*\mathbf{Y}}$	76,1	72,1	42,4	58,6	71,9	62,5	89,8	93,6	69,6	65,3
	$R_{f^*\alpha^*\mathbf{XY}}$	75,1	70,3	42,4	56,5	71,7	61,4	82,9	92,0	69,6	65,3
	$R_{f^*\alpha^*\mathbf{X}}$	88,6	70,0	69,3	76,8	100,0	100,0	79,4	86,7	86,6	80,4
$f=19$	$R_{f^*\alpha^*\mathbf{Y}}$	64,5	42,1	39,4	57,8	86,7	70,1	67,4	91,4	99,3	76,4
	$R_{f^*\alpha^*\mathbf{XY}}$	63,3	42,1	38,0	57,8	86,7	69,9	64,8	80,8	93,5	76,4
	$R_{f^*\alpha^*\mathbf{X}}$	72,0	59,4	73,7	96,9	100,0	95,2	59,3	100,0	100,0	84,2
$f=22$	$R_{f^*\alpha^*\mathbf{Y}}$	50,2	30,3	36,9	56,0	79,9	86,2	60,5	97,3	100,0	99,0
	$R_{f^*\alpha^*\mathbf{XY}}$	49,0	30,3	36,9	56,0	77,6	86,2	59,1	97,3	100,0	85,5
	$R_{f^*\alpha^*\mathbf{X}}$	61,0	57,3	66,5	82,4	100,0	95,6	64,8	100,0	84,4	84,1
$f=25$	$R_{f^*\alpha^*\mathbf{Y}}$	34,8	26,4	34,0	56,3	80,0	88,6	57,6	100,0	90,5	76,2
	$R_{f^*\alpha^*\mathbf{XY}}$	34,8	26,4	33,7	56,3	80,0	88,6	48,1	95,1	90,5	76,2

The pattern modification applied in Section 4.4 combines horizontal and vertical offsets of C_h. Although no additional improvement can be gained compared with the best patterns obtained in Section 4.3, a combined modification is in general better. The moment ratios: $R_{f^*\alpha^*\mathbf{X}}$, $R_{f^*\alpha^*\mathbf{Y}}$ and $R_{f^*\alpha^*\mathbf{XY}}$ for vertical, horizontal and combined offsets respectively, are collected in Table 6 . Each column represents results for different spread angles (α), while the rows are associated with different arch rise and configuration. For each arch rise and spread angle, grey colour in the table, indicate the most beneficial modification. It should be noted that the majority of marked results refer to XY-configuration.

The loading is an important premise for the performed analyses. The key bending moment values, i.e. maximum bending moment for each pattern, may occur for any one of the load steps (i.e. load cases). Therefore, it is suggested to use several load cases while testing or comparing different network patterns.

The present study is based on more than 12000 different radial patterns. It is shown that the introduced pattern modifications yield significant improvement in structural performance of network timber arch bridges with light decks on transversal crossbeams.

ACKNOWLEDGEMENT

This research has been made possible by several research grants. The work is associated with the projects 'Rigid joints for large timber structures' from the Research Council of Norway [grant number 208052], and the WoodWisdom-Net project 'Durable Timber Bridges' at the Research Council of Norway [project number 237135]. The projects have also received financial and technical support from The Association of Norwegian Glulam Producers, MoelvenLimtre A/S, Skogtiltaksfondet and Norwegian Public Road Authorities. All these contributions are gratefully acknowledged.

References

1. Tveit, P., *The design of network arches.* The Structural Engineer, 1966. **44**(7): p. 249-259.
2. Tveit, P., *Comparison of Steel Weights in Narrow Arch Bridges with Medium Spans.* Stahlbau, 1999. **68**(9): p. 753-757.
3. Teich, S., *The network arch bridge, an extremely efficient structure - Structural behaviour and construction.* Stahlbau, 2005. **74**(8): p. 596-605.
4. Teich, S., *Development of general design principles for the hanger arrangements of network arch bridges.* Stahlbau, 2011. **80**(2): p. 100-111.
5. Brunn, B. and F. Schanack, *Calculation of a double track railway network arch bridge applying the European standards. Graduation Thesis*. 2003, Dresden University of Technology.
6. Schanack, F. and B. Brunn, *Analysis of the structural performance of network arch bridges.* Indian Concrete Journal, 2009. **83**(1): p. 7-13.
7. De Zotti, A., C. Pellegrino, and C. Modena. *A parametric study of the hanger arrangement in arch bridges*. In *5th international conference on arch bridges ARCH '07*. 2007.
8. Pellegrino, C., G. Cupani and C. Modena, *The effect of fatigue on the arrangement of hangers in tied arch bridges.* Engineering Structures, 2010. **32**(4): p. 1140-1147.
9. Stetter, H., S. Hentschinski, and T. Fritsche, *Innovation concentrated - Regenbrücke Stefling: A tied arch bridge in concrete.* Beton- und Stahlbetonbau, 2015. **110**(10): p. 710-719.
10. Pipinato, A., *Structural analysis and design of a multispan network arch bridge.* Proceedings of the Institution of Civil Engineers: Bridge Engineering, 2016. **169**(1): p. 54-66.
11. CEN, *EN 1991-2: Eurocode 1: Actions on structures -Part 2: Traffic loads on bridges*, in 2003: Brussels, Belgium.
12. Hibbit, K., Sorensen, *ABAQUS/Standard Analysis User's Manual* 2007.
13. CEN, *EN 1990: Eurocode 0: Basis of structural design*, in 2002: Brussels, Belgium.
14. *Python Software Foundation*. https://www.python.org/.
15. Ritter, M.A., *Timber Bridges: design, construction, inspection, and maintenance*. 1992, Washington DC: U.S. Department of Agriculture, Forest Service.
16. Mettem, C.J., *Timber Bridges*. 2011, New York TRADA Technology Ltd.

Paper III

Parametric study on effects of load position on the stress distribution in network arch timber bridges with light timber deck on transverse crossbeams

(*Submitted to Engineering Structures in July 2017*)

Is not included due to copyright

Paper IV

Network arch timber bridges with light timber decks and spoked configuration of hangers - parametric study

(*Submitted to Structural Engineering International in July 2017*)

Is not included due to copyright

PART III

Appended additional paper

Paper V

A review of serviceability limit state design criteria for timber footbridges

(In: *Proceedings of the WCTE 2014, World Conference on Timber Engineering*)

WCTE 2014 Quebec City Canada August 10-14
World Conference on Timber Engineering

A REVIEW OF SERVICEABILITY LIMIT STATE DESIGN CRITERIA FOR TIMBER FOOTBRIDGES

Anna Ostrycharczyk[1], Kjell Arne Malo[2]

ABSTRACT: The paper presents a comparison of serviceability limit state design criteria for timber footbridges in Europe, Australia, Canada and the United States of America. Comparison of selected load values and load combinations for timber footbridges is also given. Deflection and dynamic parameters like natural frequency or acceleration are used for tabularization of differences between the rules. The comparison and performance are evaluated by use of a selected existing timber footbridge in Norway.

KEYWORDS: Serviceability, timber bridges, vibration

1 INTRODUCTION

For many years, safety was the most important feature of engineering constructions. The design was mostly focused on ultimate limit state criteria and related design rules. Nowadays, the importance of the serviceability limit state rises and has become almost equally important as the ultimate limit state. The reason for this is mainly the decrease in mass of the structure, which is economically beneficial, and new possibilities due to technology advancement. Consequently, more attention must be paid to deflection and vibrational issues. Considering light timber constructions like floors or footbridges, humans become a significant part of a dynamic system due to own mass contribution, and by representing vibration source and sensor simultaneously [1]. Human perception of vibration is very individual, making serviceability requirements and performance criteria on comfort issues complex and difficult to define in design codes.

The paper presents a comparison of serviceability limit state criteria found in Eurocodes for European countries, with the statement of requirements for Australia (AU), Canada (CAN) and the United States of America (USA). The Eurocodes (EU) with Norwegian national annexes have been used as basis for comparison in this paper. All collected data corresponding to other than European standards are based on the authors interpretation of the available reading materials.

[1] Anna Ostrycharczyk, Department of Structural Engineering, The Norwegian University of Science and Technology, NTNU, R. Birkelandsv 1a, 7491 Trondheim, Norway.
Email: anna.w.ostrycharczyk@ntnu.no
[2]Kjell Arne Malo, Department of Structural Engineering, The Norwegian University of Science and technology, NTNU, R. Birkelandsv 1a, 7491 Trondheim, Norway
Email: kjell.malo@ntnu.no

2 DESIGN PHILOSOPHY

Limit states design (LSD) is a design methodology used in standards in EU, as well as in AU and CAN. Load and Resistance Factor Design (LRFD) approach is used in USA. The reason for the different approaches is mainly historical since allowable stress design was used in USA before LRDF. Both methods, LSD and LRFD, are based on partial factor method and/or probabilistic methods [2 - 5]. It means that the forces in the structure caused by factored loads, have to be smaller than factored resistance of structural elements. In addition linear elastic assumptions should be applied during analysis in most design cases in all considered countries, even when inelastic behaviour is the basis of resistance of components and connections in the structure. A reason for that, among others, is incomplete knowledge of inelastic structural action [4]. Nevertheless, in all listed countries exception from above rule can be made for special cases specified in mentioned codes, or by authority approval.

Limit states, depending on country, are categorised in slightly different ways. Main existing categories of limit states are ultimate limit state (ULS) and serviceability limit state (SLS), which can be found in all considered codes. However, for instance in codes from CAN and USA, additional fatigue limit state (FLS) exists as an equal limit state category. In USA other additional category of limit state like extreme event limit state occurs. FLS category in EU and AU codes is not present, but fatigue resistance is a part of ULS requirements in EU and a part of SLS

requirements in AU. In AU also more detailed criteria are prescribed for ULS and SLS; in ULS those are; stability limit state, strength limit state, failure or deformation, deterioration of strength and brittle fracture failure. In SLS additional criteria are; deformation of foundation, permanent damage due to corrosion, cracking or fatigue, vibration and flooding.

Consequently, the variation of design criteria worldwide is rather large and additional requirements may as well be found in specific regions.

The aim of the limit state design approach is to create safe, economical and comfort structures with long-term design life, which is assumed to be equal 75 years for timber bridges in USA and CAN [4, 5], and 100 years in EU and AU [2, 3].

3 LOADS ON FOOTBRIDGES

Loads imposed on the footbridges can be divided into permanent and variable actions. Dead load from main structure elements, load from railings and other superimposed dead load, are part of permanent actions. Variable actions consist of wind loads, (acting in horizontal and vertical directions), snow loads (in reasonable cases), thermal actions and construction loads. However, the most important variable loading is related to load caused by pedestrians. In cases where there are no physical barriers to prevent vehicle access to the footbridge, additional traffic/vehicle load also occurs.

In this paper a simplified case consisting of a dead load of the structure and a pedestrian load on a timber footbridge will be considered. The example case is Dalenbrua which is a 99 m long footbridge located in Trondheim, Norway (see Figure 1). This bridge was designed by the Sweco company and built in 2012. The deck of Dalenbrua footbridge consists of stress-laminated lamellas, made of glulam timber beams class GL32c. The deck may be treated as continuous, supported at eight locations by six supporting frames in addition to the two abutments, confer sketch on Figure 4.

Figure 1: *Dalenbrua footbridge*

3.1 DEAD LOAD

In EU wood construction materials are divided into two main groups; glulam and solid timber. There are 7 classes of combined, and 7 classes of homogenous glulam. Furthermore 12 classes of solid timber for softwood species and 8 classes for hardwood can be distinguished. Strength classes and corresponding strength and stiffness properties of glulam and solid timber can be found in [6, 7]. Considering calculations with respect to SLS design, mean value density and modulus of elasticity shall be used [8]. Mean density of wood, given in [6, 7], varies between 350-550 kg/m^3 for softwood and between 570-1080 kg/m^3 for hardwood. Furthermore, for Norway additional guidance is given in [9]. For classes from C18 to C30 (not impregnated softwood) density depends on moisture content and varies between 335 kg/m^3 for 8% moisture content to 495 kg/m^3 for 18% moisture content. Wood density in other countries has similar values. In Canada it can be assumed that softwood has density of ~612 kg/m^3 (6.0 kN/m^3) and hardwood has density of ~968 kg/m^3 (9.5 kN/m^3) [5]. In USA, values of density can be assumed 0.050 kcf (~801 kg/m^3) and 0.060 kcf (~961 kg/m^3) for softwood and hardwood respectively [4].

3.2 PEDESTRIAN LOADS

In EU the recommended value of uniformly distributed load q_{fk}, which represent pedestrian loading on footbridges, should be calculated based on Equation 1, [10]:

$$q_{fk} = 2.0 + \frac{120}{L+30} \quad [\text{kN/m}^2] \qquad (1)$$

where: L is the loaded length in m, and 2.5 kN/m^2≤ q_{fk} ≤5.0 kN/m^2. It is not stated how to interpret L in case of multi span footbridges. Nonetheless, authors assume that Equation 1 was derived for simply supported beam. Thus in the example case of Dalenbrua footbridge, length of the longest span (18 m) is used.

In case of a dense crowd, value of q_{fk} shall be assumed equal to 5 kN/m^2 and considered to be static. However, this assumption is valid only for footbridges with width smaller than 6 m. In other cases individual models of loading shall be calculated [10].

In AU, according to [11], pedestrian loading is dependent on the loaded area, see Figure 2. However, in case of crowd loading, similar to Europe, a constant value of 5 kPa design load shall be used in calculations.

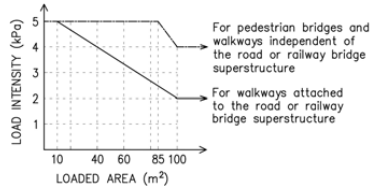

Figure 2: *Pedestrian loads in AU; after Fig. 7 in [11]*

In CAN, according to [5], pedestrian load can be calculated as follows:

$$p = 5.0 - \frac{s}{30} \quad (2)$$

where: s is the total loaded length of walkway, in meters, and $1.6 \leq p \leq 4.0$ kPa, [5].

In USA, according to [12], pedestrian loading in footbridges, shall be a uniformly distributed nominal load of constant value 90 psf (~4.31 kPa) [12].

On Figure 3 values of pedestrian loads, depending on footbridge/bridge length for EU, AU, CAN and USA are compared. To show Australian pedestrian loading, as a function of bridge length, Dalenbrua bridge width equal 5.5 m was assumed, see Figure 2. Table 1 presents maximum values of pedestrian loading.

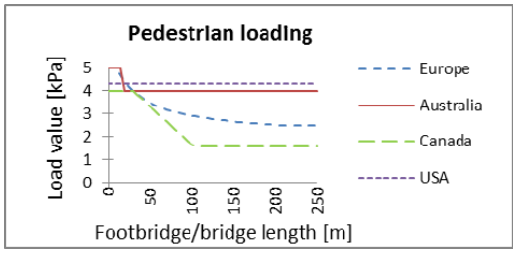

Figure 3: *Pedestrian loading in EU, AU, CAN and USA*

Table 1: *Maximum values of pedestrian loading in EU, AU, CAN and USA [10, 11, 5, 12]*

Country	EU	AU	CAN	USA
Max. value of pedestrian load [kPa]	5	5	4	~4.31

3.3 VEHICLE LOAD

In Table 2, total values of vehicle loads on pedestrian bridges in the considered countries are presented.

Table 2: *Maximum values of vehicle loads in EU, AU, CAN and USA [10, 11, 5, 12]; n.a.- 'not applicable'*

Country	EU	AU	CAN	USA
Max. value of vehicle load [kN]	120	20 / 31	n.a.	~45 / 89

In AU, the value of vehicle load given in [11] is 21 kN, which can correspond to, for instance, a park tractor. However, in [13], for footpaths subjected to wheeled vehicles, a value of a concentrated load can be assumed to be 31 kN.

In USA the value of vehicle load depends on width of the footbridge and is divided into deck with of 7 to 10 feet (2.13-3.05 m), loaded with 10 kips (~45 kN), and for width bigger than 10 feet (3.05 m) with 20 kips (~89 kN) [12].

4 LOAD COMBINATIONS

4.1 SLS LOAD COMBINATIONS IN EUROPE

There are three equations for SLS load combination in EU standards [3]. In Equations (3), (4), (5), characteristic (k), frequent (f) and quasi-permanent (qp) load combinations are given respectively by

$$E_{dk} = \sum_{j\geq 1} G_{k,j} "+" Q_{k,1} "+" \sum_{i>1} \psi_{0,i} Q_{k,i} \quad (3)$$

$$E_{df} = \sum_{j\geq 1} G_{k,j} "+" \psi_{1,1} Q_{k,1} "+" \sum_{i>1} \psi_{2,i} Q_{k,i} \quad (4)$$

$$E_{dqp} = \sum_{j\geq 1} G_{k,j} "+" \psi_{2,1} Q_{k,1} "+" \sum_{i>1} \psi_{2,i} Q_{k,i} \quad (5)$$

where: E_d is a design value of the effects of actions due to serviceability criterion, G is a permanent action, and Q is a variable action.

As it can be noticed, design load combinations divide loads into groups depending on load duration. Considering SLS for footbridges, design load values are dependent on a load factor (usually equal to 1.0), prescribed both to permanent and variable actions, and combination factors ψ which works only with variable actions. In Table 3 values of combination factors are presented.

Table 3: *Recommended values of combination factors for footbridges; after Tables A2.2 and NA.A2.2 in [14]*

Load	Combination factor		
	ψ_0	ψ_1	ψ_2
Traffic loads	0.7	0.7	0.2

For simple load cases, considering the condition that both traffic loads cannot occur simultaneously [10], load combinations for the case study of Dalenbrua are as follows

$$E_{dk} = \text{dead load} + \text{pedestrian load} \quad (6)$$

$$E_{df} = \text{dead load} + 0.7\text{pedestrian load} \quad (7)$$

$$E_{dqp} = \text{dead load} + 0.2\text{pedestrian load} \quad (8)$$

4.2 SLS LOAD COMBINATIONS IN AUSTRALIA, CANADA AND THE UNITED STATES OF AMERICA

In AU and USA, SLS load combination equations are made in a similar way, i.e. both load factors and combination factors appear. In regulations from CAN, only load factors appear, but there are two SLS load

combinations; one general and one for superstructure vibrations.

For AU, the SLS load combination can be expressed as:

$$\mathrm{PE}+\left(\text{SDL for one TE}\right)+ \\ \mathrm{k}\cdot\left(\text{SDL for one or more other TE or TH}\right) \tag{9}$$

where: *PE*, *TE*, and *TH* are permanent, transient and thermal effects respectively and *SDL* is serviceability design load [11]. Coefficient *k* takes into account possibility of transient and thermal loads occurring simultanously, and is equal to 0.7 for one additional effect and 0.5 for two additional effects [15].

In regulations for CAN, the relation is as follows:

$$\sum \mathrm{PE}+\sum \mathrm{TE}+\sum \mathrm{EE} \tag{10}$$

where: *EE* are exceptional loads.

Finally, for USA the SLS load combination reads:

$$Q=\sum \eta_i \gamma_i Q_i \tag{11}$$

where: Q_i is singular load, η_i is load modifier and γ_i is a load factor. The value of a load modifier is dependent on ductility, redundancy, and operational classification. For the considered SLS (timber footbridges), value of load modifier is equal 1.0 for all load cases. In general, there are four SLS load combinations presented in [4], but only SLS1 can be related to timber footbridges.

4.3 COMPARISON OF SLS LOAD COMBINATIONS IN EUROPE, AUSTRALIA, CANADA AND THE UNITED STATES OF AMERICA

Loads and load combination factors are presented in Table 4 are for SLS load combinations. In the various codes all the coefficients and forces were selected for the case of Dalenbrua footbridge.

Table 4: *Load and combination factors for SLS in EU, AU, CAN and USA; where DL is a dead load and PL is a pedestrian load*

	Load factor		Combination factor	
	DL	PL	DL	PL
EU SLS1	1.0	1.0	-	-
EU SLS2	1.0	1.0	-	0.7(ψ_1)
EU SLS3	1.0	1.0	-	0.2(ψ_2)
AU SLS1	1.0	1.0	-	0.7
CAN SLS1	1.0	0.9	-	-
CAN SLS2	0.0	0.9	-	-
USA SLS1	1.0	1.0	1.0	1.0

5 NUMERICAL MODEL

In the next sections of this paper, the guidelines for calculation of deflection and deflection criteria will be presented, as well as issues related to dynamics and comfort criteria. To compare theoretical requirements with a real object, simplified numerical model of Dalenbrua deck was made. Seven-span deck is modelled using shell elements with transversely isotropic material. Engineering constants, shown in Table 5, were calculated on base of mean value of elastic modulus for GL32, and requirements for system properties of stress-laminated deck plates, presented in Table 5.1. in [16].

Table 5: *Engineering constants in simplified deck model of Dalenbrua, [N/mm²]*

E_1	E_2, E_3	ν_{12}, ν_{13}, ν_{23}	G_{12}, G_{13}	G_{23}
13500	270	0	810	81

The averaged mean density of the deck material including asphalt layers and steel bars, was assumed to be 824 kg/m^3. The model was loaded with pedestrian loading located in the most unfavourable manner, which means on one of the longest span of the bridge, i.e. 18 m length. Pedestrian loading calculated after Equation (1) is 4.5 kPa. Deflection and dynamic analyses were performed. Instantaneous deflections under self-weight, and with added pedestrian loading were obtained, and are visualized on Figure 5 and Figure 6, with maximum values of 15 mm and 27 mm respectively. The deflection was calculated considering the characteristic load combination (most unfavourable case). Figure 4 shows a sketch of Dalenbrua construction, based on a drawing from SWECO [17], where axes 1 and 8 correspond to the edge supports in the numerical model.

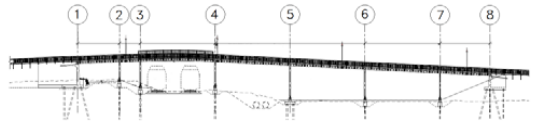

Figure 4: *Sketch of Dalenbrua footbridge; after SWECO* ***[17]***

Figure 5: *Deck deflection under self-weight*

Figure 6: *Deck deflection under pedestrian load*

Natural frequencies and the corresponding mode shapes were also computed for the modelled bridge. Figures 7, 8 and 9 present the first three vertical modes, while Figure 10 presents first horizontal/torsional mode. In Table 6 values of natural frequencies of the deck from numerical computations and calculations provided by designers, are given.

Figure 7: *First vertical mode shape of the deck*

Figure 8: *Second vertical mode shape of the deck*

Figure 9: *Third vertical mode shape of the deck*

Figure 10: *First horizontal/torsional mode shape of the deck*

Table 6: *Natural frequencies of the deck*

	Natural frequencies f [Hz]	
Direction of mode shape	Numerical model	Designer calculations
Vertical 1	2.703	2.717
Vertical 2	3.373	3.377
Vertical 3	4.240	4.220
Hor./Tors. 1	4.519	n.a.

6 DEFLECTION DESIGN GUIDANCE AND CRITERIA

In this section, deflections of Dalenbrua footbridge are calculated with respect to EU rules, and compared to the requirements from AU, CAN and USA.

6.1 CALCULATION OF DEFLECTION

In EU, deflection shall be calculated in two steps. In the first step, the instantaneous deflection is calculated, and secondly the effect of creep is added in order to obtain the final deflection. Values for instantaneous deflection for dead load and pedestrian load were obtained from the numerical model. Final deflection [8]: shall be calculated from:

$$u_{fin} = u_{fin,G} + u_{fin,Q1} \tag{12}$$

$$u_{fin,G} = u_{inst,G}\left(1 + k_{def}\right) \tag{13}$$

$$u_{fin,Q1} = u_{inst,Q1}\left(1 + \psi_{2,1} k_{def}\right) \tag{14}$$

where: k_{def} is a deformation factor, dependent on type of material and service class, which is related to moisture content in wood. The service class depends on the expected moisture content vs. time in the wood [8]. By use of effective water sealing or cover, service class 2 can be used in Norway [9]. Then $k_{def} = 0.8$, after [8], and $\psi = 0.2$ is stated in national annex [14]. Calculated after Equations (12), (13) and (14), values of final deflections are presented in Table 7.

Table 7: *Deflection of Dalenbrua deck, [mm]*

	Deflection	
	self-weight	pedestrian load
Instantaneous	15	27
Final - partial	27	31.3
Final - combined	58.3	

6.2 DEFLECTION REQUIREMENTS

In Table 8, calculated deflection is compared with requirements from EU, AU, CAN and USA.

Table 8: *Juxtaposition of deflection requirements in EU, AU, CAN and USA to deflection in Dalenbrua footbridge; after [16, 11, 5, 4]*

Country	Requirement	Deflection value
EU	l/200	90mm
AU	l/600	30mm
CAN	l/500	36mm
USA	l/425	42mm

Presented results shows, that the final deflection of Dalenbrua footbridge (with assumption of l=18 m) meet requirements from EU only. However, authors are not sure about how creep effects the requirements of other countries. It should also be mentioned, that the EU deflection requirement is a recommended range between l/200 to l/400 and is to be supplied by national choices [16]. In addition, authors decided to refer USA deflection requirements for wood structures [4], and not to deflection requirements for footbridges (l/500) [12], the latter condition is stricter.

7 VIBRATION DESIGN GUIDANCE AND CRITERIA

Vibration criteria in EU shall be considered in two ways: as caused by pedestrians or wind. This paper focuses on vibrations caused by pedestrian only.

7.1 CALCULATION OF VIBRATION CRITERIA

Considering vibrations, it is intuitive that the natural frequency is an important factor for comparison with requirements. However, it is alone not sufficient. In EU,

natural frequency is used to calculate acceleration, which can be used in comfort criteria related to vibrations. A simplified method in EU for assessing the vibrations of timber footbridges is given below, [16].

Equations (15), (16) and (17) present vertical accelerations caused by one person, several persons or running persons crossing the bridge, respectively:

$$a_{vert,1} = \frac{200}{Mζ} \qquad \text{for } f_{vert} \le 2.5 \text{ Hz} \qquad (15a)$$

$$a_{vert,1} = \frac{100}{Mζ} \qquad \text{for } 2.5 \text{ Hz} < f_{vert} \le 5.0 \text{ Hz} \qquad (15b)$$

$$a_{vert,n} = 0.23 a_{vert,1} n k_{vert} \qquad (16)$$

$$a_{vert,1} = \frac{600}{Mζ} \qquad \text{for } 2.5 \text{ Hz} < f_{vert} \le 3.5 \text{ Hz} \qquad (17)$$

M is total mass of the bridge, given by $M=ml$; l is a span of the bridge, m is a mass per unit length (self-weight), ζ is damping ratio (equal 0.01 for structures without and 0.015 for structures with mechanical joints), f_{vert} is the fundamental frequency for vertical deformation of the bridge, n is number of pedestrians and k_{vert} is a coefficient according to Figure 11. Number of people should be taken as $n = 13$ for a distinct group of people and $n = 0.6A$ for continuous stream of pedestrians, where A is area of the bridge deck [16].

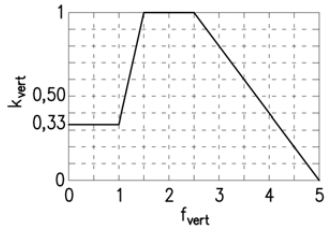

Figure 11: *Relation between the vertical fundamental natural frequency f_{vert} and the coefficient k_{vert}; after Fig. B.1 in [16]*

Acceleration in horizontal direction shall also be checked and calculated after Equations (18) and (19), for one person or several persons crossing the bridge, respectively:

$$a_{hor,1} = \frac{50}{Mζ} \qquad \text{for } 0.5 \text{ Hz} \le f_{hor} \le 2.5 \text{ Hz} \qquad (18)$$

$$a_{hor,n} = 0.18 a_{hor,1} n k_{hor} \qquad (19)$$

where: k_{hor} is a coefficient according to Figure 12.

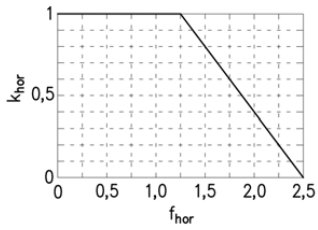

Figure 12: *Relation between the horizontal fundamental natural frequency f_{hor} and the coefficient k_{hor}; after Fig. B.2 in [16]*

7.2 CASE STUDY - DALENBRUA

For Dalenbrua footbridge, first vertical natural frequency (f_{vert}) is 2.7 Hz. Because 2.5 Hz ≤ f_{vert} ≤ 5.0 Hz, Equations (15b), (16) and (17) are used to calculate vertical acceleration of the bridge according to EU guideline. Horizontal acceleration do not need to be checked, due to high value of first natural horizontal frequency. Mass per unit length of the footbridge equals 1962 kg/m, and the deck has mechanical joints so damping ratio is taken equal to 0.015. Value of k_{vert} equals 0.9, see Figure 10, and number of people crossing the bridge is 13 as suggested in [16]. Values of calculated accelerations are presented in Table 9.

Table 9: *Vertical acceleration of Dalenbrua deck*

$a_{vert,1}$ [m/s^2] one person walks	$a_{vert,n}$ [m/s^2] 13 persons walk/ stream of people	$a_{vert,1}$ [m/s^2] one running person
0.189	0.509 / 2.324	1.133

7.3 VIBRATION CRITERIA IN EUROPE

Due to the EU regulations for vibrations caused by pedestrians, maximum acceptable acceleration levels should be defined. Maximum recommended values of acceleration for any part of the deck are: 0.7 m/s^2 for vertical vibrations and 0.2 m/s^2 for horizontal vibrations due to normal use, and 0.4 m/s^2 for exceptional crowds [14]. Verification of the comfort criteria shall be checked in case when fundamental frequency of the deck is less than 5.0 Hz for vertical vibrations, and 2.5 Hz for horizontal and torsional vibrations [14]. From Table 9 it is seen that the footbridge meets the criteria for walking people. However, the criteria for a running person and stream of people are not met. The method of calculation is developed for simply supported beams and it is questionable for other structural systems. Moreover, the requirements is merely guidance, it is the responsibility of the bridge owner to set performance requirements of the bridge in SLS state.

7.4 VIBRATION CRITERIA IN AUSTRALIA

In many countries vibration criteria need to be checked if natural frequency is lower than a fixed value, or is contained in a specified range. In AU, frequencies for vertical vibrations which are between 1.5 – 3.5 Hz, are treated as resonant ones and investigation of superstructure vibration shall be made in SLS. However, due to [15], when pedestrian bridge is calculated with resonant frequencies of 5 Hz and higher, it is highly unlikely that problematic vibration occurs. Figure 13 shows limits for maximum dynamic deflection caused by one pedestrian giving load of 700 N, crossing the footbridge with the speed of 1.75-2.5 footfalls per second. Special attention shall be paid when horizontal vibration is less than 1.5 Hz. With such a low frequency value, pedestrians might cause unacceptable magnitude of lateral vibrations to footbridges, [11]. Above requirements, [11, 15], differ from EU and a comparison based on Dalenbrua with respect to AU rules is not feasible. However, the dynamic amplitude of vertical deflection under a 700 N impact force was obtained from the numerical model of Dalenbrua footbridge, and is less than 1 mm. Consequently, compared to the requirements in Figure 13, the AU requirements are fulfilled.

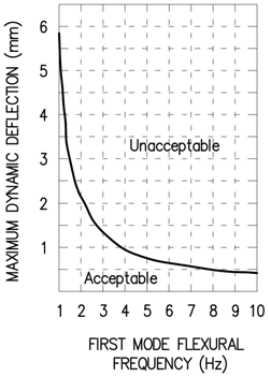

Figure 13: *Dynamic amplitude limits for pedestrian bridges; after Fig. 12.4 in [11]*

It should be noted that the requirements and acceptance criteria for dynamic behaviour of bridges provided in [11] do not apply to bridges longer than 100 m and suspension or cable-stayed bridges.

7.5 VIBRATIONA CRITERIA IN CANADA

Basic CAN standard [5] is considering vibration requirements for bridges depending on presence of sidewalks. The requirements relate the deflection to the first flexural frequency, as presented on Figure 14, and defines the acceptable domains.

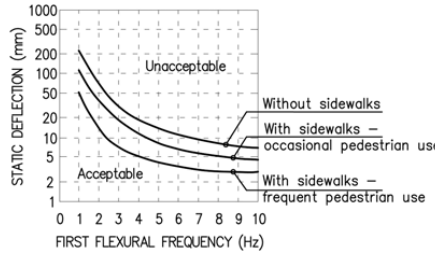

Figure 14: *Deflection limits for highway bridge superstructure vibration; after Fig. 3.1 in [5]*

Figure 14 is applying to road bridges, so the CAN vibrational requirements are not directly applicable to the case of Dalenbrua. However, according to [18], a walking person of average weight of ~70 kg should not give acceleration exceeding the limit given in Figure 15.

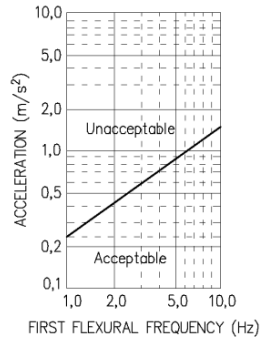

Figure 15: *Acceleration limit for pedestrian bridge serviceability; after Fig. C3.3 in [18]*

Considering Dalenbrua footbridge, the acceleration level calculated after Equation (15b) will meet the requirements of [18].

However, by applying the requirements given in Figure 14 [5], it is observed that they cannot be fulfilled. Probably these requirements are not meant for pure footbridges.

7.6 VIBRATION CRITERIA IN THE UNITED STATES OF AMERICA

Vibrational criteria for pedestrian bridge in USA are based on vertical and lateral vibrational modes and corresponding fundamental frequencies, obtained for a load case without live load, see Table 10.

Table 10: *Minimum values of fundamental frequencies, [12]*

Fundamental frequency mode direction	Value [Hz]
Vertical	3.0
Lateral	1.5

In case of too low fundamental frequencies, or when second harmonic might be of a concern, additional evaluation is needed. In that case, analysis considering, among others, frequency and magnitude of pedestrian footfall loadings, structural damping and frequency dependent limits on acceleration and velocity shall be performed, or one of the Equations (20) or (21) shall be satisfied.

$$f \geq 2.86 \ln\left(\frac{180}{W}\right) \qquad (20)$$

$$W \geq 180 e^{(-0.35f)} \qquad (21)$$

where: *W* is the weight of the supported structure including only dead load (kip), and *f* is the fundamental frequency in the vertical direction (Hz).

For Dalenbrua footbridge, first natural frequency is equal to 2.7 Hz, and *W* for 18 m span is equal 35316 kg (77.9 kip). Considering Equation (20), first natural frequency shall be bigger than 2.4 Hz, which is fulfilled. Considering Equation (21), weight (given in kip), shall be bigger than 70 kip, which is also fulfilled. To conclude, Dalenbrua footbridge meets USA vibration requirements.

8 CONCLUSIONS

In this paper a comparison of loading and SLS criteria for timber footbridges in EU, AU, CAN and USA are presented. Requirements and results are applied to an existing footbridge case and compared.

Table 11: *Comparison of footbridge loading in EU, AU, CAN and USA*

	Country			
Load	EU	AU	CAN	USA
Dead load softwood [kg/m^3]	350-550 (335-495)	n.a.	612	801
Dead load hardwood [kg/m^3]	570-1080	n.a.	968	961
Pedestrian loading [kPa]	$q_k = 2.0 + \frac{120}{L+30}$	n.a.	$p = 5.0 - \frac{s}{30}$	4
Crowd (max value) [kPa]	5	5	4.0	~4.31
Pedestrian loading for Dalenbrua [kPa]	4.5	~4.0	4.0	~4.31
Vehicle load [kN]	120	21/31	n.a.	~45/89

Table 12: *Comparison of footbridge vibrational criteria and performance in EU, AU, CAN and USA*

	Country			
Requirement	EU	AU	CAN	USA
Deflection	l/200	l/600	l/500	l/425
Dalenbrua case; max deflection =59 [mm]	90	30	36	42
Requirement fulfilled	yes	no	no	no
Min of vertical fundamental frequency [Hz]; for Dalenbrua =2.7	5.0	5.0 (3.0)	n.a.	3.0
Min of hor./tors. fundamental frequency [Hz]; for Dalenbrua =4.5	2.5	1.5	n.a.	1.5
Accepted vertical acceleration [m/s^2] in Dalenbrua case (1 person walks)	0.7	n.a.	~0.55	n.a.
Requirement fulfilled; accaler. for Dalenbrua =0.189 [m/s^2]	yes	n.a.	yes	n.a.
Max dyn. defl. to first frequency under 700 N force; [mm]	n.a.	~1.6	n.a.	n.a.
Requirement fulfilled	n.a.	yes	n.a.	n.a.
Min frequency or weight criteria	n.a.	n.a.	n.a.	Eq. (21), (22)
Requirement fulfilled	n.a.	n.a.	n.a.	yes

It is shown in Table 11 and 12 that considered parameters like dead load, pedestrian or vehicle load, as well as deflection or acceleration of the footbridge, vary among the countries. Some similarities can be noticed between the values of pedestrian load and dead load, and minimum values of first natural frequency, which implies that there is no need to check vibrational criteria for these footbridges. There are considerable differences in SLS requirements and approaches. Information about the procedures for calculations differs as well as the additional limitations with respect to footbridge/bridge width and length.

To conclude, the SLS design recommendations for timber footbridges vary significantly among countries. Especially vibrational criteria is an area for further work, development and harmonization.

ACKNOWLEDGEMENT

This work has been made possible by a project grant: Rigid joints for large timber (10381500) received from The Research Council of Norway and financial and technical support from The Association of Norwegian Glulam Producers, Skogtiltaksfondet and Norwegian Public Road

Authorities. The design documentation of Dalenbrua footbridge has been very helpful and was made available from the company SWECO Norway. All these contributions are gratefully acknowledged.

REFERENCES

[1] Thelandersson S. and Larsen H. J.: Timber Engineering. Wiley & Sons London, 2003.

[2] AS 5100.1-2004. Australian Standard. Bridge design. Part 1: Scope and general principles. Standards Australia, Sydney, 2004.

[3] NS-EN 1990:2002+NA:2008. Eurocode - Basis of structural design. European Committee for Standardization, Brussels, 2002.

[4] AASHTO LRFD BRIDGE. Design Specifications, American Association of State Highway and Transportation Officials, Washington, 2012.

[5] CAN/CSA-S6-06. Canadian highway bridge design code, Canadian Standard Association, Ontario, 2011.

[6] NS-EN 14080:2013. Timber structures. Glued laminated timber and glued solid timber. Requirements. European Committee for Standardization, Brussels, 2013.

[7] NS-EN 338:2009. Structural Timber. Strength classes, European Committee for Standardization, Brussels, 2009.

[8] NS-EN 1995-1-1:2004+A1:2008+NA:20010. Eurocode 5: Design of timber structures. Part 1-1: General. Common rules and rules for buildings. European Committee for Standardization, Brussels, 2004.

[9] Bruprosjektering, (Basis of Bridge Design, Handbook 185), Statens vegvesen Vegdirektoratet, Oslo, 2009.

[10] NS-EN 1991-2:2003+NA:2010. Eurocode1: Actions on structures. Part 2: Traffic loads on bridges. European Committee for Standardization, Brussels, 2003.

[11] AS 5100.2-2004. Australian Standard. Bridge design. Part 2: Design loads. Standards Australia, Sydney, 2004.

[12] LRFD Guide specifications for the design of pedestrian bridges. American Association of State Highway and Transportation Officials, Washington, 2009.

[13] AS/NZS 1170.1:2002. Australian/New Zeland Standard. Structural design actions. Part 1: Permanent, imposed and other actions. Standards Australia/Standards New Zeland, Sydney, 2002.

[14] NS-EN 1990:2002/A1:2005+NA:2010. Amendment A1. Eurocode - Basis of structural design. European Committee for Standardization, Brussels, 2005.

[15] AS 5100.2 Supplement 1 - 2007. Bridge design - Design loads – Commentary. Standards Australia, Sydney, 2007.

[16] NS-EN 1995-2:2004+NA:2010. Eurocode 5: Design of timber structures. Part 2: Bridges. European Committee for Standardization, Brussels, 2004.

[17] SWECO NORWAY, Drawings and documentation of Dalenbrua, Lillehammer, 2012.

[18] Commentary on CAN/CSA-S6-06. Canadian highway bridge design code, Canadian Standard Association, Ontario, 2006.

DEPARTMENT OF STRUCTURAL ENGINEERING
NORWEGIAN UNIVERSITY OF SCIENCE AND TECHNOLOGY

N–7491 TRONDHEIM, NORWAY
Telephone: +47 73 59 47 00 Telefax: +47 73 59 47 01

"Reliability Analysis of Structural Systems using Nonlinear Finite Element Methods",
C. A. Holm, 1990:23, ISBN 82-7119-178-0.

"Uniform Stratified Flow Interaction with a Submerged Horizontal Cylinder",
Ø. Arntsen, 1990:32, ISBN 82-7119-188-8.

"Large Displacement Analysis of Flexible and Rigid Systems Considering Displacement-Dependent Loads and Nonlinear Constraints",
K. M. Mathisen, 1990:33, ISBN 82-7119-189-6.

"Solid Mechanics and Material Models including Large Deformations",
E. Levold, 1990:56, ISBN 82-7119-214-0, ISSN 0802-3271.

"Inelastic Deformation Capacity of Flexurally-Loaded Aluminium Alloy Structures",
T. Welo, 1990:62, ISBN 82-7119-220-5, ISSN 0802-3271.

"Visualization of Results from Mechanical Engineering Analysis",
K. Aamnes, 1990:63, ISBN 82-7119-221-3, ISSN 0802-3271.

"Object-Oriented Product Modeling for Structural Design",
S. I. Dale, 1991:6, ISBN 82-7119-258-2, ISSN 0802-3271.

"Parallel Techniques for Solving Finite Element Problems on Transputer Networks",
T. H. Hansen, 1991:19, ISBN 82-7119-273-6, ISSN 0802-3271.

"Statistical Description and Estimation of Ocean Drift Ice Environments",
R. Korsnes, 1991:24, ISBN 82-7119-278-7, ISSN 0802-3271.

“Properties of concrete related to fatigue damage: with emphasis on high strength concrete”,
G. Petkovic, 1991:35, ISBN 82-7119-290-6, ISSN 0802-3271.

"Turbidity Current Modelling",
B. Brørs, 1991:38, ISBN 82-7119-293-0, ISSN 0802-3271.

"Zero-Slump Concrete: Rheology, Degree of Compaction and Strength. Effects of Fillers as Part Cement-Replacement",
C. Sørensen, 1992:8, ISBN 82-7119-357-0, ISSN 0802-3271.

"Nonlinear Analysis of Reinforced Concrete Structures Exposed to Transient Loading",
K. V. Høiseth, 1992:15, ISBN 82-7119-364-3, ISSN 0802-3271.

"Finite Element Formulations and Solution Algorithms for Buckling and Collapse Analysis of Thin Shells",
R. O. Bjærum, 1992:30, ISBN 82-7119-380-5, ISSN 0802-3271.

"Response Statistics of Nonlinear Dynamic Systems",
J. M. Johnsen, 1992:42, ISBN 82-7119-393-7, ISSN 0802-3271.

"Digital Models in Engineering. A Study on why and how engineers build and operate digital models for decisison support",
J. Høyte, 1992:75, ISBN 82-7119-429-1, ISSN 0802-3271.

"Sparse Solution of Finite Element Equations",
A. C. Damhaug, 1992:76, ISBN 82-7119-430-5, ISSN 0802-3271.

"Some Aspects of Floating Ice Related to Sea Surface Operations in the Barents Sea",
S. Løset, 1992:95, ISBN 82-7119-452-6, ISSN 0802-3271.

"Modelling of Cyclic Plasticity with Application to Steel and Aluminium Structures",
O. S. Hopperstad, 1993:7, ISBN 82-7119-461-5, ISSN 0802-3271.

"The Free Formulation: Linear Theory and Extensions with Applications to Tetrahedral Elements
with Rotational Freedoms",
G. Skeie, 1993:17, ISBN 82-7119-472-0, ISSN 0802-3271.

"Høyfast betongs motstand mot piggdekkslitasje. Analyse av resultater fra prøving i Veisliter'n",
T. Tveter, 1993:62, ISBN 82-7119-522-0, ISSN 0802-3271.

"A Nonlinear Finite Element Based on Free Formulation Theory for Analysis of Sandwich Structures",
O. Aamlid, 1993:72, ISBN 82-7119-534-4, ISSN 0802-3271.

"The Effect of Curing Temperature and Silica Fume on Chloride Migration and Pore Structure of High Strength Concrete",
C. J. Hauck, 1993:90, ISBN 82-7119-553-0, ISSN 0802-3271.

"Failure of Concrete under Compressive Strain Gradients",
G. Markeset, 1993:110, ISBN 82-7119-575-1, ISSN 0802-3271.

"An experimental study of internal tidal amphidromes in Vestfjorden",
J. H. Nilsen, 1994:39, ISBN 82-7119-640-5, ISSN 0802-3271.

"Structural analysis of oil wells with emphasis on conductor design",
H. Larsen, 1994:46, ISBN 82-7119-648-0, ISSN 0802-3271.

"Adaptive methods for non-linear finite element analysis of shell structures",
K. M. Okstad, 1994:66, ISBN 82-7119-670-7, ISSN 0802-3271.

"On constitutive modelling in nonlinear analysis of concrete structures",
O. Fyrileiv, 1994:115, ISBN 82-7119-725-8, ISSN 0802-3271.

"Fluctuating wind load and response of a line-like engineering structure with emphasis on motion-induced wind forces",
J. Bogunovic Jakobsen, 1995:62, ISBN 82-7119-809-2, ISSN 0802-3271.

"An experimental study of beam-columns subjected to combined torsion, bending and axial actions",
A. Aalberg, 1995:66, ISBN 82-7119-813-0, ISSN 0802-3271.

"Scaling and cracking in unsealed freeze/thaw testing of Portland cement and silica fume concretes",
S. Jacobsen, 1995:101, ISBN 82-7119-851-3, ISSN 0802-3271.

"Damping of water waves by submerged vegetation. A case study of laminaria hyperborea",
A. M. Dubi, 1995:108, ISBN 82-7119-859-9, ISSN 0802-3271.

"The dynamics of a slope current in the Barents Sea",
Sheng Li, 1995:109, ISBN 82-7119-860-2, ISSN 0802-3271.

"Modellering av delmaterialenes betydning for betongens konsistens",
Ernst Mørtsell, 1996:12, ISBN 82-7119-894-7, ISSN 0802-3271.

"Bending of thin-walled aluminium extrusions",
Birgit Søvik Opheim, 1996:60, ISBN 82-7119-947-1, ISSN 0802-3271.

"Material modelling of aluminium for crashworthiness analysis",
Torodd Berstad, 1996:89, ISBN 82-7119-980-3, ISSN 0802-3271.

"Estimation of structural parameters from response measurements on submerged floating tunnels",
Rolf Magne Larssen, 1996:119, ISBN 82-471-0014-2, ISSN 0802-3271.

“Numerical modelling of plain and reinforced concrete by damage mechanics”,
Mario A. Polanco-Loria, 1997:20, ISBN 82-471-0049-5, ISSN 0802-3271.

“Nonlinear random vibrations - numerical analysis by path integration methods”,
Vibeke Moe, 1997:26, ISBN 82-471-0056-8, ISSN 0802-3271.

"Numerical prediction of vortex-induced vibration by the finite element method",
Joar Martin Dalheim, 1997:63, ISBN 82-471-0096-7, ISSN 0802-3271.

"Time domain calculations of buffeting response for wind sensitive structures",
Ketil Aas-Jakobsen, 1997:148, ISBN 82-471-0189-0, ISSN 0802-3271.

"A numerical study of flow about fixed and flexibly mounted circular cylinders",
Trond Stokka Meling, 1998:48, ISBN 82-471-0244-7, ISSN 0802-3271.

"Estimation of chloride penetration into concrete bridges in coastal areas",
Per Egil Steen, 1998:89, ISBN 82-471-0290-0, ISSN 0802-3271.

"Stress-resultant material models for reinforced concrete plates and shells",
Jan Arve Øverli, 1998:95, ISBN 82-471-0297-8, ISSN 0802-3271.

"Chloride binding in concrete. Effect of surrounding environment and concrete composition",
Claus Kenneth Larsen, 1998:101, ISBN 82-471-0337-0, ISSN 0802-3271.

"Rotational capacity of aluminium alloy beams",
Lars A. Moen, 1999:1, ISBN 82-471-0365-6, ISSN 0802-3271.

"Stretch Bending of Aluminium Extrusions",
Arild H. Clausen, 1999:29, ISBN 82-471-0396-6, ISSN 0802-3271.

"Aluminium and Steel Beams under Concentrated Loading",
Tore Tryland, 1999:30, ISBN 82-471-0397-4, ISSN 0802-3271.

"Engineering Models of Elastoplasticity and Fracture for Aluminium Alloys",
Odd-Geir Lademo, 1999:39, ISBN 82-471-0406-7, ISSN 0802-3271.

"Kapasitet og duktilitet av dybelforbindelser i trekonstruksjoner",
Jan Siem, 1999:46, ISBN 82-471-0414-8, ISSN 0802-3271.

"Etablering av distribuert ingeniørarbeid; Teknologiske og organisatoriske erfaringer fra en norsk ingeniørbedrift",
Lars Line, 1999:52, ISBN 82-471-0420-2, ISSN 0802-3271.

"Estimation of Earthquake-Induced Response",
Símon Ólafsson, 1999:73, ISBN 82-471-0443-1, ISSN 0802-3271.

"Coastal Concrete Bridges: Moisture State, Chloride Permeability and Aging Effects"
Ragnhild Holen Relling, 1999:74, ISBN 82-471-0445-8, ISSN 0802-3271.

"Capacity Assessment of Titanium Pipes Subjected to Bending and External Pressure",
Arve Bjørset, 1999:100, ISBN 82-471-0473-3, ISSN 0802-3271.

“Validation of Numerical Collapse Behaviour of Thin-Walled Corrugated Panels”,
Håvar Ilstad, 1999:101, ISBN 82-471-0474-1, ISSN 0802-3271.

“Strength and Ductility of Welded Structures in Aluminium Alloys”,
Miroslaw Matusiak, 1999:113, ISBN 82-471-0487-3, ISSN 0802-3271.

“Thermal Dilation and Autogenous Deformation as Driving Forces to Self-Induced Stresses in High Performance Concrete”,
Øyvind Bjøntegaard, 1999:121, ISBN 82-7984-002-8, ISSN 0802-3271.

“Some Aspects of Ski Base Sliding Friction and Ski Base Structure”,
Dag Anders Moldestad, 1999:137, ISBN 82-7984-019-2, ISSN 0802-3271.

"Electrode reactions and corrosion resistance for steel in mortar and concrete",
Roy Antonsen, 2000:10, ISBN 82-7984-030-3, ISSN 0802-3271.

"Hydro-Physical Conditions in Kelp Forests and the Effect on Wave Damping and Dune Erosion. A case study on Laminaria Hyperborea",
Stig Magnar Løvås, 2000:28, ISBN 82-7984-050-8, ISSN 0802-3271.

"Random Vibration and the Path Integral Method",
Christian Skaug, 2000:39, ISBN 82-7984-061-3, ISSN 0802-3271.

"Buckling and geometrical nonlinear beam-type analyses of timber structures",
Trond Even Eggen, 2000:56, ISBN 82-7984-081-8, ISSN 0802-3271.

”Structural Crashworthiness of Aluminium Foam-Based Components”,
Arve Grønsund Hanssen, 2000:76, ISBN 82-7984-102-4, ISSN 0809-103X.

“Measurements and simulations of the consolidation in first-year sea ice ridges, and some aspects of mechanical behaviour”,
Knut V. Høyland, 2000:94, ISBN 82-7984-121-0, ISSN 0809-103X.

”Kinematics in Regular and Irregular Waves based on a Lagrangian Formulation”,
Svein Helge Gjøsund, 2000-86, ISBN 82-7984-112-1, ISSN 0809-103X.

”Self-Induced Cracking Problems in Hardening Concrete Structures”,
Daniela Bosnjak, 2000-121, ISBN 82-7984-151-2, ISSN 0809-103X.

"Ballistic Penetration and Perforation of Steel Plates",
Tore Børvik, 2000:124, ISBN 82-7984-154-7, ISSN 0809-103X.

"Freeze-Thaw resistance of Concrete. Effect of: Curing Conditions, Moisture Exchange and Materials",
Terje Finnerup Rønning, 2001:14, ISBN 82-7984-165-2, ISSN 0809-103X

"Structural behaviour of post tensioned concrete structures. Flat slab. Slabs on ground",
Steinar Trygstad, 2001:52, ISBN 82-471-5314-9, ISSN 0809-103X.

"Slipforming of Vertical Concrete Structures. Friction between concrete and slipform panel",
Kjell Tore Fosså, 2001:61, ISBN 82-471-5325-4, ISSN 0809-103X.

"Some numerical methods for the simulation of laminar and turbulent incompressible flows",
Jens Holmen, 2002:6, ISBN 82-471-5396-3, ISSN 0809-103X.

“Improved Fatigue Performance of Threaded Drillstring Connections by Cold Rolling”,
Steinar Kristoffersen, 2002:11, ISBN: 82-421-5402-1, ISSN 0809-103X.

"Deformations in Concrete Cantilever Bridges: Observations and Theoretical Modelling",
Peter F. Takâcs, 2002:23, ISBN 82-471-5415-3, ISSN 0809-103X.

"Stiffened aluminium plates subjected to impact loading",
Hilde Giæver Hildrum, 2002:69, ISBN 82-471-5467-6, ISSN 0809-103X.

"Full- and model scale study of wind effects on a medium-rise building in a built up area",
Jónas Thór Snæbjørnsson, 2002:95, ISBN82-471-5495-1, ISSN 0809-103X.

“Evaluation of Concepts for Loading of Hydrocarbons in Ice-infested water”,
Arnor Jensen, 2002:114, ISBN 82-417-5506-0, ISSN 0809-103X.

”Numerical and Physical Modelling of Oil Spreading in Broken Ice”,
Janne K. Økland Gjøsteen, 2002:130, ISBN 82-471-5523-0, ISSN 0809-103X.

”Diagnosis and protection of corroding steel in concrete”,
Franz Pruckner, 20002:140, ISBN 82-471-5555-4, ISSN 0809-103X.

“Tensile and Compressive Creep of Young Concrete: Testing and Modelling”,
Dawood Atrushi, 2003:17, ISBN 82-471-5565-6, ISSN 0809-103X.

“Rheology of Particle Suspensions. Fresh Concrete, Mortar and Cement Paste with Various Types of Lignosulfonates”,
Jon Elvar Wallevik, 2003:18, ISBN 82-471-5566-4, ISSN 0809-103X.

“Oblique Loading of Aluminium Crash Components”,
Aase Reyes, 2003:15, ISBN 82-471-5562-1, ISSN 0809-103X.

“Utilization of Ethiopian Natural Pozzolans”,
Surafel Ketema Desta, 2003:26, ISSN 82-471-5574-5, ISSN:0809-103X.

“Behaviour and strength prediction of reinforced concrete structures with discontinuity regions”, Helge Brå, 2004:11, ISBN 82-471-6222-9, ISSN 1503-8181.

“High-strength steel plates subjected to projectile impact. An experimental and numerical study”, Sumita Dey, 2004:38, ISBN 82-471-6282-2 (printed version), ISBN 82-471-6281-4 (electronic version), ISSN 1503-8181.

“Alkali-reactive and inert fillers in concrete. Rheology of fresh mixtures and expansive reactions.”
Bård M. Pedersen, 2004:92, ISBN 82-471-6401-9 (printed version), ISBN 82-471-6400-0 (electronic version), ISSN 1503-8181.

“On the Shear Capacity of Steel Girders with Large Web Openings”.
Nils Christian Hagen, 2005:9 ISBN 82-471-6878-2 (printed version), ISBN 82-471-6877-4 (electronic version), ISSN 1503-8181.

”Behaviour of aluminium extrusions subjected to axial loading”.
Østen Jensen, 2005:7, ISBN 82-471-6873-1 (printed version), ISBN 82-471-6872-3 (electronic version), ISSN 1503-8181.

”Thermal Aspects of corrosion of Steel in Concrete”.
Jan-Magnus Østvik, 2005:5, ISBN 82-471-6869-3 (printed version), ISBN 82-471-6868 (electronic version), ISSN 1503-8181.

”Mechanical and adaptive behaviour of bone in relation to hip replacement.” A study of bone remodelling and bone grafting.
Sébastien Muller, 2005:34, ISBN 82-471-6933-9 (printed version), ISBN 82-471-6932-0 (electronic version), ISSN 1503-8181.

“Analysis of geometrical nonlinearities with applications to timber structures”.
Lars Wollebæk, 2005:74, ISBN 82-471-7050-5 (printed version), ISBN 82-471-7019-1 (electronic version), ISSN 1503-8181.

“Pedestrian induced lateral vibrations of slender footbridges”,
Anders Rönnquist, 2005:102, ISBN 82-471-7082-5 (printed version), ISBN 82-471-7081-7 (electronic version), ISSN 1503-8181.

“Initial Strength Development of Fly Ash and Limestone Blended Cements at Various Temperatures Predicted by Ultrasonic Pulse Velocity”,
Tom Ivar Fredvik, 2005:112, ISBN 82-471-7105-8 (printed version), ISBN 82-471-7103-1 (electronic version), ISSN 1503-8181.

“Behaviour and modelling of thin-walled cast components”,
Cato Dørum, 2005:128, ISBN 82-471-7140-6 (printed version), ISBN 82-471-7139-2 (electronic version), ISSN 1503-8181.

“Behaviour and modelling of selfpiercing riveted connections”,
Raffaele Porcaro, 2005:165, ISBN 82-471-7219-4 (printed version), ISBN 82-471-7218-6 (electronic version), ISSN 1503-8181.

”Behaviour and Modelling og Aluminium Plates subjected to Compressive Load”,
Lars Rønning, 2005:154, ISBN 82-471-7169-1 (printed version), ISBN 82-471-7195-3 (electronic version), ISSN 1503-8181.

”Bumper beam-longitudinal system subjected to offset impact loading”,
Satyanarayana Kokkula, 2005:193, ISBN 82-471-7280-1 (printed version), ISBN 82-471-7279-8 (electronic version), ISSN 1503-8181.

“Control of Chloride Penetration into Concrete Structures at Early Age”,
Guofei Liu, 2006:46, ISBN 82-471-7838-9 (printed version), ISBN 82-471-7837-0 (electronic version), ISSN 1503-8181.

“Modelling of Welded Thin-Walled Aluminium Structures”,
Ting Wang, 2006:78, ISBN 82-471-7907-5 (printed version), ISBN 82-471-7906-7 (electronic version), ISSN 1503-8181.

”Time-variant reliability of dynamic systems by importance sampling and probabilistic analysis of ice loads”,
Anna Ivanova Olsen, 2006:139, ISBN 82-471-8041-3 (printed version), ISBN 82-471-8040-5 (electronic version), ISSN 1503-8181.

“Fatigue life prediction of an aluminium alloy automotive component using finite element analysis of surface topography”.
Sigmund Kyrre Ås, 2006:25, ISBN 82-471-7791-9 (printed version), ISBN 82-471-7791-9 (electronic version), ISSN 1503-8181.

”Constitutive models of elastoplasticity and fracture for aluminium alloys under strain path change”,
Dasharatha Achani, 2006:76, ISBN 82-471-7903-2 (printed version), ISBN 82-471-7902-4 (electronic version), ISSN 1503-8181.

“Simulations of 2D dynamic brittle fracture by the Element-free Galerkin method and linear fracture mechanics”,
Tommy Karlsson, 2006:125, ISBN 82-471-8011-1 (printed version), ISBN 82-471-8010-3 (electronic version), ISSN 1503-8181.

“Penetration and Perforation of Granite Targets by Hard Projectiles”,
Chong Chiang Seah, 2006:188, ISBN 82-471-8150-9 (printed version), ISBN 82-471-8149-5 (electronic version), ISSN 1503-8181.

“Deformations, strain capacity and cracking of concrete in plastic and early hardening phases”,
Tor Arne Hammer, 2007:234, ISBN 978-82-471-5191-4 (printed version), ISBN 978-82-471-5207-2 (electronic version), ISSN 1503-8181.

“Crashworthiness of dual-phase high-strength steel: Material and Component behaviour”, Venkatapathi Tarigopula, 2007:230, ISBN 82-471-5076-4 (printed version), ISBN 82-471-5093-1 (electronic version), ISSN 1503-8181.

“Fibre reinforcement in load carrying concrete structures”,
Åse Lyslo Døssland, 2008:50, ISBN 978-82-471-6910-0 (printed version), ISBN 978-82-471-6924-7 (electronic version), ISSN 1503-8181.

“Low-velocity penetration of aluminium plates”,
Frode Grytten, 2008:46, ISBN 978-82-471-6826-4 (printed version), ISBN 978-82-471-6843-1 (electronic version), ISSN 1503-8181.

“Robustness studies of structures subjected to large deformations”,
Ørjan Fyllingen, 2008:24, ISBN 978-82-471-6339-9 (printed version), ISBN 978-82-471-6342-9 (electronic version), ISSN 1503-8181.

“Constitutive modelling of morsellised bone”,
Knut Birger Lunde, 2008:92, ISBN 978-82-471-7829-4 (printed version), ISBN 978-82-471-7832-4 (electronic version), ISSN 1503-8181.

“Experimental Investigations of Wind Loading on a Suspension Bridge Girder”,
Bjørn Isaksen, 2008:131, ISBN 978-82-471-8656-5 (printed version), ISBN 978-82-471-8673-2 (electronic version), ISSN 1503-8181.

“Cracking Risk of Concrete Structures in The Hardening Phase”,
Guomin Ji, 2008:198, ISBN 978-82-471-1079-9 (printed version), ISBN 978-82-471-1080-5 (electronic version), ISSN 1503-8181.

“Modelling and numerical analysis of the porcine and human mitral apparatus”,
Victorien Emile Prot, 2008:249, ISBN 978-82-471-1192-5 (printed version), ISBN 978-82-471-1193-2 (electronic version), ISSN 1503-8181.

“Strength analysis of net structures”,
Heidi Moe, 2009:48, ISBN 978-82-471-1468-1 (printed version), ISBN 978-82-471-1469-8 (electronic version), ISSN1503-8181.

“Numerical analysis of ductile fracture in surface cracked shells”,
Espen Berg, 2009:80, ISBN 978-82-471-1537-4 (printed version), ISBN 978-82-471-1538-1 (electronic version), ISSN 1503-8181.

"Subject specific finite element analysis of bone – for evaluation of the healing of a leg lengthening and evaluation of femoral stem design",
Sune Hansborg Pettersen, 2009:99, ISBN 978-82-471-1579-4 (printed version), ISBN 978-82-471-1580-0 (electronic version), ISSN 1503-8181.

"Evaluation of fracture parameters for notched multi-layered structures",
Lingyun Shang, 2009:137, ISBN 978-82-471-1662-3 (printed version), ISBN 978-82-471-1663-0 (electronic version), ISSN 1503-8181.

"Modelling of Dynamic Material Behaviour and Fracture of Aluminium Alloys for Structural Applications"
Yan Chen, 2009:69, ISBN 978-82-471-1515-2 (printed version), ISBN 978-82 471-1516-9 (electronic version), ISSN 1503-8181.

"Nanomechanics of polymer and composite particles"
Jianying He 2009:213, ISBN 978-82-471-1828-3 (printed version), ISBN 978-82-471-1829-0 (electronic version), ISSN 1503-8181.

"Mechanical properties of clear wood from Norway spruce"
Kristian Berbom Dahl 2009:250, ISBN 978-82-471-1911-2 (printed version) ISBN 978-82-471-1912-9 (electronic version), ISSN 1503-8181.

"Modeling of the degradation of TiB_2 mechanical properties by residual stresses and liquid Al penetration along grain boundaries"
Micol Pezzotta 2009:254, ISBN 978-82-471-1923-5 (printed version) ISBN 978-82-471-1924-2 (electronic version) ISSN 1503-8181.

"Effect of welding residual stress on fracture"
Xiabo Ren 2010:77, ISBN 978-82-471-2115-3 (printed version) ISBN 978-82-471-2116-0 (electronic version), ISSN 1503-8181.

"Pan-based carbon fiber as anode material in cathodic protection system for concrete structures"
Mahdi Chini 2010:122, ISBN 978-82-471-2210-5 (printed version) ISBN 978-82-471-2213-6 (electronic version), ISSN 1503-8181.

"Structural Behaviour of deteriorated and retrofitted concrete structures"
Irina Vasililjeva Sæther 2010:171, ISBN 978-82-471-2315-7 (printed version) ISBN 978-82-471-2316-4 (electronic version) ISSN 1503-8181.

"Prediction of local snow loads on roofs"
Vivian Meløysund 2010:247, ISBN 978-82-471-2490-1 (printed version) ISBN 978-82-471-2491-8 (electronic version) ISSN 1503-8181.

"Behaviour and modelling of polymers for crash applications"
Virgile Delhaye 2010:251, ISBN 978-82-471-2501-4 (printed version) ISBN 978-82-471-2502-1 (electronic version) ISSN 1503-8181.

“Blended cement with reducted CO_2 emission – Utilizing the Fly Ash-Limestone Synergy”,
Klaartje De Weerdt 2011:32, ISBN 978-82-471-2584-7 (printed version) ISBN 978-82-471-2584-4 (electronic version) ISSN 1503-8181.

“Chloride induced reinforcement corrosion in concrete” Concept of critical chloride content – methods and mechanisms.
Ueli Angst 2011:113, ISBN 978-82-471-2769-9 (printed version) ISBN 978-82-471-2763-6 (electronic version) ISSN 1503-8181.

“A thermo-electric-Mechanical study of the carbon anode and contact interface for Energy savings in the production of aluminium”.
Dag Herman Andersen 2011:157, ISBN 978-82-471-2859-6 (printed version) ISBN 978-82-471-2860-2 (electronic version) ISSN 1503-8181.

“Structural Capacity of Anchorage Ties in Masonry Veneer Walls Subjected to Earthquake”. The implications of Eurocode 8 and Eurocode 6 on a typical Norwegain veneer wall.
Ahmed Mohamed Yousry Hamed 2011:181, ISBN 978-82-471-2911-1 (printed version) ISBN 978-82-471-2912-8 (electronic ver.) ISSN 1503-8181.

“Work-hardening behaviour in age-hardenable Al-Zn-Mg(-Cu) alloys”.
Ida Westermann , 2011:247, ISBN 978-82-471-3056-8 (printed ver.) ISBN 978-82-471-3057-5 (electronic ver.) ISSN 1503-8181.

“Behaviour and modelling of selfpiercing riveted connections using aluminium rivets”.
Nguyen-Hieu Hoang, 2011:266, ISBN 978-82-471-3097-1 (printed ver.) ISBN 978-82-471-3099-5 (electronic ver.) ISSN 1503-8181.

“Fibre reinforced concrete”.
Sindre Sandbakk, 2011:297, ISBN 978-82-471-3167-1 (printed ver.) ISBN 978-82-471-3168-8 (electronic ver) ISSN 1503:8181.

“Dynamic behaviour of cablesupported bridges subjected to strong natural wind”.
Ole Andre Øiseth, 2011:315, ISBN 978-82-471-3209-8 (printed ver.) ISBN 978-82-471-3210-4 (electronic ver.) ISSN 1503-8181.

“Constitutive modeling of solargrade silicon materials”
Julien Cochard, 2011:307, ISBN 978-82-471-3189-3 (printed ver). ISBN 978-82-471-3190-9 (electronic ver.) ISSN 1503-8181.

“Constitutive behavior and fracture of shape memory alloys”
Jim Stian Olsen, 2012:57, ISBN 978-82-471-3382-8 (printed ver.) ISBN 978-82-471-3383-5 (electronic ver.) ISSN 1503-8181.

“Field measurements in mechanical testing using close-range photogrammetry and digital image analysis”
Egil Fagerholt, 2012:95, ISBN 978-82-471-3466-5 (printed ver.) ISBN 978-82-471-3467-2 (electronic ver.) ISSN 1503-8181.

“Towards a better under standing of the ultimate behaviour of lightweight aggregate concrete in compression and bending”,
Håvard Nedrelid, 2012:123, ISBN 978-82-471-3527-3 (printed ver.) ISBN 978-82-471-3528-0 (electronic ver.) ISSN 1503-8181.

“Numerical simulations of blood flow in the left side of the heart”
Sigrid Kaarstad Dahl, 2012:135, ISBN 978-82-471-3553-2 (printed ver.) ISBN 978-82-471-3555-6 (electronic ver.) ISSN 1503-8181.

“Moisture induced stresses in glulam”
Vanessa Angst-Nicollier, 2012:139, ISBN 978-82-471-3562-4 (printed ver.) ISBN 978-82-471-3563-1 (electronic ver.) ISSN 1503-8181.

“Biomechanical aspects of distraction osteogensis”
Valentina La Russa, 2012:250, ISBN 978-82-471-3807-6 (printed ver.) ISBN 978-82-471-3808-3 (electronic ver.) ISSN 1503-8181.

“Ductile fracture in dual-phase steel. Theoretical, experimental and numerical study”
Gaute Gruben, 2012:257, ISBN 978-82-471-3822-9 (printed ver.) ISBN 978-82-471-3823-6 (electronic ver.) ISSN 1503-8181.

“Damping in Timber Structures”
Nathalie Labonnote, 2012:263, ISBN 978-82-471-3836-6 (printed ver.) ISBN 978-82-471-3837-3 (electronic ver.) ISSN 1503-8181.

“Biomechanical modeling of fetal veins: The umbilical vein and ductus venosus bifurcation”
Paul Roger Leinan, 2012:299, ISBN 978-82-471-3915-8 (printed ver.) ISBN 978-82-471-3916-5 (electronic ver.) ISSN 1503-8181.

“Large-Deformation behaviour of thermoplastics at various stress states”
Anne Serine Ognedal, 2012:298, ISBN 978-82-471-3913-4 (printed ver.) ISBN 978-82-471-3914-1 (electronic ver.) ISSN 1503-8181.

“Hardening accelerator for fly ash blended cement”
Kien Dinh Hoang, 2012:366, ISBN 978-82-471-4063-5 (printed ver.) ISBN 978-82-471-4064-2 (electronic ver.) ISSN 1503-8181.

“From molecular structure to mechanical properties”
Jianyang Wu, 2013:186, ISBN 978-82-471-4485-5 (printed ver.) ISBN 978-82-471-4486-2 (electronic ver.) ISSN 1503-8181.

“Experimental and numerical study of hybrid concrete structures”
Linn Grepstad Nes, 2013:259, ISBN 978-82-471-4644-6 (printed ver.) ISBN 978-82-471-4645-3 (electronic ver.) ISSN 1503-8181.

“Mechanics of ultra-thin multi crystalline silicon wafers”
Saber Saffar, 2013:199, ISBN 978-82-471-4511-1 (printed ver.) ISBN 978-82-471-4513-5 (electronic ver). ISSN 1503-8181.

“Through process modelling of welded aluminium structures”
Anizahyati Alisibramulisi, 2013:325, ISBN 978-82-471-4788-7 (printed ver.) ISBN 978-82-471-4789-4 (electronic ver.) ISSN 1503-8181.

“Combined blast and fragment loading on steel plates”
Knut Gaarder Rakvåg, 2013:361, ISBN978-82-471-4872-3 (printed ver.) ISBN 978-82-4873-0 (electronic ver.). ISSN 1503-8181.

“Characterization and modelling of the anisotropic behaviour of high-strength aluminium alloy”
Marion Fourmeau, 2014:37, ISBN 978-82-326-0008-3 (printed ver.) ISBN 978-82-326-0009-0 (electronic ver.) ISSN 1503-8181.

“Behaviour of threated steel fasteners at elevated deformation rates”
Henning Fransplass, 2014:65, ISBN 978-82-326-0054-0 (printed ver.) ISBN 978-82-326-0055-7 (electronic ver.) ISSN 1503-8181.

“Sedimentation and Bleeding”
Ya Peng, 2014:89, ISBN 978-82-326-0102-8 (printed ver.) ISBN 978-82-326-0103-5 (electric ver.) ISSN 1503-8181.

“Impact against X65 offshore pipelines”
Martin Kristoffersen, 2014:362, ISBN 978-82-326-0636-8 (printed ver.) ISBN 978-82-326-0637-5 (electronic ver.) ISSN 1503-8181.

“Formability of aluminium alloy subjected to prestrain by rolling”
Dmitry Vysochinskiy, 2014:363,, ISBN 978-82-326-0638-2 (printed ver.) ISBN 978-82-326-0639-9 (electronic ver.) ISSN 1503-8181.

“Experimental and numerical study of Yielding, Work-Hardening and anisotropy in textured AA6xxx alloys using crystal plasticity models”
Mikhail Khadyko, 2015:28, ISBN 978-82-326-0724-2 (printed ver.) ISBN 978-82-326-0725-9 (electronic ver.) ISSN 1503-8181.

“Behaviour and Modelling of AA6xxx Aluminium Alloys Under a Wide Range of Temperatures and Strain Rates”
Vincent Vilamosa, 2015:63, ISBN 978-82-326-0786-0 (printed ver.) ISBN 978-82-326-0787-7 (electronic ver.) ISSN 1503-8181.

“A Probabilistic Approach in Failure Modelling of Aluminium High Pressure Die-Castings”
Octavian Knoll, 2015:137, ISBN 978-82-326-0930-7 (printed ver.) ISBN 978-82-326-0931-4 (electronic ver.) ISSN 1503-8181.

“Ice Abrasion on Marine Concrete Structures”
Egil Møen, 2015:189, ISBN 978-82-326-1034-1 (printed ver.) ISBN 978-82-326-1035-8 (electronic ver.) ISSN 1503-8181.

“Fibre Orientation in Steel-Fibre-Reinforced Concrete”
Giedrius Zirgulis, 2015:229, ISBN 978-82-326-1114-0 (printed ver.) ISBN 978-82-326-1115-7 (electronic ver.) ISSN 1503-8181.

“Effect of spatial variation and possible interference of localised corrosion on the residual capacity of a reinforced concrete beam”
Mohammad Mahdi Kioumarsi, 2015:282, ISBN 978-82-326-1220-8 (printed ver.) ISBN 978-82-1221-5 (electronic ver.) ISSN 1503-8181.

“The role of concrete resistivity in chloride-induced macro-cell corrosion”
Karla Horbostel, 2015:324, ISBN 978-82-326-1304-5 (printed ver.) ISBN 978-82-326-1305-2 (electonic ver.) ISSN 1503-8181.

“Flowable fibre-reinforced concrete for structural applications”
Elena Vidal Sarmiento, 2015-335, ISBN 978-82-326-1324-3 (printed ver.) ISBN 978-82-326-1325-0 (electronic ver.) ISSN 1503-8181.

“Development of chushed sand for concrete production with microproportioning”
Rolands Cepuritis, 2016:19, ISBN 978-82-326-1382-3 (printed ver.) ISBN 978-82-326-1383-0 (electronic ver.) ISSN 1503-8181.

“Withdrawal properties of threaded rods embedded in glued-laminated timer elements”
Haris Stamatopoulos, 2016:48, ISBN 978-82-326-1436-3 (printed ver.) ISBN 978-82-326-1437-0 (electronic ver.) ISSN 1503-8181.

“An Experimental and numerical study of thermoplastics at large deformation”
Marius Andersen, 2016:191, ISBN 978-82-326-1720-3 (printed ver.) ISBN 978-82-326-1721-0 (electronic ver.) ISSN 1503-8181.

“Modeling and Simulation of Ballistic Impact”
Jens Kristian Holmen, 2016:240, ISBN 978-82-326-1818-7 (printed ver). ISBN 978-82-326-1819-4 (electronic ver.) ISSN 1503-8181.

“Early age crack assessment of concrete structures”
Anja B. Estensen Klausen, 2016:256, ISBN 978-82-326-1850-7 (printed ver). ISBN 978-82-326-1851-4 (electronic ver.) ISSN 1503-8181.

“Uncertainty quantification and sensitivity analysis for cardiovascular models”
Vinzenz Gregor Eck, 2016:234, ISBN 978-82-326-1806-4 (printed ver.) ISBN 978-82-326-1807-1 (electronic ver.) ISSN 1503-8181.

“Dynamic behaviour of existing and new railway catenary systems under Norwegain conditions”
Petter Røe Nåvik, 2016:298, ISBN 978-82-326-1935-1 (printed ver.) ISBN 978-82-326-1934-4 (electronic ver.) ISSN 1503-8181.

“Mechanical behaviour of particle-filled elastomers at various temperatures”
Arne Ilseng, 2016-295, ISBN978-82-326-1928-3 (printed ver.) ISBN 978-82-326-1929-0 (electronic ver.) ISSN 1503-8181.

“Nanotechnology for Anti-Icing Application”
Zhiwei He, 2016:348, ISBN 978-82-326-2038-8 (printed ver.) ISBN 978-82-326-2019-5 (electronic ver.) ISSN 1503-8181.

“Conduction Mechanisms in Conductive Adhesives with Metal-Coated Polyer Spheres”
Sigurd Rolland Pettersen, 2016:349, ISBN 978-326-2040-1 (printed ver,) ISBN 978-82-326-2041-8 (electronic ver.) ISSN 1503-8181.

“The interaction between calcium lignosulfonate and cement”
Alessia Colombo, 2017:20, ISBN 978-82-326-2122-4 (printed ver.) ISBN 978-82-326-2123-1 (electronic ver.) ISSN 1503-8181.

“Behaviour and Modelling of Flexible Structures Subjected to Blast Loading”
Vegard Aune, 2017:101, ISBN 978-82-326-2274-0 (printed ver.) ISBN 978-82-326-2275-7 (electronic ver.) ISSN 1503-8181.

“Behaviour of steel connections under quasi-static and impact loading”
Erik Løhre Grimsmo, 2017:159, ISBN 978-82-326-2390-7 (printed ver.) ISBN 978-82-326-2391-4 (electronic ver.) ISSN 1503-8181.

“An experimental and numerical study of cortical bone at he macro and Nano-scale”
Masoud Ramenzanzadehkoldeh,, 2017:208, ISBN 978-82-326-2488-1 (printed ver.) ISBN 978-82-326-2489-8 (electronic ver.) ISSN 1503-8181.

“Optoelectrical Properties of a Novel Organic Semiconductor: 6,13-Dichloropentacene”
Mao Wang, 2017:130, ISBN 978-82-326-2332-7 (printed ver.) ISBN 978-82-326-2333-4) (electronic ver.) ISSN 1503-8181.

“Core-shell structured microgels and their behavior at oil and water interface”
Yi Gong, 2017:182, ISBN 978-82-326-2436-2 (printed. ver.) ISBN 978-82-326-2437-9 (electronic ver.) ISSN 1503-8181.

“Aspects of design of reinforced concrete structures using nonliear finite element analyses”
Morten Engen, 2017:149, ISBN 978-82-326-2370-9 (printed ver.) ISBN 978-82-326-2371-6 (electronic ver.) ISSN 1503-8181.

“Numerical studies on ductile failure of aluminium alloys”
Lars Edvard Dæhli, 2017:284, ISBN 978-82-326-2636-6 (printed ver.) ISBN 978-82-326-2637-3 (electronic ver.) ISSN 1503-8181.

“Modelling and Assessment of Hydrogen Embrittlement in Steels and Nickel Alloys”
Haiyang Yu, 2017:278, ISBN 978-82-326-2624-3 (printed. ver.) ISBN 978-82-326-2625-0 (electronic ver.) ISSN 1503-8181.